DANMARKS OG GRØNLANDS GEOLOGISKE UNDERSØGELSE **RAPPORT 2024/35**

Re-assessment of diamond potential for South Greenland

Stefan Bernstein, Thomas Kokfelt, Diogo Rosa, Nynke Keulen,
Anette Juul-Nielsen, Jakob K. Keiding & Nima Hajir Azad

GEOLOGICAL SURVEY OF DENMARK AND GREENLAND
DANISH MINISTRY OF CLIMATE, ENERGY AND UTILITIES

G E U S

DANMARKS OG GRØNLANDS GEOLOGISKE UNDERSØGELSE **RAPPORT 2024/35**

Re-assessment of diamond potential for South Greenland

Stefan Bernstein, Thomas Kokfelt, Diogo Rosa, Nynke Keulen,
Anette Juul-Nielsen, Jakob K. Keiding & Nima Hajir Azad

GEOLOGICAL SURVEY OF DENMARK AND GREENLAND
DANISH MINISTRY OF CLIMATE, ENERGY AND UTILITIES

G E U S

Contents

Executive summary

Johan Dahl Land in South Greenland is regarded to hold a potential for diamond prospecting based on its suitable geology that includes carbonatite-related (*s.l.*) intrusions, and previous findings of diamond-indicator minerals in sediment samples. Work in the mid-1990's by 'Quadrant Resources' and 'Major General Resources' revealed some samples with diamond-indicator minerals, primarily Cr-rich garnets and spinel, but also chrome-diopside, olivine, Mg-rich ilmenite and orthopyroxene. The positive indications from stream and lake sediments were not followed up on since the 1990's, nor was an attempt made to tie indicator minerals to specific outcrops of carbonatite/lamprophyre/kimberlite intrusions.

This report summarises the results of new field work in 2021 by GEUS/MMR to the Johan Dahl Land area with the following tasks: (1) to re-collect and supplement sediment samples for diamond-indicator minerals, (2) to conduct reconnaissance with the aim to identify rocks of potential source character for indicator minerals, i.e., ultramafic lamprophyre-related intrusions, either in-situ or as floats, and (3) to visit the dykes and breccias in the island of Illutalik, to collect samples for laboratory testing – which would involve identification of possible mantle xenoliths or their alteration products and the possible occurrence of diamond indicator minerals.

The newly collected sediment samples were analysed for their content of diamond-indicator minerals. The samples were processing at SRC, Geoanalytical Laboratories Diamond Services in Saskatoon, Canada, followed by analysis at GEUS using Automated Quantitative Mineralogy maps to obtain the proportions and chemical compositions of the minerals. Out of 265 hand-picked mineral grains, none could be classified as diamond-indicator minerals: garnet (3 grains) classifies as G0 type; ilmenite (82 grains) is Mg-poor and plot away from the kimberlite field; diopside (16 grains) is Cr-absent; olivine (112 grains) is generally relatively Mg-poor (Mg# <76).

The present study does not confirm previous positive findings regarding diamond prospectivity in Johan Dahl Land, South Greenland. However, this does not invalidate the previously established potential due to several factors, including the limited sample size, small investigation area, intense rock alteration, and evidence of past magmatic activity. Despite challenges, South Greenland's tectonic setting and geological history indicate an underexplored but promising diamond potential. Future exploration should focus on identifying primary sources, such as lamprophyre or kimberlite intrusions, to assess economic viability.

Introduction

Sediment samples collected across South Greenland for diamond prospecting in the mid-1990's revealed a number of samples from Johan Dahl Land with some diamond-indicator minerals, primarily Cr-rich garnets and spinel, but also some chrome-diopside, olivine, Mg-rich ilmenite and orthopyroxene (Quadrant Resources, 1996; Major General Resources, 1997) (Fig. 1). Johan Dahl Land lies a few tens of kilometres north of Narsarsuaq airport, bounded to the SE of the Kiatuut Sermiat glacier, to the North by the Eqalorutsit Kangilliit Sermiat glacier and to the West by the Nordre Sermilik fjord. The terrain at Johan Dahl Land consists of broad river valleys with lush vegetation and parsley vegetated highlands with rugged hills and numerous lakes.

The area immediately north of Narsarsuaq airport and to the west at Qassiarsuk hosts a number of carbonatite-related intrusions (Walton, 1965; Stewart,1970; Andersen, 2008; Bartels & Kokfelt, 2014). Some of the intrusions are described as having been emplaced violently into the host granitoid rocks, forming strong brecciation. At least at one location, although some 50 km west near the town of Narsaq, there is a lamprophyre dyke with a suite of altered ultramafic inclusions (Upton, 1991) and another carbonatitic breccia is reported to contain magnetite-rich inclusions (Walton, 1965). From the descriptions referenced above, several of the intrusions bear strong resemblance to ultramafic lamprophyre-related intrusions in the Ataa region in NE Disko Bay, of which a few have proved to be diamond-bearing (Bernstein et al., 2013).

Since the identification of the indicator minerals in lake and stream sediments in Johan Dahl Land (Quadrant Resources, 1996; Major General Resources, 1997), there has not been a dedicated investigation of the area and likewise, the carbonatite-related (*s.l.*) intrusions have not been investigated for potential to carry diamonds. The purpose of this study is to re-evaluate the diamond potential in the Johan Dahl Land which was done by resampling sediments from some of the steams which returned diamond-indicator minerals i the 1990's and by searching the field for kimberlite (*s.l.*)/ultramafic lamprophyre intrusive rocks.

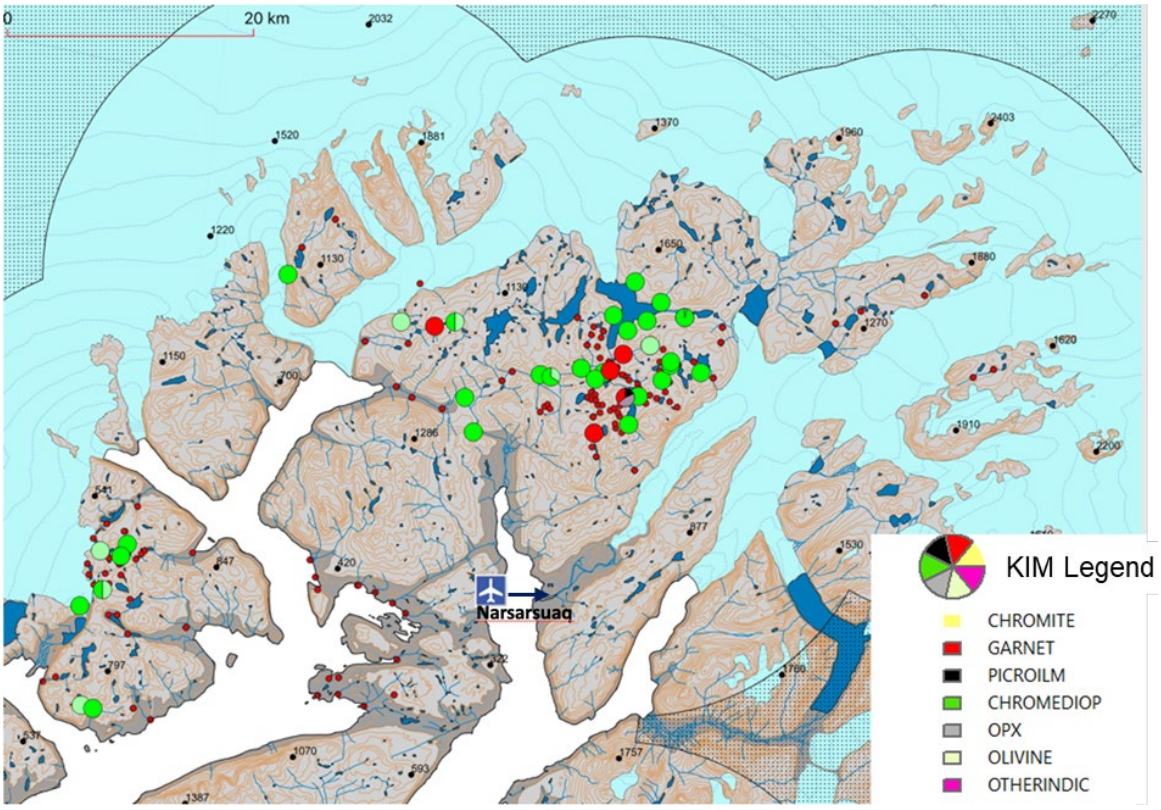

Figure 1. *showing the location of stream sediment samples collected in 1995 and 1996 during diamond exploration – samples with identified KIM are shown with large colour-keyed symbols, while small red circles indicate samples from which no indicator minerals were retrieved.*

Fieldwork

During an eleven-day field programme conducted from 23rd of August to 3rd of September 2021, a team from GEUS and MMR visited Johan Dahl Land in order to assess the significance of the reported diamond-indicator minerals and the general potential for diamond-bearing intrusions in this region of South Greenland. The work was designed to address of following tasks:

- Re-collect stream sediment samples in Johan Dahl Land that have been reported to contain the diamond-indicator minerals and supplement sampling to obtain better area coverage.

- Conduct reconnaissance of Johan Dahl Land with the aim to identify rocks with lamprophyre/carbonatite/kimberlite affinity, either in-situ or as floats, and which could be the source of the reported indicator minerals.

- Visit the dykes and breccias reported by Upton (1991) and Walton (1965), respectively, to collect samples for laboratory testing – which would involve identification of possible mantle xenoliths or their alteration products and the possible occurrence of diamond indicator minerals.

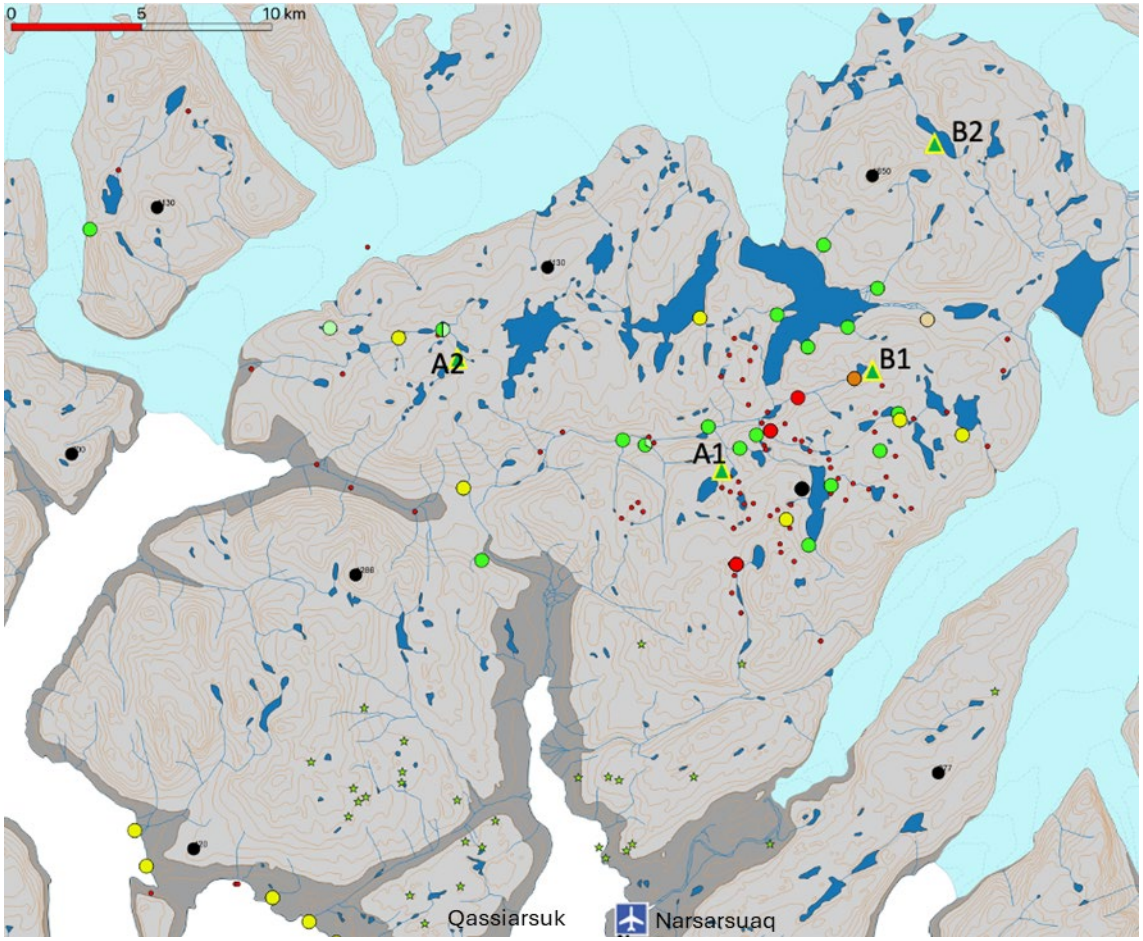

Figure 2. *showing the distribution of field camps A1, A2 and B1, B2, from which the work was carried out.*

Work was carried out from a total of four field camps, two for each two-person team (Fig. 2). The field camps were mobilised by chartered helicopter from Sermeq helicopters, stationed at Qaqortoq, and ground was reached by foot from the field camps. In addition, one day of helicopter support on August 29th, allowed for a visit to the island of Illutalik, SW of Narsaq (Fig. 13a), in addition to sampling streams at the high ground, N of Qassiarsuk some 15-20 km NW of Narsarsuaq and moving the field camps to new locations.

Participants: Stefan Bernstein (pm), Jakob K. Keiding, Diogo Rosa (GEUS) and Anette Juul Nielsen (MMR).

Stream sediment sampling

A total of 14 stream sediment samples were collected during the fieldwork (see Table A1). Sampling of streams was planned so to cover the historic samples sites which returned the most indicator mineral grains, prioritizing those with G9/G10 garnets since e.g., chrome diopside and chrome spinel can have several other sources than mantle peridotite. A total of 12 samples were collected un the vicinity of the four field camps with locations given in Figure 2 along with three additional samples that were collected North of Qassiarsuk. Samples were collected from streams by gathering gravel and sand from their beds (Fig. 3), as well as from

grass roots and moss growing in rock cracks present along their banks. These were carefully disaggregated by hand within a pan or bucket filled with water, to liberate soil from roots and separate sand and gravel from clay. The resulting loose vegetable material was picked and discarded. If the material was granulometrically very heterogeneous it would undergo a first stage of panning, to remove a portion of the clay and coarser rock fragments components (Fig. 4), before any sieving. Otherwise, or subsequently, the gravel, sand and clay mixture was sieved into a pan. The coarser grained fraction was discarded whereas the finer grained mixture was panned. Panning took place by shaking back and forth and side to side, as well as swirling the pan, always with the pan within running water. This resulted in the removal of clays and lighter sand grains, resulting in the concentration of heavier sand grains. The 15 stream samples weighted between 9.95 kg and 15.30 kg and were sent to SRC in Canada for heavy mineral separation processing as described in the Section on the Analytical work.

Figure 3. *Collecting sand and gravel from stream beds.*

Figure 4. *First stage of panning, to remove coarser rock fragments and part of the clays, before sieving.*

Ultramafic lamprophyre dykes

Dykes of ultramafic lamprophyre and carbonatite are well known from South Greenland and are mostly confined to the Gardar rift zone. Based on this, and cross-cutting relations to young Gardar dykes, the age of the ultramafic lamprophyres and carbonatites are believed to be that of the early Gardar rifting (see discussion by Upton, 1991). Such ultramafic lamprophyres and carbonatite intrusive rocks are particularly abundant in the vicinity of Qassiarsuk and Narsarsuaq airport, where they have been described in detail by Walton (1965), Stewart (1970) and Bartels & Kokfelt (2014). Within the area visited by the GEUS/MMR parties, there are no reports of intrusions of such origin, being a few tens of kilometres north of those reported by the aforementioned authors.

The late Gardar dykes are often encountered. They are distinctly of mafic composition with medium to coarse grained gabbroic texture and with rather evolved chemical compositions based on their primary mineral assemblage of pyroxene, plagioclase and Fe-Ti oxides.

A total of 14 rock samples were collected as either floats or solid outcrops of kimberlites (*s.l.*)/ ultramafic lamprophyres (see Table A1). Near Camp A1 (Fig. 5), on the southern banks of a ca 1 km wide lake, a yellow-brown weathered ultramafic lamprophyre dyke cuts across the host metasediments and metavolcanics (samples 591205-7, Fig. 7). The dyke is 0.5-1.5 m thick, near vertical and strikes ca 50°. It can be traced for about 1.3 km along strike, of which several hundred meters towards the SW are covered by moraine/lake. The dyke becomes

increasingly narrow, 5-10 cm across, towards both ends (Fig. 6). Within the length of the exposed dyke, it occasionally jumps a few meters en-echelon. The dyke contains a brownish groundmass with altered olivine phenocrysts (Fig. 8), scattered megacrysts of silicates (5-10 mm; not seen in Fig. 8) – now mostly altered to clay/Fe-Ti oxide mixtures; some scattered black opaque megacrysts (≤10 mm) with a metallic lustre on freshly broken surfaces – marked with red circles in Figure 8. The lamprophyre dyke also contains subangular felsic fragments of what is interpreted to represent gneissic host rock, and some rounded and some angular enclaves of fine-grained intergrowth of minerals, which could represent altered ultramafic xenoliths – possibly of mantle origin.

Near the N-S trending elongated lake, from where stream sediment sample 591201 was collected (Fig. 5), a series of floats of similar ultramafic lamprophyre dyke rock was found in frost boils, some 10 m west of stream bed (sample 591202). The fragments are 5-20 cm in size, angular and appear similar to the larger in-situ lamprophyre dyke rock referred to above (samples 591205-07) and possibly contains relic olivine grains, ≤5 mm in size. The overburden here is relatively thin, and although the fragments could originate as a broken, ice-transported block from the ultramafic lamprophyre dyke at the camp lake, the linear arrangement of the fragments over 10-20 m suggests it to be of local origin. A search in the surroundings for more floats was not fruitful.

One other location was found with a possible ultramafic lamprophyre dyke, at Camp A2 (Fig. 9, sample 591212). It is a red-brown 20-30 cm wide dyke striking 70-80° and vertical and can be followed for ca 100 m along strike. At either end it terminates in overburden, but also becomes thinner.

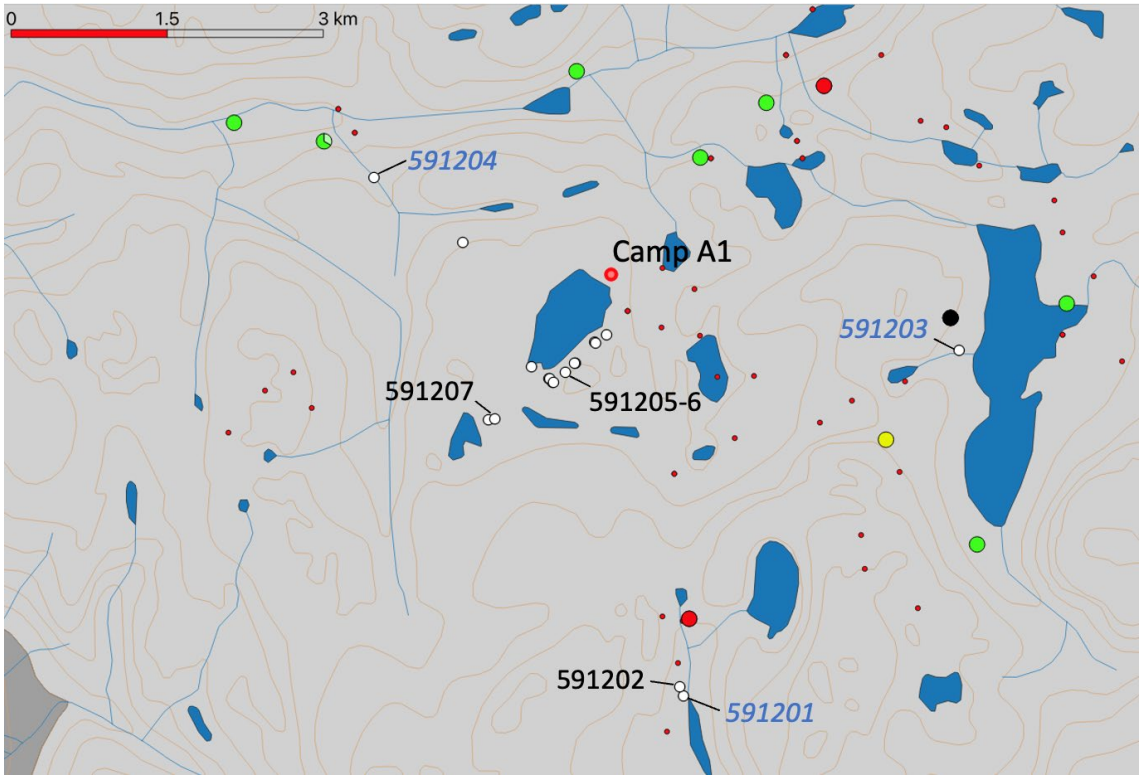

Figure 5. *showing the position of field camp A1 and the distribution of samples taken.*

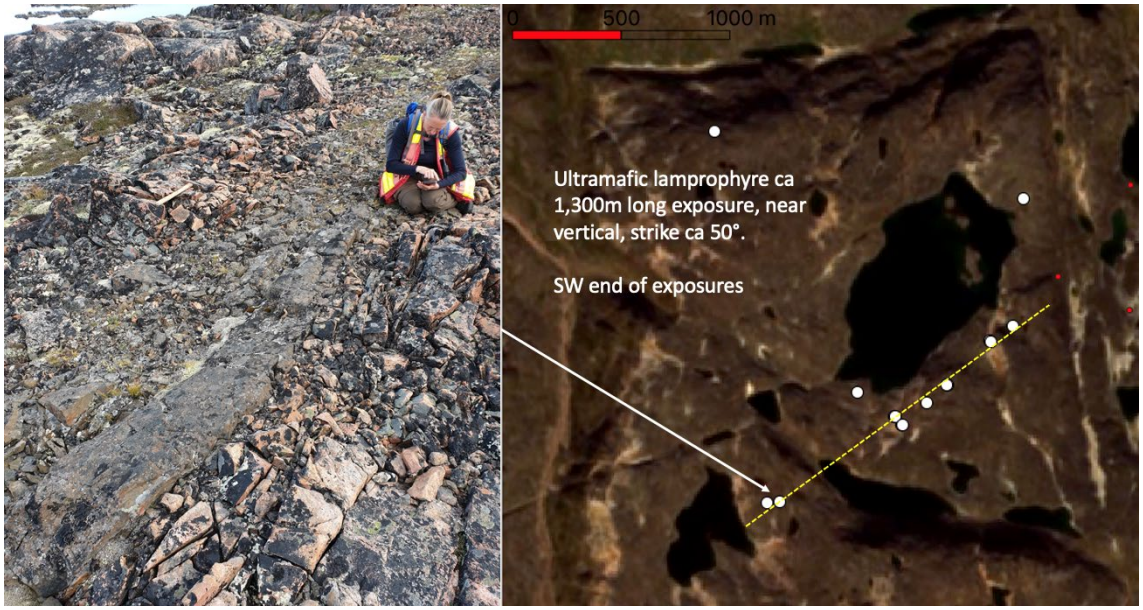

Figure 6. *Outcrop of a 0.5-1.5m wide ultramafic lamprophyre dyke that can be followed for ca 1300m along strike.*

Figure 7. *A yellow-brown weathered ultramafic lamprophyre dyke cuts across the host meta-sediments and meta-volcanics.*

Figure 8. *Detail of ultramafic lamprophyre dyke (591205) with iron-oxide megacrysts (red circles), olivine phenocrysts (?) (yellow circles) subangular xenoliths to 15 mm across of gneissic material, and rounded, brownish enclaves, 5-10 mm across.*

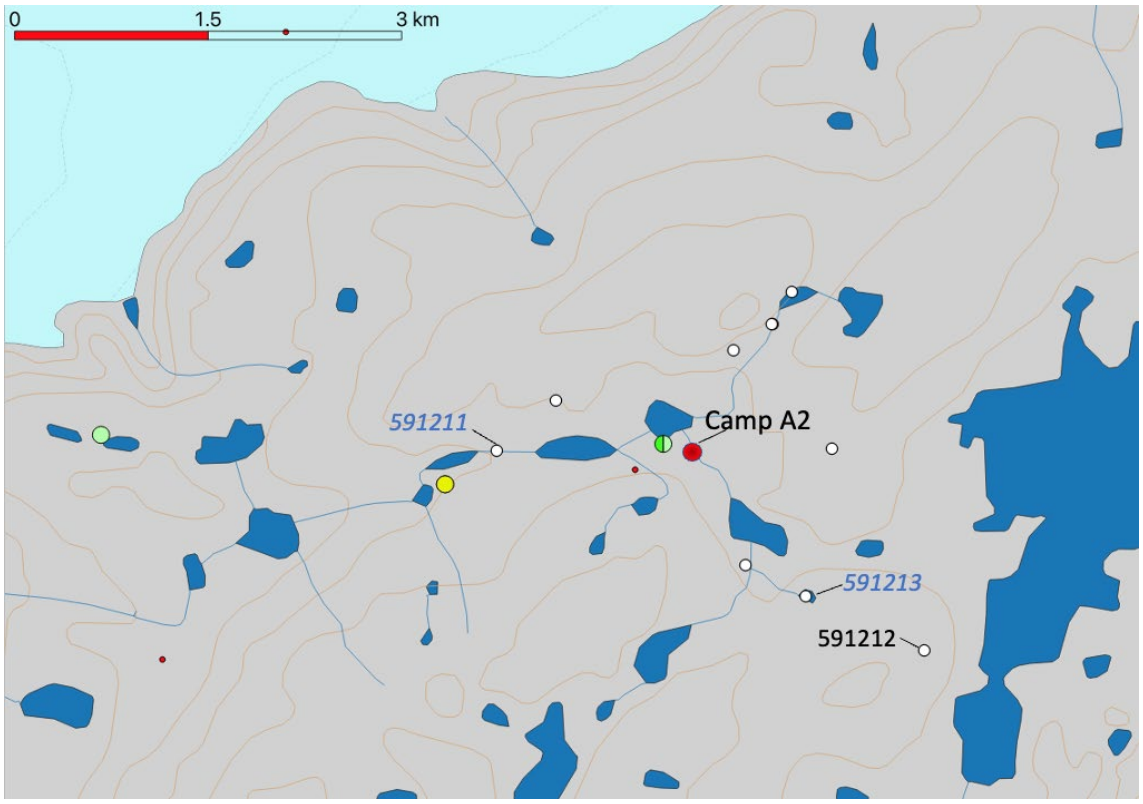

Figure 9. *Sample 591212 is a red-brown 20-30 cm wide dyke striking 70-80° and vertical and can be followed for ca 100 m along strike.*

Lamprophyres were also observed Northwest of camp B2, Valhaltinde (See Fig A1 for location). Two floats of lamprophyre were found and sampled (Fig. 10) the latter of these samples 524515 is believed to be related to two outcrops exposed along a lake edge: a 5×1 m exposure (sample 524514) and a larger 7×2 m exposure (sample 591416), see Figure 11 and 12. Due to the overburden and abundant scree, it was difficult to deduce the relationship between the outcrops. The larger outcrop exhibits a general 170° trend and is subvertical (Fig. 11b) and appears to be an approximately 2 m wide dyke but terminates in a lake. The smaller exposure could be a segment of the same dyke or an unrelated intrusive body. The lithology consists of a heterogeneous, xenolith-bearing lamprophyre hosted within a light grey to white, medium-grained pyroxene-biotite monzonite. The lamprophyres exposed are fine-grained, highly vesicular, strongly altered and contains numerous, mostly subangular xenoliths, of crustal origin. The xenoliths have highly variable sizes ranging from mm-size up to 15 cm wide bodies, and they are predominantly of felsic compositions with monzonite (host rock), gneiss and granite being the predominant lithologies.

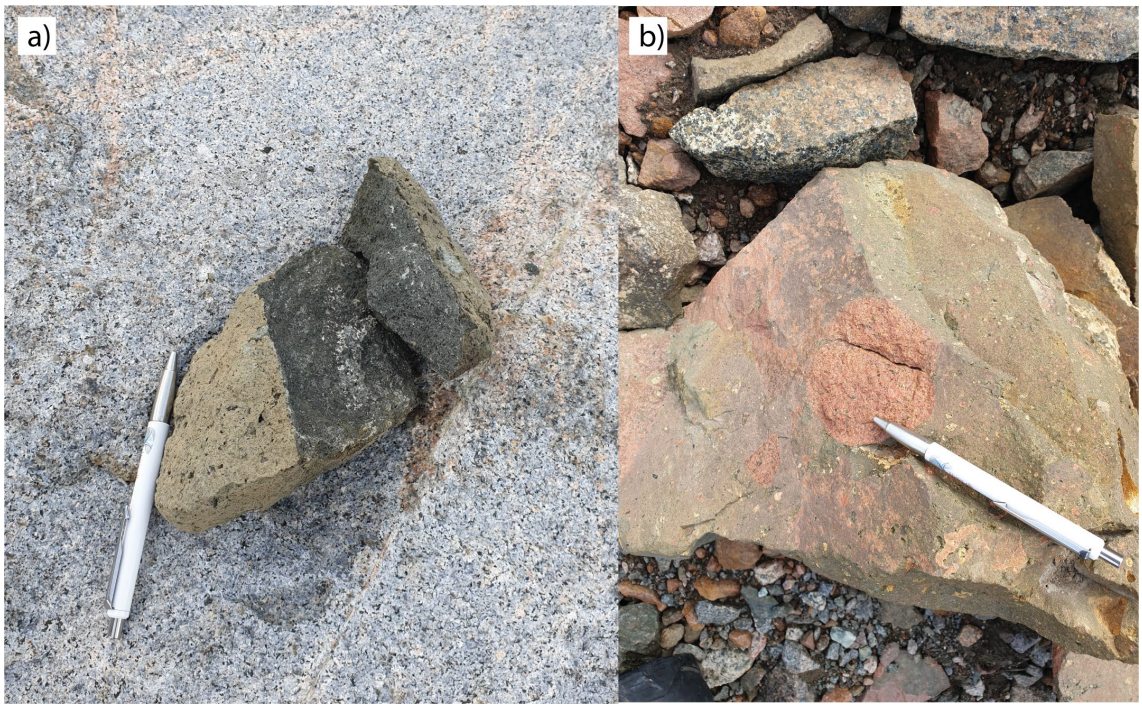

Figure 10. *Float samples of lamprophyres. a) Small brown-weathering relatively homogeneous ultramafic lamprophyre (sample 584512). b) Float sample with large granitic xenolith in the centre and other smaller xenoliths of crustal origin (sample 584514).*

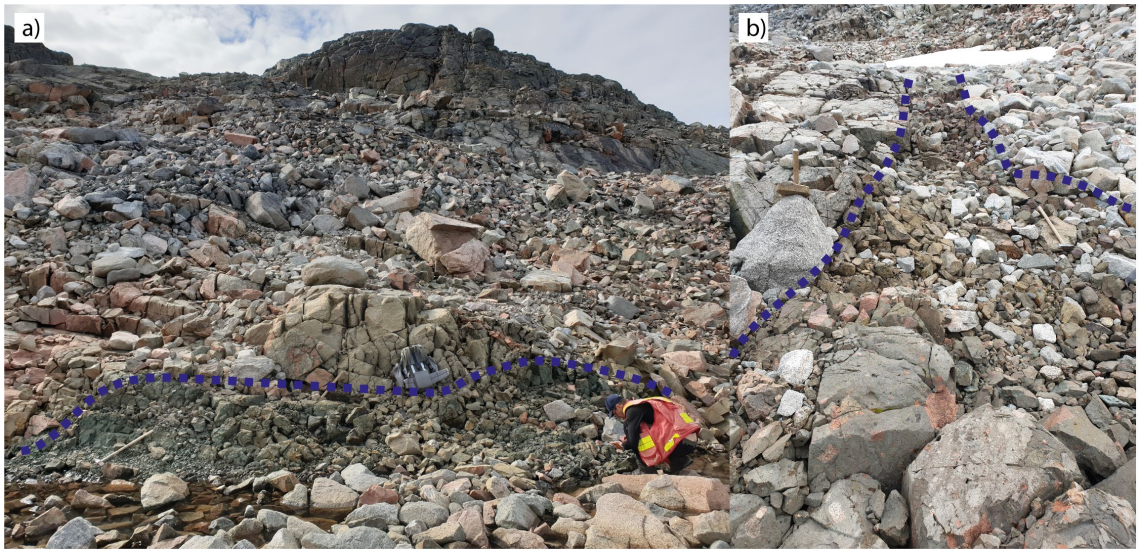

Figure 11. *Ultramafic lamprophyres. a) Contact between lamprophyre and host monzonite. b) subvertical lamprophyre dyke, note hammer for scale to the right.*

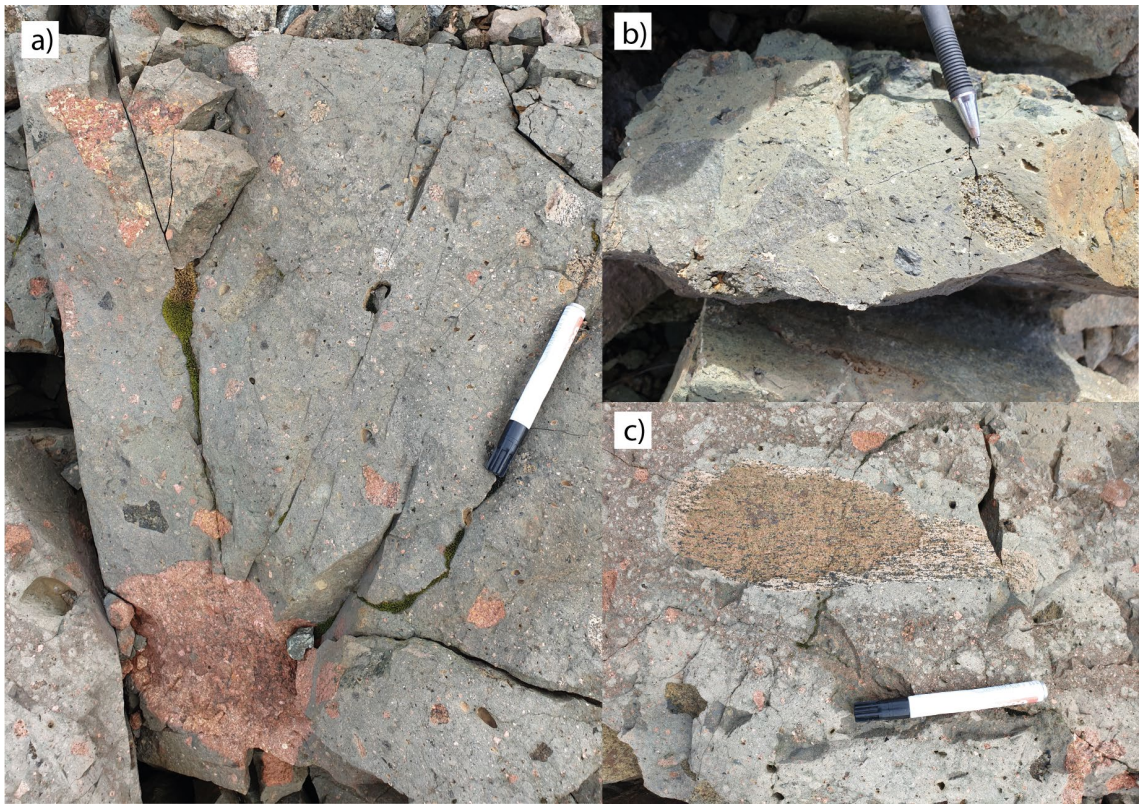

Figure 12. *Vesicular fine-grained lamprophyre with abundant crustal xenoliths.*

Ultramafic lamprophyre dyke on Illutalik island

The ultramafic lamprophyre occurring on the island of Illutalik near Narsaq was visited on 29th of August during a joint helicopter reconnaissance including all field participants (Fig. 13). The ultramafic lamprophyre is part of the Gardar igneous province in South Greenland and is significant due to the abundance of mantle-derived xenoliths it contains. The dyke is associated with shearing along the Tugtutôq lineament. The xenoliths are believed to originate from the lithospheric mantle, likely from depths greater than 60 km based on the observation of what has been interpreted as an altered garnet grain in a xenolith (Upton 1991).

A brief description of the lamprophyre dyke based on Upton (1991) is given below:

Host Rock: The host rock is an ultramafic lamprophyre, a part of the suite known from the Tugtutôq-Illímaussaq-Nunataq zone. It has undergone metamorphism, and its original mineral assemblage has largely been replaced by tremolite, chlorite, and magnetite.

Xenoliths: The intrusion contains an abundance of mantle xenoliths, which constitute over 50% of the rock's volume. These xenoliths are closely packed, primarily consisting of peridotites (possibly garnet-bearing – see above) and some glimmerites. The xenoliths fall into two main categories of which (1) was targeted for sampling:

- Pale-coloured xenoliths: These are thought to be former peridotite blocks now composed mostly of tremolite, with lesser chlorite, magnetite, and chrome-spinel.
- Glimmerite xenoliths: These are rich in phlogopite (>85%) and contain minor amounts of calcite, zircon, and sphene. They show similarities to the MARID (mica-amphibole-rutile-ilmenite-diopside) suite xenoliths known from kimberlite occurrences (Dawson & Smith 1977).

Metamorphism and Alteration: Both the host rock and the xenoliths have been extensively altered and recrystallised, with the original mineral assemblages replaced by secondary minerals due to hydrothermal processes. The host rock itself is mainly composed of tremolite and chlorite, with magnetite and hematite giving it a darker colour. The recrystallisation obscured much of the original magmatic texture, though the host rock is inferred to have originally been highly olivine-phyric.

Geochemical Evidence: The chemical composition of the host rock indicates it was a primitive, silica-poor ultramafic rock, likely feldspar-free. The rock is rich in Ni and Cr, supporting its primitive nature. Xenoliths show significant compositional changes due to metasomatic processes, with high contents of iron and calcium as well as trace elements like zirconium and rare earth elements.

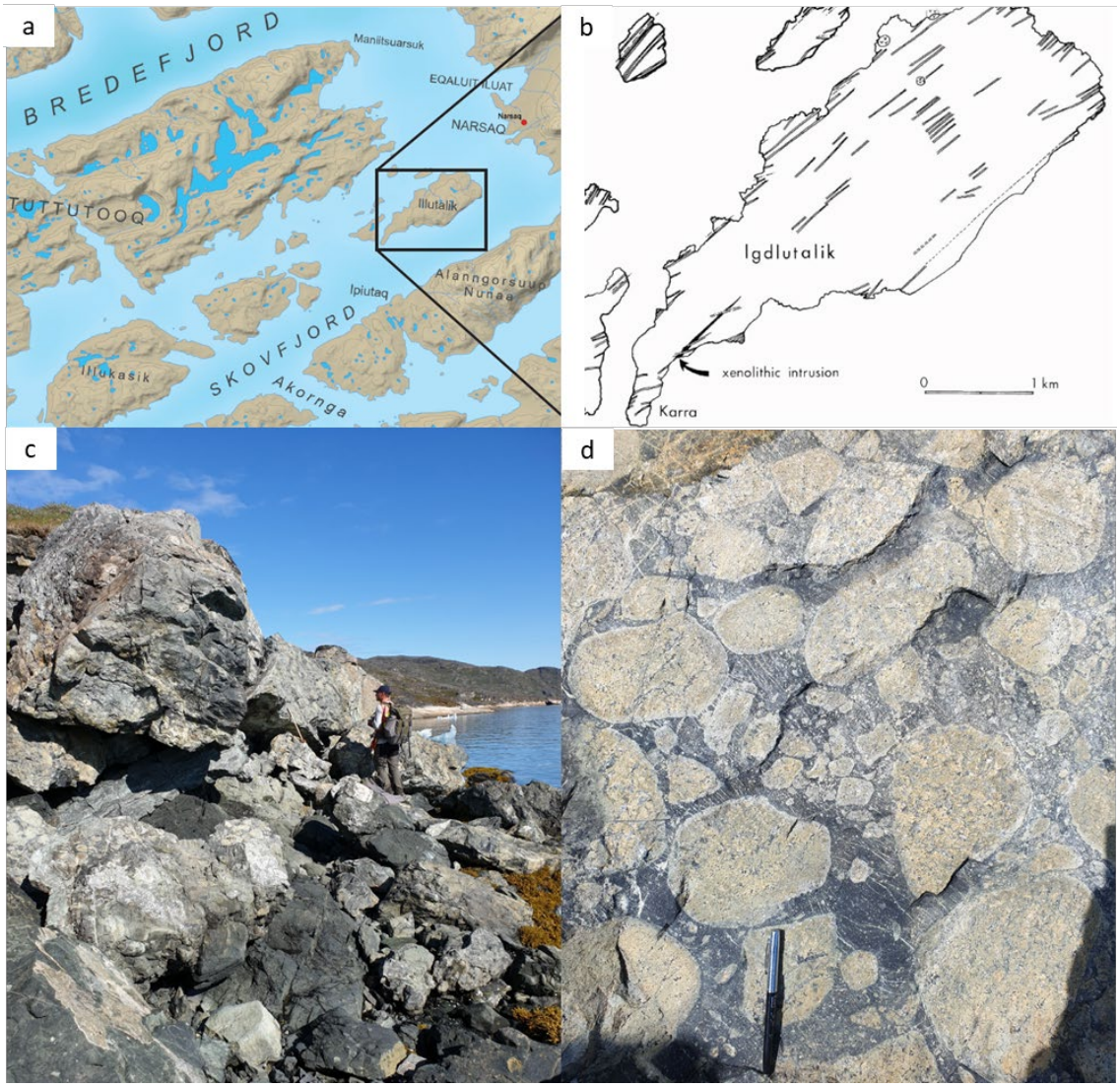

Figure 13. *(a) Map of Illutalik island situated southwest of Narsaq town; (b) Sketch map of Illutalik and the locality of the xenolith-bearing ultramafic lamprophyre; (c)-(d) Field photographs showing the coastal outcrop and a close-up of the ultramafic lamprophyre which is characterised by cm-dm-sized rounded xenoliths of pale (altered) mantle peridotite set in a dark matrix.*

Analytical work

Processing of stream sediment samples

The stream sediment samples were processed by SRC, Geoanalytical Laboratories Diamond Services in Saskatoon, Canada following the flowsheet in Figure 14. Here, samples were sieved to collect the size fractions 1.0 to 0.50 mm (+0.5 mm in the following) and 0.50 to 0.25 mm (+0.25 mm in the following). A two-stage density separation followed for both fractions (+0.5 mm and +0.25 mm), using firstly a dense media separator (cut point 2.7 g/cm^3) and a subsequent heavy liquid (cut point 3.23 g/cm^3). The resulting two size fractions of mineral grains heavier than 3.23 g/cm^3 were treated by magnetic separator to yield a magnetic fraction and a non-magnetic fraction. KIM's are usually picked from the latter, but as Mg-rich ilmenites sometime can have an altered outer rim containing magnetite (M. Morrison, pers. comm., July 2021) and thus become included in the magnetic fraction, these fractions were also sent to I.M. Morrison Lab for visual KIM identification. The procedures for KIM identification are outlined in Figure 14.

Optical microscopy and automated quantitative mineralogy analysis

Twentynine polished thin sections were made at Precision Petrographics Ltd. in Canada. Thin sections were investigated by optical microscopy at GEUS using a ZEISS Axioskop 40 equipped with an AxioCam MRc5 for photo documentation.

Samples were scanned in plane polarised light and cross-polarised light, coated with carbon and investigated with the ZEISS Sigma 300 VP field emission scanning electron microscope (SEM) at GEUS equipped with two Bruker Xflash 6|30 30 mm^2, 129 eV EDS detectors. Automated quantitative mineral mapping (AQM) on the samples were performed on the SEM at GEUS, using the Zeiss Mineralogic™ software platform. For Mineralogic™ analyses, the backscattered electron contrast (BSE) is applied to enhance the contrast between different mineral phases in the sample. During Mineralogic™ analysis, a mosaic of BSE frames of a representative part of the sample is taken. Each frame in the mosaic is thereafter analysed with Energy Dispersive X-ray Spectrometry (EDS) detectors in a grid with a user defined step-size of 5-20 µm between EDS analytical spots. The chemistry in each spot is interpreted as a mineral species and assigned a colour, which is then forming one pixel in the false-coloured mineral map. The classification of minerals is operator-based, where obtained mineral compositions are compared to known compositions in Deer et al. (1985) and the online databases www.webminerals.com and www.mineralienatlas.com. Some thin sections, especially those with few scheelite or cassiterite grains, or those with a range of minerals suitable for dating, were screened for suitable minerals with the Bright Phase Search routine. Here, the BSE greyscale values were darkened, such that only the densest phases could be selected by thresholding. Only these phases were mapped out with the Mineralogic™ software, ignoring all other minerals. EDS analyses, and thus also the Mineralogic™ method, cannot distinguish between mineral phases of the same chemistry (e.g., anatase and rutile),

between hydrous and anhydrous minerals of the same composition (e.g., goethite and magnetite). Further details on the software and applied method can be found in Keulen et al. (2020). Analyses were performed with acceleration voltages of 15kV, a 120 µm^2 aperture and an EDS throughput rate of 275-400 kcps/detector. The mineral maps shown in this study were made with a step size of 20 µm, unless indicated differently.

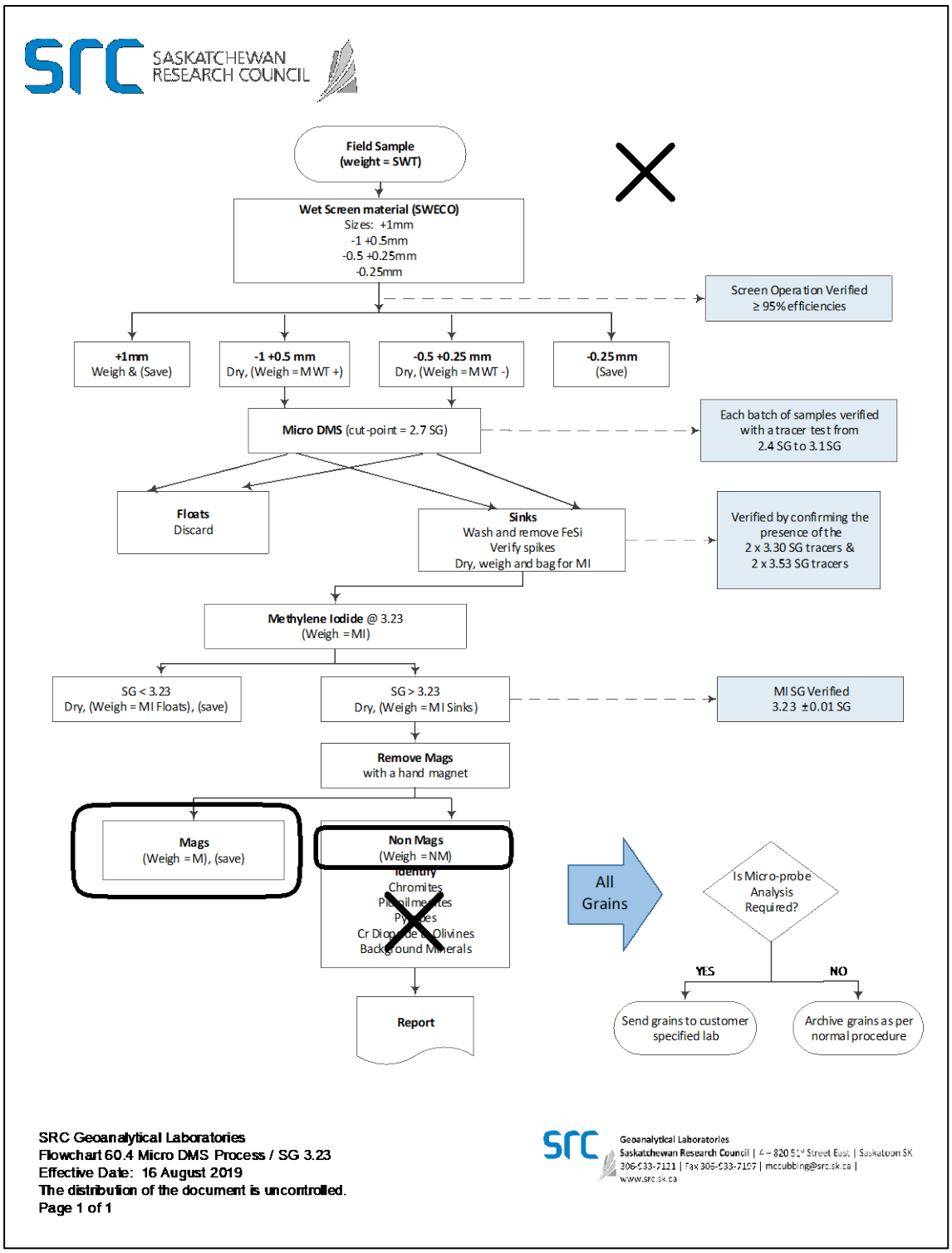

Figure 14. *SRC-flowsheet, documenting the processing of sediment samples using a variety of size screening and density and magnetic separation.*

SEM analyses of hand-picked KIM

As only relatively few KIM were picked from the selected field work samples, the grains have been analysed twice. First, the hand-picked KIM were analysed from the sticky tape on which the samples were delivered by SRC, by placing the entire cardboard and sticky tape on a holder into the SEM. As a result, in this procedure we analysed the outside of all grains.

Secondly, all grains were picked, mounted in epoxy and polished such that interior part of the grains was available for analysis. All grains were now reanalysed by SEM. Only 3 grains were lost in the picking and polishing process. A two-step procedure was implemented to secure data for all grains, in view of the potential risk of losing grains during casting and polishing.

For both runs, analyses were performed with acceleration voltages of 15kV, a 120 μm^2 aperture and an EDS throughput rate of 275-400 kcps/detector. The mineral maps shown in this study were made with a step size of 20 µm. It has been demonstrated previously that automated SEM analyses are a suitable alternative for electron microprobe analyses, with reasonable precision and a good accuracy (see Keulen et al. 2009).

Results

Optical microscopy

Seven samples analysed on the SEM by AQM (see below) were also investigated using standard optical microscopy (Appendix B). Figure 15 shows an example of a typical ultramafic lamprophyre sample from Johan Dahl Land (sample 591206, same locality as sample 591205, see Fig. 7-8) showing a porphyritic texture with intense alteration of the matrix into various clay minerals and partial alteration of the olivine megacrysts into serpentine.

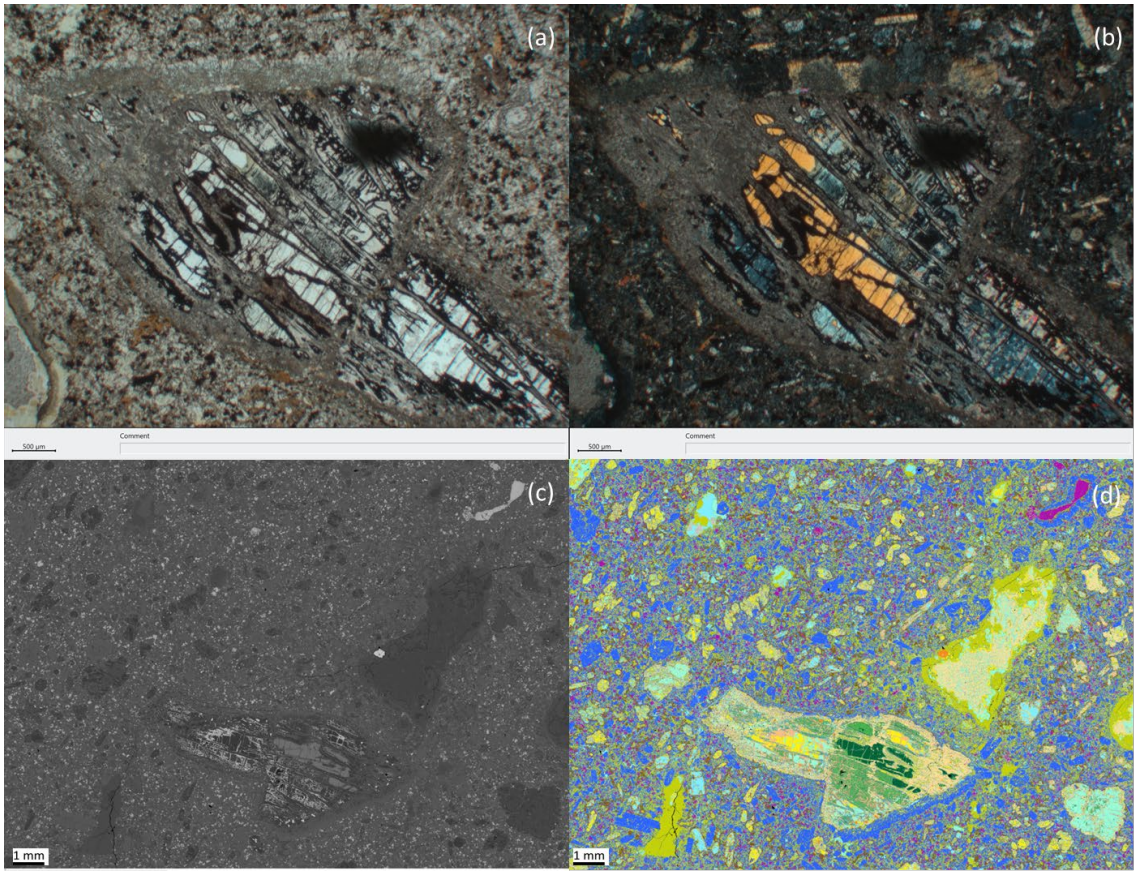

Figure 15. *Detail of ultramafic lamprophyre dyke (591206) viewed by (a-b) optical microscopy (PPL: plane polarised light, XPL: cross-polarised light), (c) back-scattered electron (BSE) imaging, (d) automated quantitative mineralogy (AQM) imaging (for colour code: see Appendix).*

Automated Quantitative Mineralogy maps

Automated Quantitative Mineralogy (AQM) maps for seven rock samples are given in the Appendix. An example of a AQM map is given in Figure 15.

SEM analyses of hand-picked KIM

The KIM samples returned after hand-picking were indicated by SRC as the following minerals: ilmenite, chromite, pyrope, olivine, zircon, chrome-diopside, sulphide, hematite, zircon, and a mineral abbreviated as ECL. In total, approximately 265 grains were picked (Table 1). SEM-EDS analyses of the same grains yielded chrome-spinel rather than chromite, almandine rather than pyrope garnet and diopside without chrome. The sulphide is chalcopyrite and the mineral abbreviated ECL is spessartine.

Table 1: *Summary of the SEM-EDS investigation of 265 hand-picked Kimberlite Indicator Minerals from stream sediment samples from Johan Dahl Land, listed per mineral and per sample. Results are for sample cores (polished grains).*

Sample #	Oli	Diop	Gar (Alm)	Gar (Sps)	Ilm	Epi	Zir	Chp	Bio	Sid	Cr-sp
524501	3	2			5	2					
524502		2			2						
524503		2	1		2						
524504		1									
524505		4			4						
524506	10			1	4		22				
524508a					1			2	1	4	
524508b					17			1			
524510a		1			2			16			
524510b	6				1						
524511	23					1					
591201			1		16						1
591203		1			4					2	
591204	1	1			6						
591211	15	1			11						
591213	54	1			7						
Sum	**112**	**16**	**2**	**1**	**82**	**3**	**22**	**19**	**1**	**6**	**1**

Oli: olivine, Diop: diopside; Gar: garnet; Alm: almandine; Sps: Spessartine; Ilm: ilmenite; Epi: epidote; Zir: zircon; Chp: chalcopyrite; Bio: biotite; Sid: siderite; Cr-sp: chrome-spinel.

The three garnet grains, including spessartine, were classified following the schedule of Grütter et al. (2004); they all plotted in garnet group G0 (non-kimberlitic), see Figure 16.

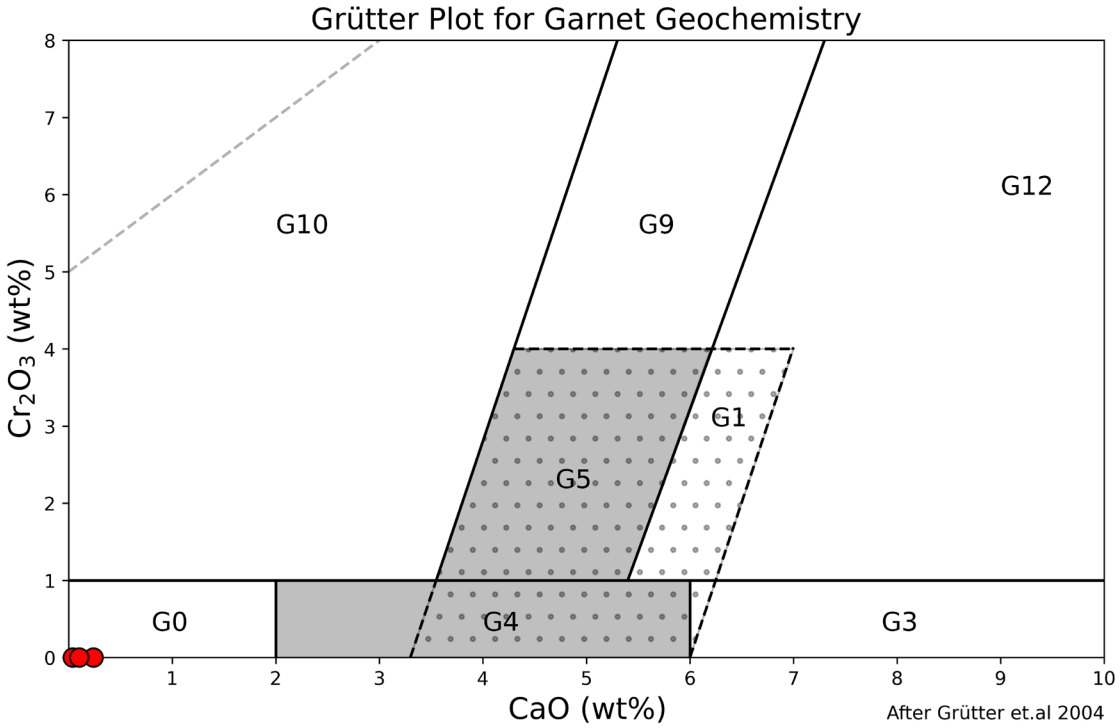

Figure 16. *Garnet classification diagram for potentially kimberlitic garnets, after Grütter et al. (2004). The studied garnets (red dots) all plot in the G0 (non-kimberlitic) field.*

The Mg-number for olivine was determined from the average of the KIMs (in cross-section) and plotted as an average per sample (Fig. 17). To better compare to EMP analyses (where spot analyses in the core of the grain are made), the highest value in the core of each olivine grain was listed and plotted additionally (Fig. 17). This yields higher Mg-numbers.

Ilmenite grains were plotted in the same manner, both as the average of the ilmenite grain in cross-section, and by manually reading off the values in the core of the grain (Fig. 18). The ilmenite contains ca. 55 wt.% TiO_2, with only little MgO on average, and the highest MgO values found in the core of the grain. All grains plot below the kimberlitic MgO concentration (after Wyatt et al. 2004).

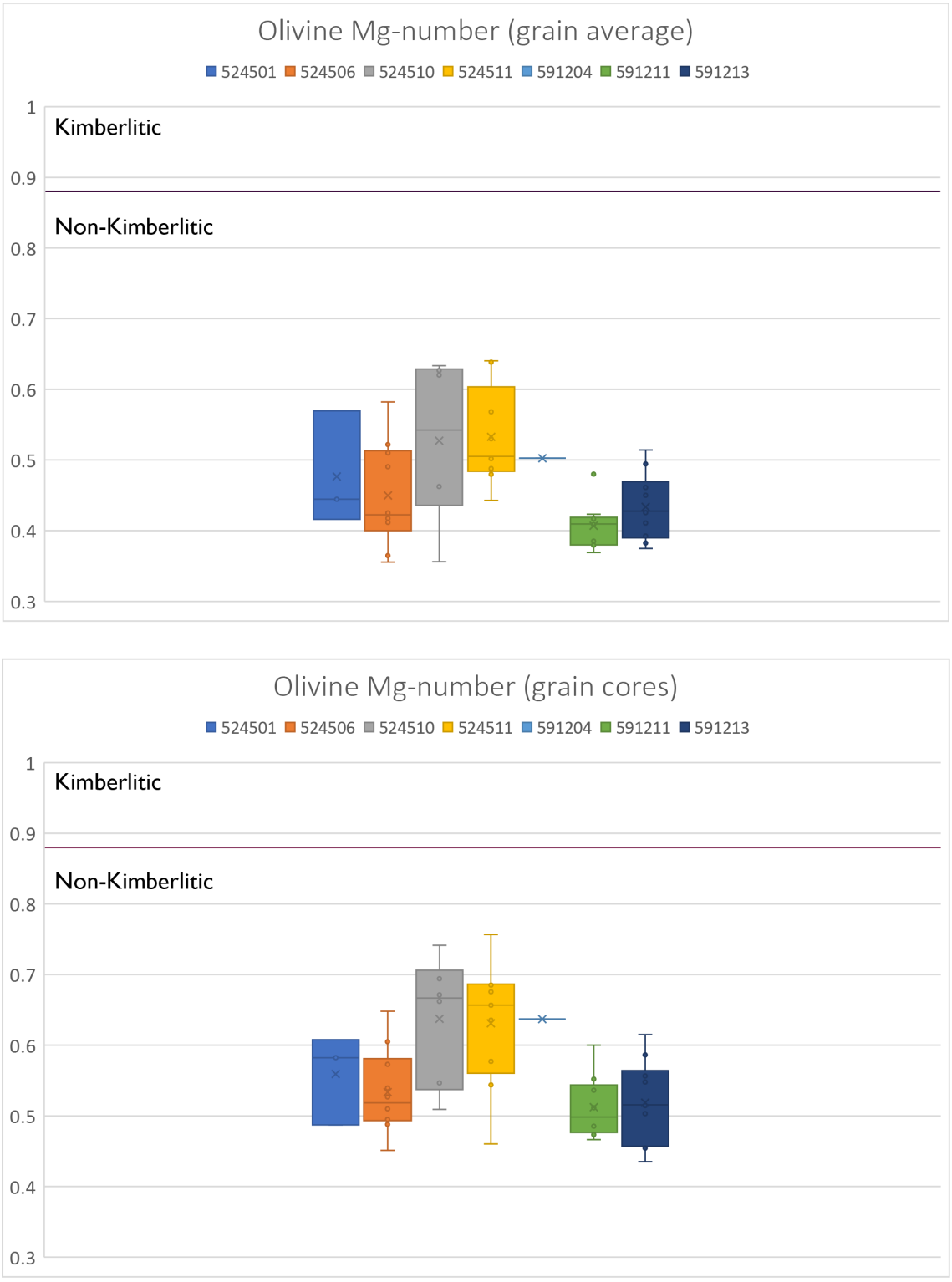

Figure 17. *Olivine Mg-number for grain averages (top) and grain cores (bottom) of hand-picked olivine grains.*

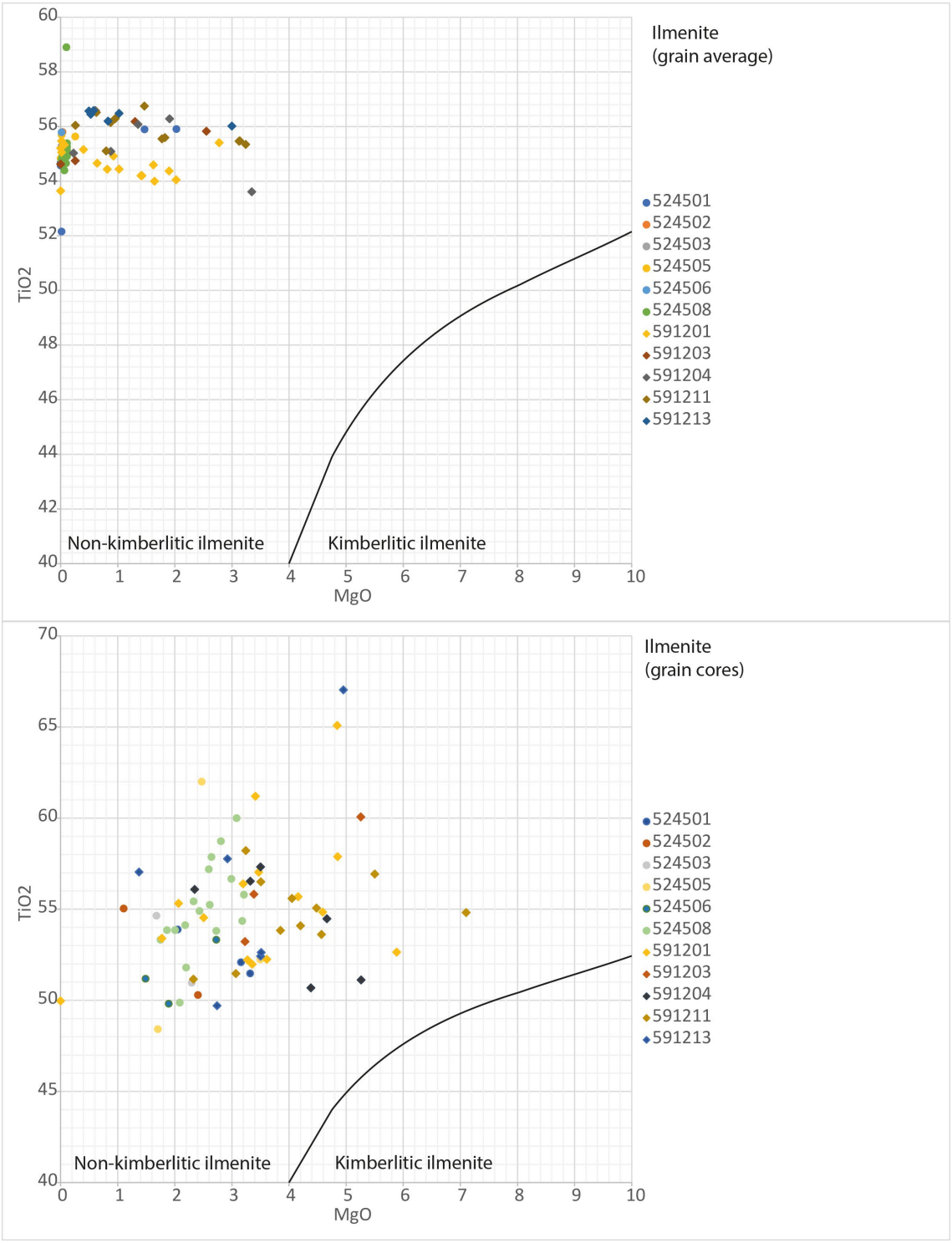

Figure 18. *Ilmenite MgO vs TiO_2 concentrations for grain averages (top) and grain cores (bottom) of hand-picked ilmenite grains. Line indicating boundary between kimberlitic and non-kimberlitic grains after Wyatt et al. (2004).*

Discussion

The potential for diamond occurrences in South Greenland, and specifically Johan Dahl Land, is supported by favourable geological conditions and evidence from previous exploration. However, challenges in identifying primary diamond-hosting sources have highlighted the need for targeted investigations. The present study has tried to address this need but was unsuccessful in finding new evidence in favour of the diamond prospectivity.

Although much of the direct evidence for diamondiferous material comes from West Greenland, such as the Qeqertaa lamprophyre dyke, where highly refractory cratonic mantle extends into the diamond stability field, similar geological processes could be present in South Greenland. In West Greenland, mantle compositions featuring high Mg# olivine, Cr-rich spinel, and garnet inclusions demonstrate conditions favourable for diamond formation and preservation.

Additionally, micro- and macro-diamonds recovered from lamprophyric intrusions in West Greenland further confirm the potential for diamondiferous materials in cratonic settings. While South Greenland lacks direct discoveries of this type, the tectonic environment and lithospheric characteristics suggest that similar opportunities may exist.

Despite these encouraging indicators, exploration efforts in South Greenland have faced limitations. The 1995 exploration report from the Narsarsuaq area noted difficulties in confirming primary diamond-hosting sources, such as lamprophyric intrusions. Although some geophysical anomalies and heavy mineral samples showed promise, no definitive diamondiferous intrusions have been identified. Without such sources, the economic viability of diamond mining remains uncertain.

Furthermore, large portions of South Greenland remain underexplored. Existing data only cover limited areas, leaving significant gaps in understanding the region's diamond potential. Systematic exploration, including advanced geophysical surveys and targeted heavy mineral sampling, is essential to refine exploration targets.

Conclusions

The results presented in this report do not confirm previous positive findings in the target area (Johan Dahl Land, South Greenland) in terms of its diamond prospectivity. It is important to state that this does not exclude remaining diamond potential as several factors could explain why the present study did not find any diamond-indicator minerals: (1) The number of indicator mineral grains found in the 1990's sampling is quite small compared to other parts of Greenland so could potentially be missed by the 2021 sampling; (2) The investigated area is rather small; by including a larger target area (hence hinterland) would enhance the potential for finding diamond-indicator minerals; (3) The degree of alteration in the rock samples is significant and indicator minerals (also in the sediments) could have been altered and therefore overlooked in the chemical screening.

While most direct evidence for diamonds in Greenland comes from West Greenland, South Greenland's tectonic setting and geological history suggest a promising but relatively underexplored potential. The discovery of ultramafic lamprophyres in several places in Johan Dahl Land, albeit generally strongly altered, demonstrates that potentially diamondiferous magmatic activity has occurred in the region. Future exploration efforts should prioritize the identification of primary sources, such as lamprophyre or kimberlite intrusions, to assess the region's economic viability for diamond mining. Despite current challenges, the combination of favourable geological settings and the broader context of diamond discoveries in Greenland highlights South Greenland as a region warranting further investigation.

Based on the above we therefore conclude that additional detailed work in South Greenland, including Johan Dahl Land, is still warranted to further characterize the true diamond potential in this part of Greenland.

References

Andersen, T. 2008: Coexisting silicate and carbonatitic magmas in the Qassiarsuk complex, Gardar Rift, Southwest Greenland. *The Canadian Mineralogist* **46**, 933-950. https://doi.org/10.3749/canmin.46.4.933

Bartels, A. & Kokfelt, T.F. 2014: Field investigations of carbonatitic - alkaline – silicic intrusive rocks near Qorlortoq, Qassiarsuk area, South Greenland. *Danmarks og Grønlands Geologiske Undersøgelse Rapport* **2014/63**, 27 pp. https://doi.org/10.22008/gpub/30631

Bernstein, S., Szilas, K. & Kelemen, P.B. 2013: Highly depleted cratonic mantle in West Greenland extending into diamond stability field in the Proterozoic. *Lithos* **168-169**, 160-172. https://doi.org/10.1016/j.lithos.2013.02.011

Dawson, J.B. & Smith, J.V. 1977: The MADRID (mica-amphibole-rutile-ilmenite-diopside suite of xenoliths in kimberlite. *Geochimica et Cosmochimica Acta* **41**, 409-323. 10.1016/0016-7037(77)90239-3

Deer, W.A., Howie, R.A. & Zussman, J. 1985: An introduction to the rock-forming minerals. Longman Group Ltd., Essex, England, 528p.

Grütter, H.S., Gurney, J.J., Menzies, A.H. & Winter, F. 2004: An updated classification scheme for mantle-derived garnet, for use by diamond explorers. *Lithos* **77**, 841–857. https://doi.org/10.1016/j.lithos.2004.04.012

Hutchison M.T. 2022: Diamond Exploration and Prospectivity of Greenland. Govt Greenland Dept. Geol. Record, vol 1, 228 pp. GEUS Dataverse. https://doi.org/10.22008/FK2/HMLDVH

Keulen, N., Frei D. & Hutchison, M. 2009: Computer-controlled scanning electron microscopy: A fast and reliable tool for diamond prospecting. *Journal of Geochemical Exploration*, **103**, 1-5. https://doi.org/10.1016/j.gexplo.2009.04.001

Keulen, N., Malkki, S.N. & Graham S. 2020: Automated Quantitative Mineralogy Applied to Metamorphic Rocks. *Minerals* **10**, 47, 29pp. https://doi.org/10.3390/min10010047

Major General Resources, 1997: Major General Resources LTD. Report on 19956 exploration activities: Narsarsuaq licence area (licence 22/95). p. 1-95. *GEUS Report File* **21512**.

Mitchell, R.H., 1995: Kimberlites, Orangeites and Related Rocks. Plenum, New York. 410 pp.

Quadrant Resources, 1996: Quadrant Resources PTY LTD and Major General Resources LTD – Gardar project. Report on the 1995 exploration activities in the Narsarsuaq licence area. p. 1-56. *GEUS Report File* **21433**.

Stewart, J.W. 1970: Precambrian alkaline-ultramafic/carbonatite volcanism at Qagssiarssuk, South Greenland. *GGU Bulletin*, **84**. pp 84. https://tidsskrift.dk/meddrgroenland/article/view/152175

Upton, B.G.J., 1991: Gardar mantle xenoliths: Igdlutalik, South Greenland. *GGU Report* **150**. 37-43. https://doi.org/10.34194/rapggu.v150.8139

Walton, B.J., 1965: Sanerutian appinitic rocks and Gardar dykes and diatremes, North of Narssarssuaq, South Greenland. *GGU Bulletin*, **57**. pp 66. https://tidsskrift.dk/meddrgroenland/article/view/155280

Wyatt, B.A., Baumgartner, M., Anckar, E., Grütter, H., 2004: Compositional classification of “kimberlitic” and “non-kimberlitic” ilmenite. *Lithos* **77**, 819–840. https://doi.org/10.1016/j.lithos.2004.04.025

Appendices

Appendix A. Sample table and sample maps

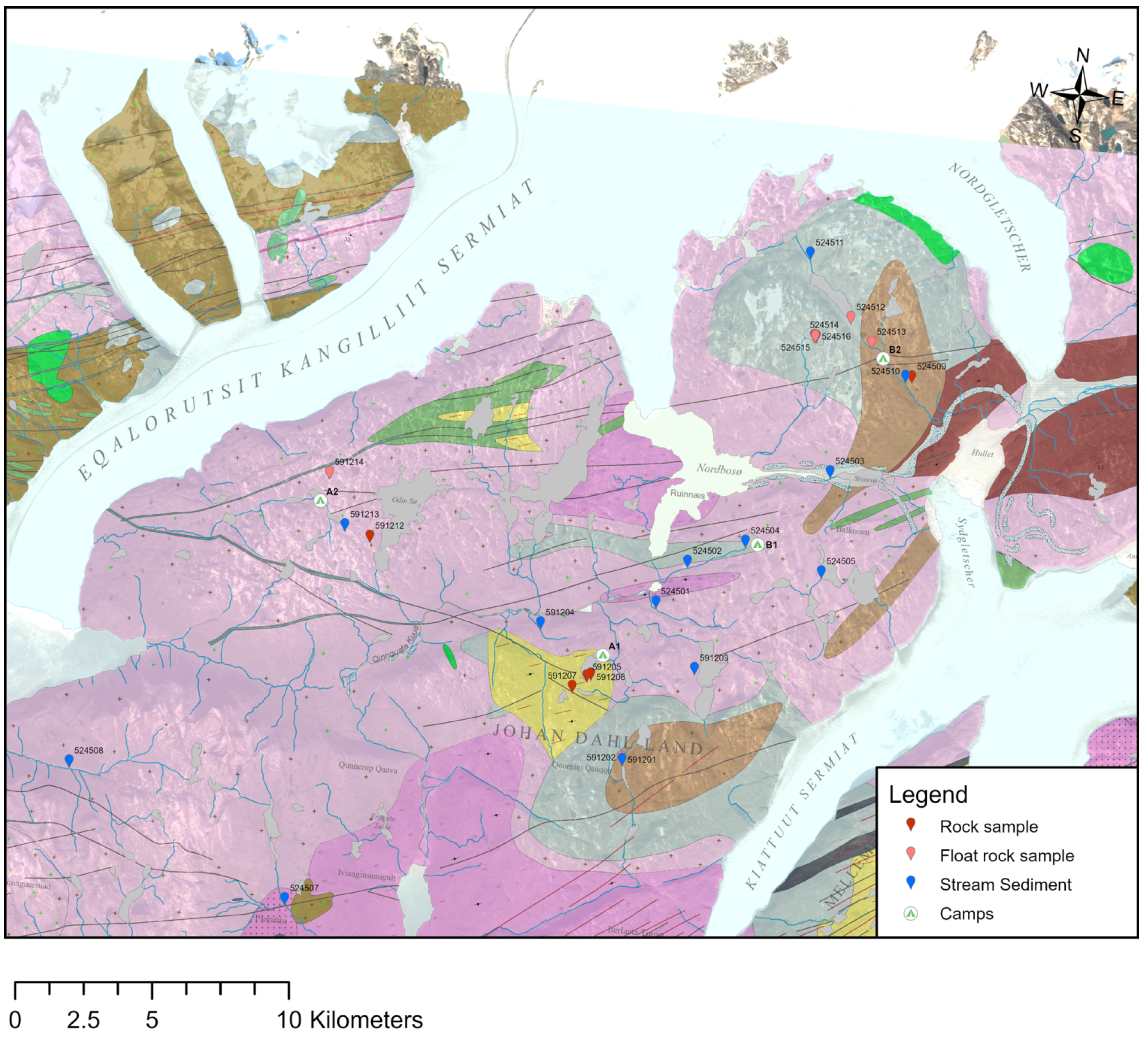

Figure A1. *Map showing the distribution of field camps (A1, A2 and B1, B2) and rock + stream sediment samples collected.*

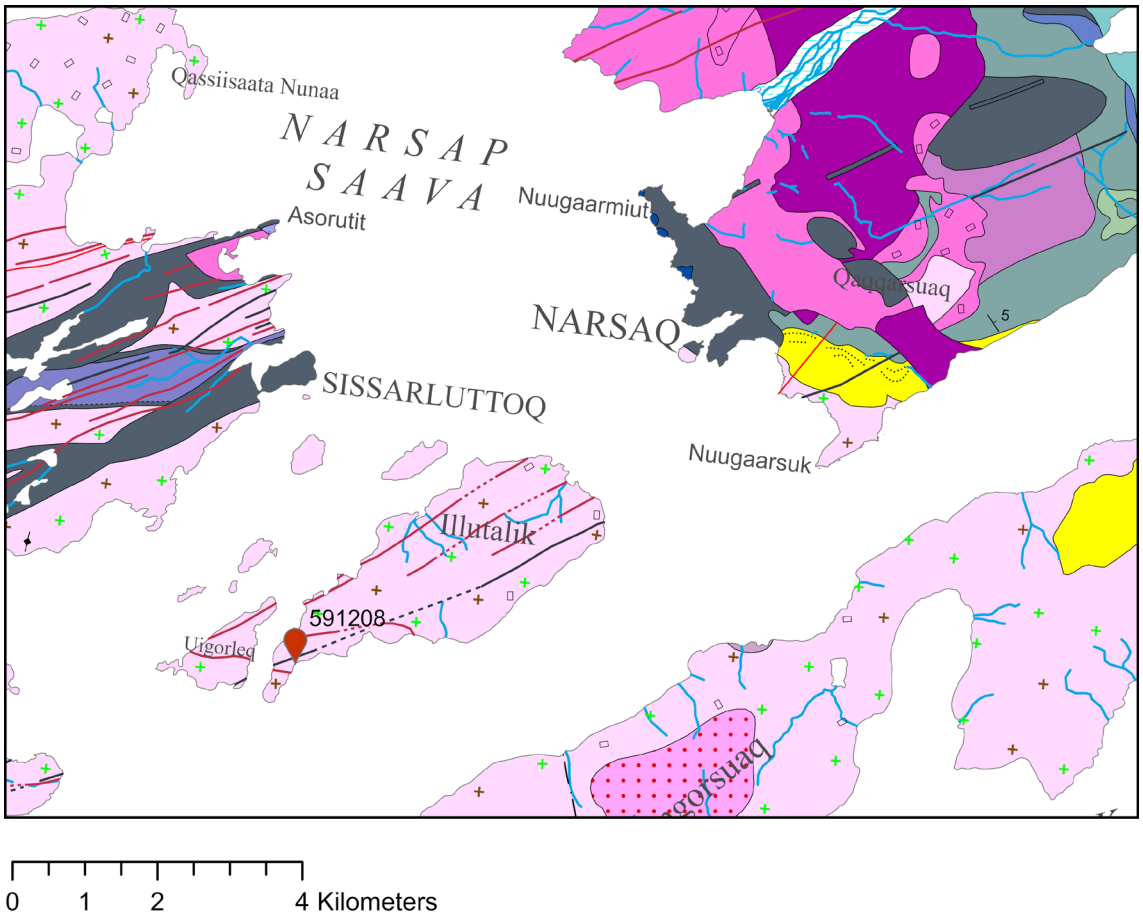

Figure A2. *Map showing the position of rock sample (591208) collected on Illutalik during a reco to the island on August 29.*

Table A1: Sample list of stream sediment samples (14) and rock samples (14) collected in South Greenland in 2021 by GEUS/MMR.

GeusNo	Collector*	Latitude	Longitude	Elevation	SampleType	Notes	InsertDate
591201	SB+AJN	61.28474	-45.37766	953	Stream Sediment	At stream entering lake.	24/08/2021 16:40
591202	SB+AJN	61.28544	-45.37846	946	Float rock sample	Lamprophyre with olivine megacrysts?	24/08/2021 17:21
591203	SB+AJN	61.31669	-45.33460	957	Stream Sediment	Near Heavy Mineral Concentrate 2.	25/08/2021 16:07
591204	SB+AJN	61.32661	-45.44210	592	Stream Sediment	Bed sediments.	26/08/2021 16:16
591205	SB+AJN	61.31087	-45.40715	877	Rock sample	Mafic dyke w 1-5mm oxide crysts, subcrop in scree.	27/08/2021 16:54
591206	SB+AJN	61.31156	-45.40456	916	Rock sample	Ultramafic lamprophyre -as 591205.	27/08/2021 17:51
591207	SB+AJN	61.30691	-45.41633	926	Rock sample	Thin 20cm wide ultramafic lamprophyre. No inclusions seen.	28/08/2021 14:24
591208	SB+AJN	60.86198	-46.15131	42	Rock sample	Ilutalik island, ultramafic lamprophyre w xenoliths.	29/08/2021 15:32
591209	SB+AJN	61.19767	-45.74260	328	Rock sample	0,5m thick dyke near stream sediment sample.	29/08/2021 18:05
591212	SB+AJN	61.34929	-45.56370	998	Rock sample	0.3m thick ultramafic lamprophyre.	01/09/2021 13:40
591213	SB+AJN	61.35221	-45.58148	944	Stream Sediment	Small stream entering lake.	01/09/2021 17:19
591214	SB+AJN	61.36872	-45.59547	929	Float rock sample	ca 1 m thick alkaline dyke.	02/09/2021 16:39
524501	JKK+DRO	61.33715	-45.36518	763	Stream Sediment	Stream sediment sample rich in pyroxene and qtz+fsp. Some magnetite possibly a few olivines. Sample taken ca 200m SW of 21433 Heavy Mineral Concentrate 5. Sampled over 40-50m.	24/08/2021 18:28
524502	JKK+DRO	61.35138	-45.34640	726	Stream Sediment	Sample taken predominantly from beach spot but also along 40m around this area on the SE side of the river. Sample quite felsic but some green minerals Cr-diopside? Observed.	25/08/2021 15:13
524503	JKK+DRO	61.38510	-45.25539	708	Stream Sediment	Very silty or fine grained sample, difficult to get enough coarse sandy material due to low energy and slow running water.	26/08/2021 11:53
524504	JKK+DRO	61.35980	-45.30843	883	Stream Sediment	Stream sediment sample from braided stream close to run off from lake, sandy with some silt.	27/08/2021 09:54
524505	JKK+DRO	61.35218	-45.25486	958	Stream Sediment	1.order stream connecting two lakes. Difficult to find material for sampling in running water. Sample from small designated bank spot close to where the stream runs in to lake.	28/08/2021 12:12
524506	JKK+DRO	61.19710	-45.74313	323	Stream Sediment	Powerful creek with small waterfalls. Much sandy material to sample.	29/08/2021 13:41
524507	JKK+DRO	61.22840	-45.59664	461	Stream Sediment	Meandering river after fork where two creeks meet. Sampled from rocky and sandy bank.	29/08/2021 14:39
524508	JKK+DRO	61.26603	-45.75196	286	Stream Sediment	Ravine with fast running water many boulders and sandy sediment.	29/08/2021 15:34
524509	JKK+DRO	61.41856	-45.20596	1033	Rock sample	Lamprophyre fgr brown homogeneous, small pico-ilmenite crystals, 30 cm wide at sampling spot. Subvertical strike 34.	30/08/2021 09:26
524510	JKK+DRO	61.41853	-45.21040	1003	Stream Sediment	Fast flowing stream sample at the point where creek flows into steep gully. Sampled over 50 m on the western bank.	30/08/2021 14:09
524511	JKK+DRO	61.45576	-45.28320	1061	Stream Sediment	Sampled downstream just after fork of two smaller streams. Relatively fast flowing creek.	01/09/2021 11:06
524512	JKK+DRO	61.43599	-45.25135	1098	Float rock sample	Float sample lamprophyre?	01/09/2021 12:41
524513	JKK+DRO	61.42856	-45.23560	1071	Float rock sample	Vuggy float sample, mafic. Possible lamprophyre?	01/09/2021 13:08
524514	JKK+DRO	61.42896	-45.27492	1200	Rock sample	Lamprophyre dyke with abundant crustal xenoliths some peridotite nodules?	02/09/2021 10:59
524515	JKK+DRO	61.42873	-45.27431	1198	Float rock sample	Float of lamprophyre.	01/01/2018 15:57
524516	JKK+DRO	61.42883	-45.27372	1208	Rock sample	Lamprophyre dyke.	27/01/2018 13:50

*SB: Stefan Bernstein; ANJ: Anette Juul-Nielsen; JKK: Jakob Kløve Keiding; DRO: Diogo Rosa

Appendix B. Sample documentation by optical microscopy and Automated Quantitative Mineralogy (AQM) maps

524512: Float sample of ultramafic lamprohyre, vuggy texture, calcite-altered

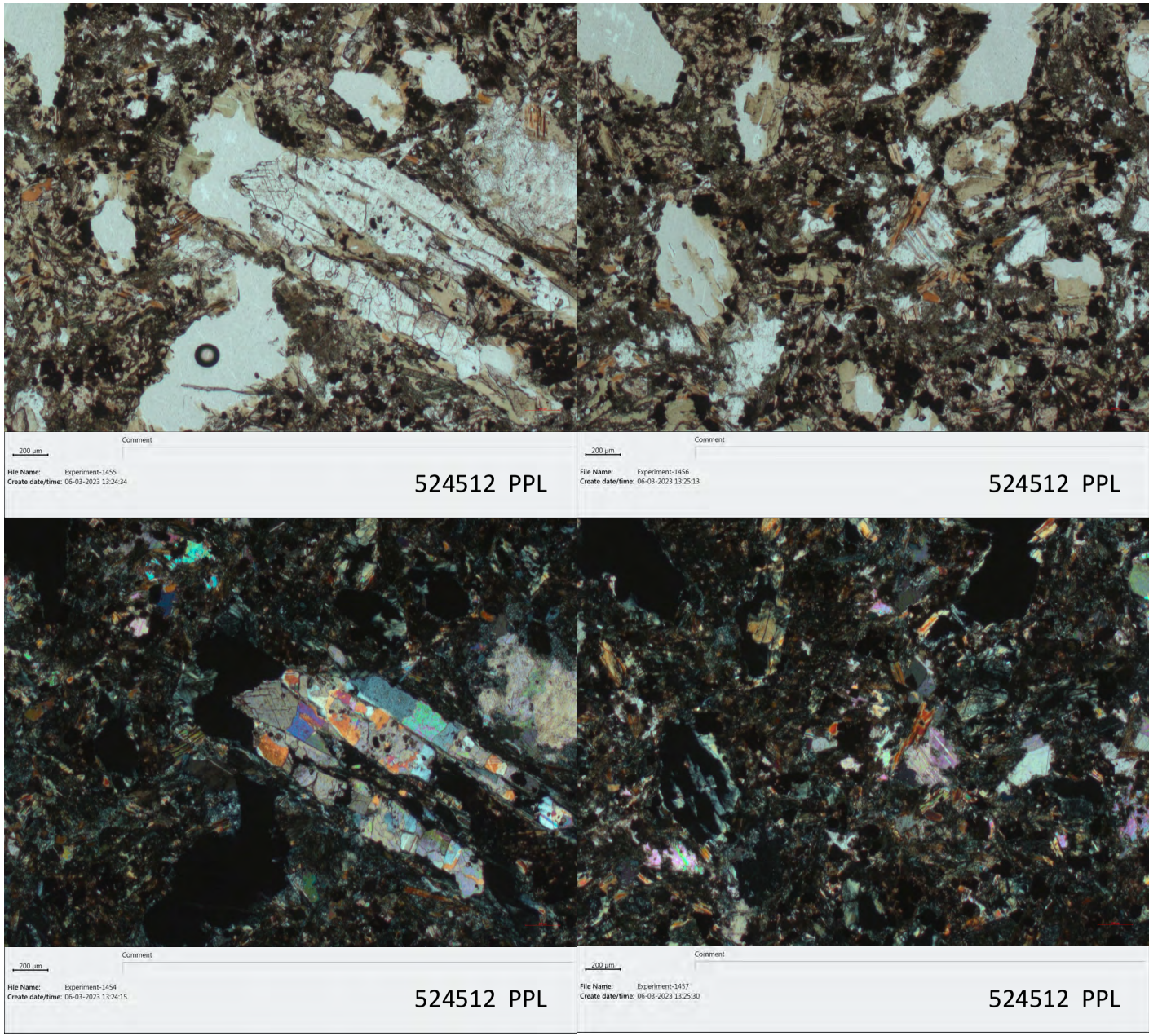

524512: Float sample of ultramafic lamprohyre

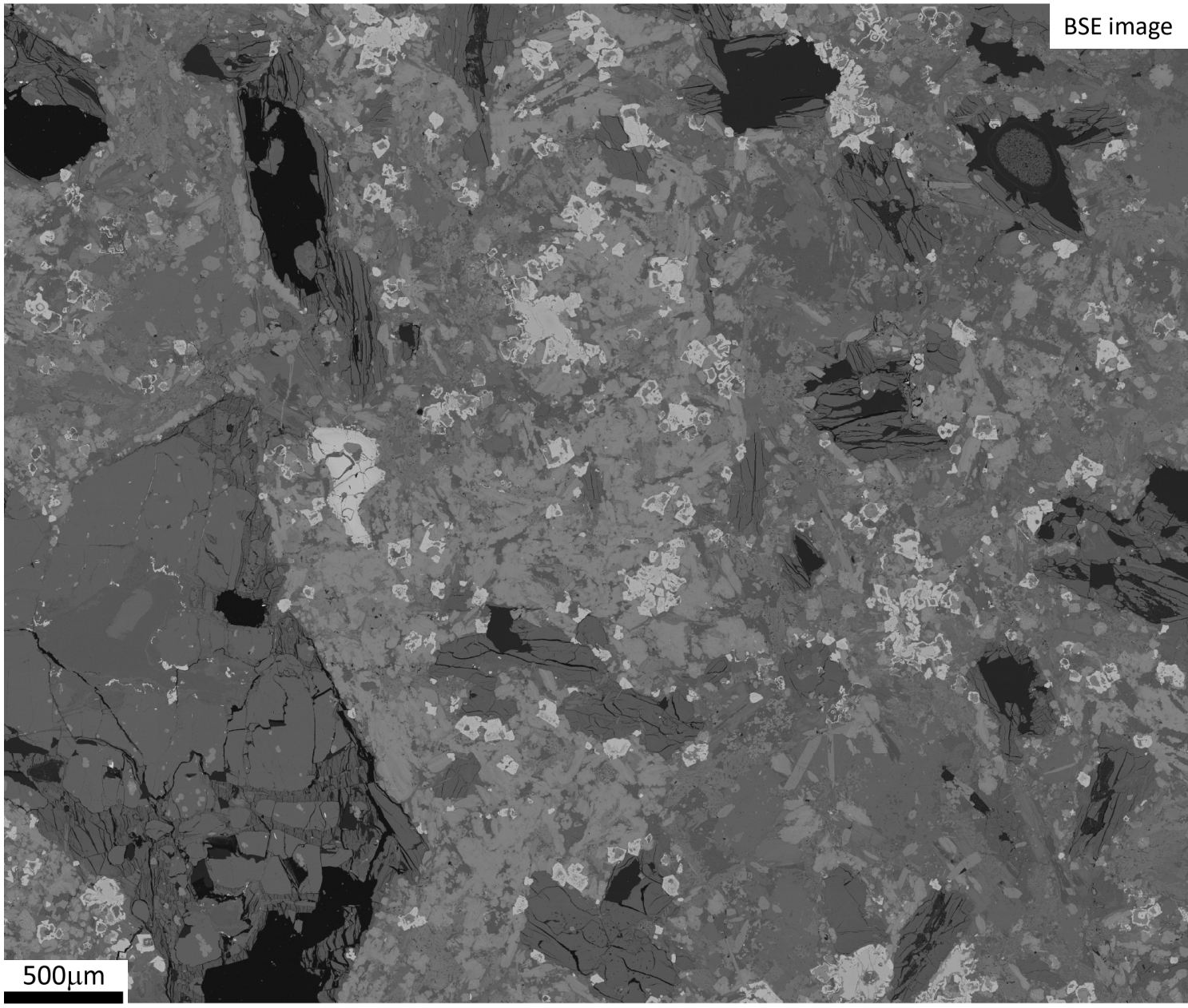

524512: Float sample of ultramafic lamprohyre

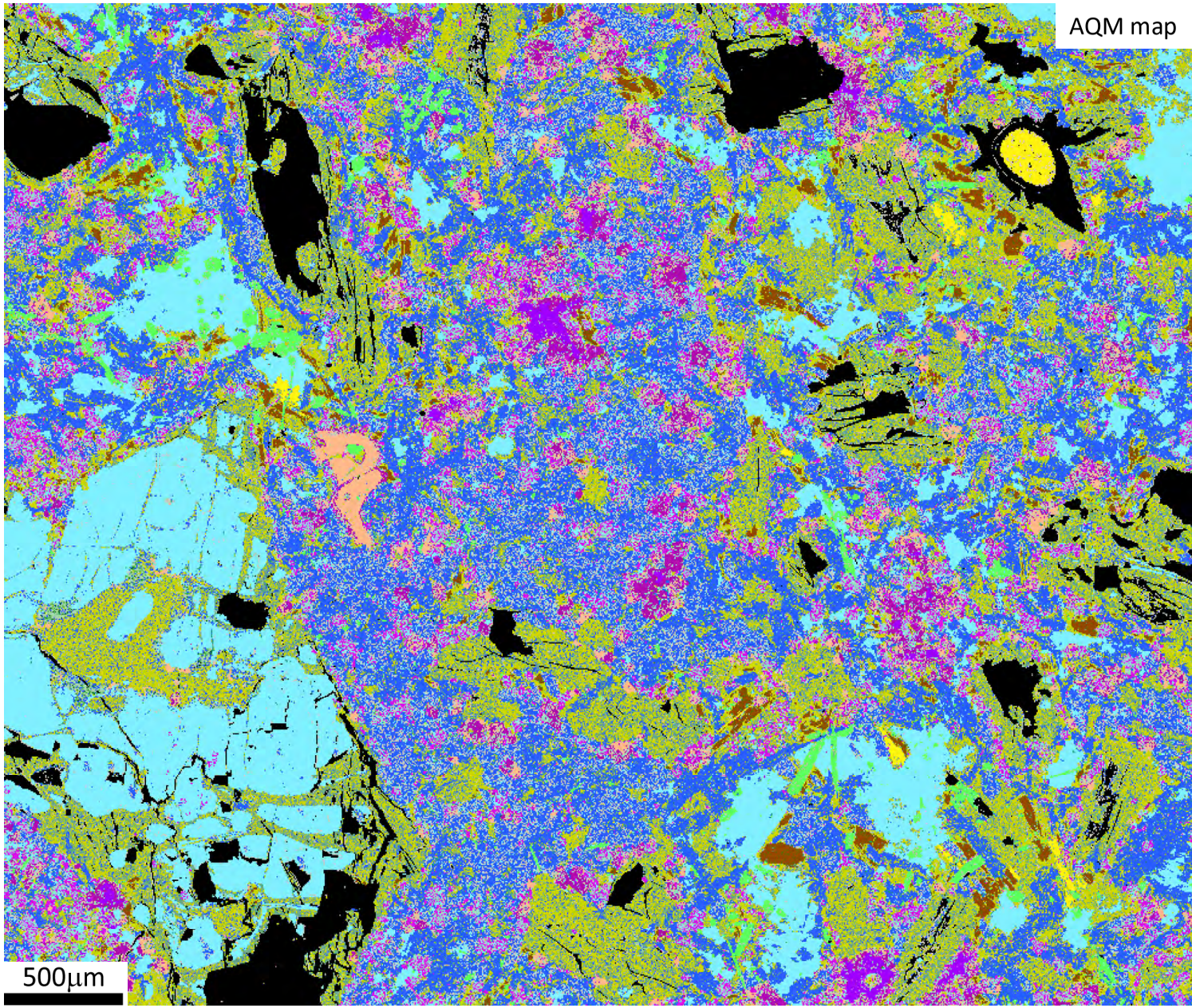

524514: Lamprophyre body with crustal xenoliths

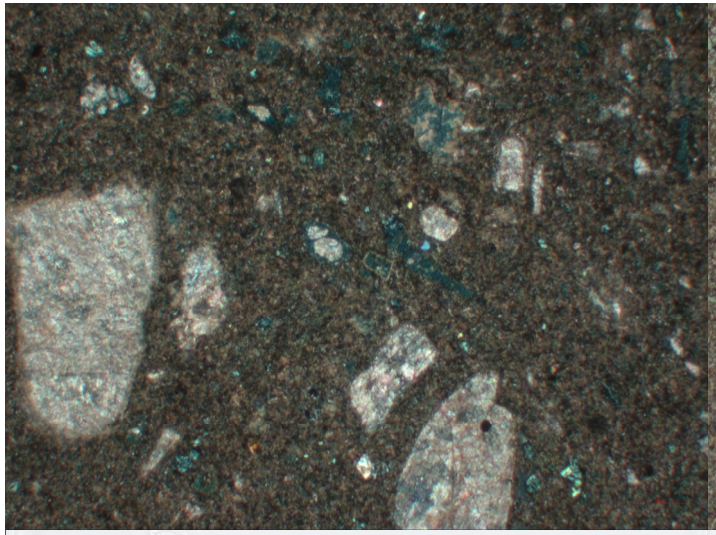

524514-02 XPL

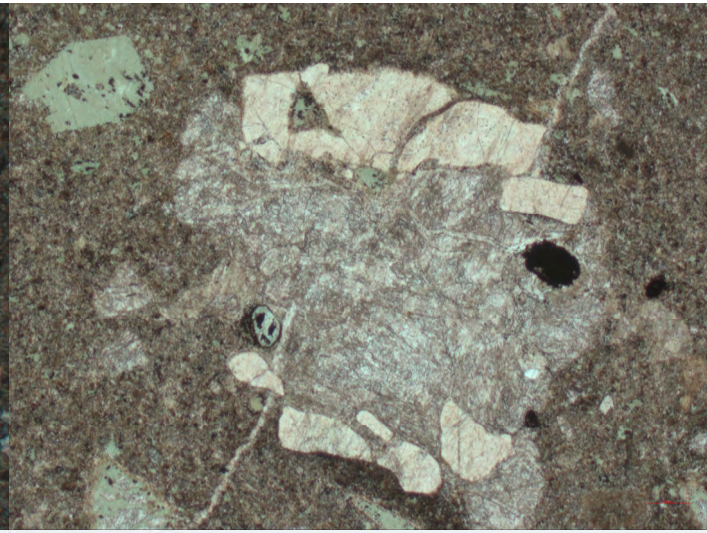

524514-01 PPL

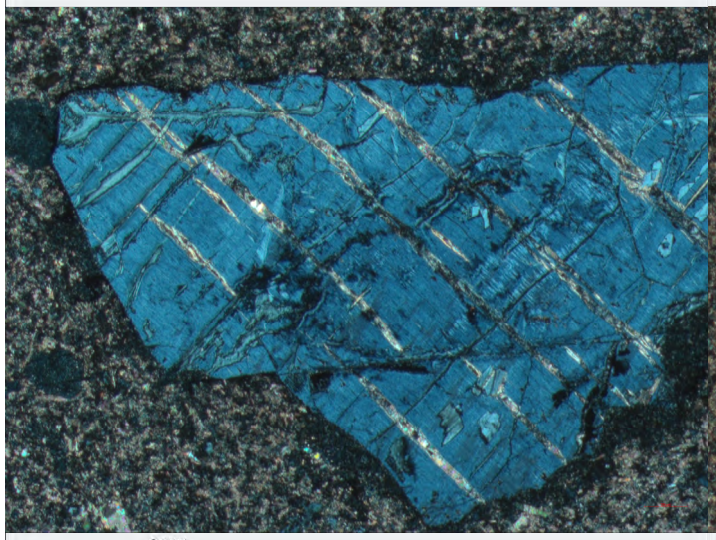

524514-04 XPL

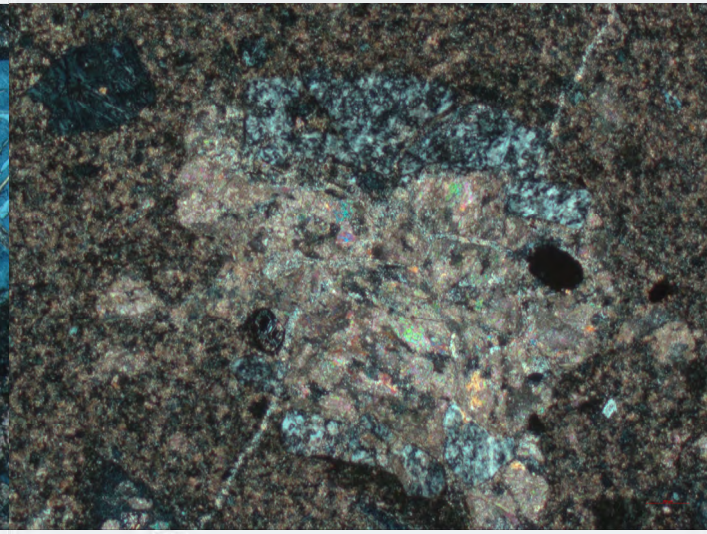

524514-01 XPL

524514_01: Lamprophyre body with crustal xenoliths

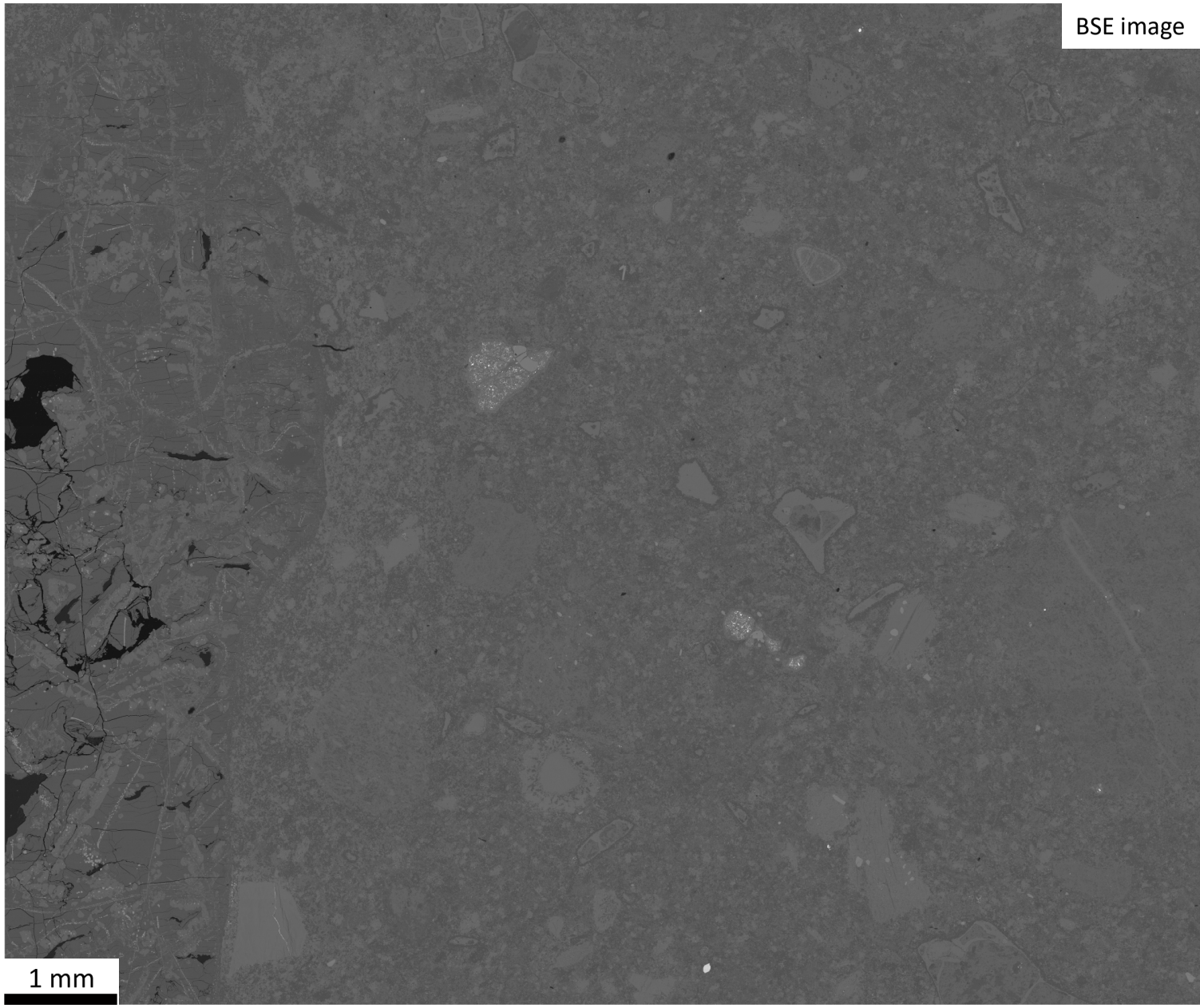

524514_01: Lamprophyre body with crustal xenoliths

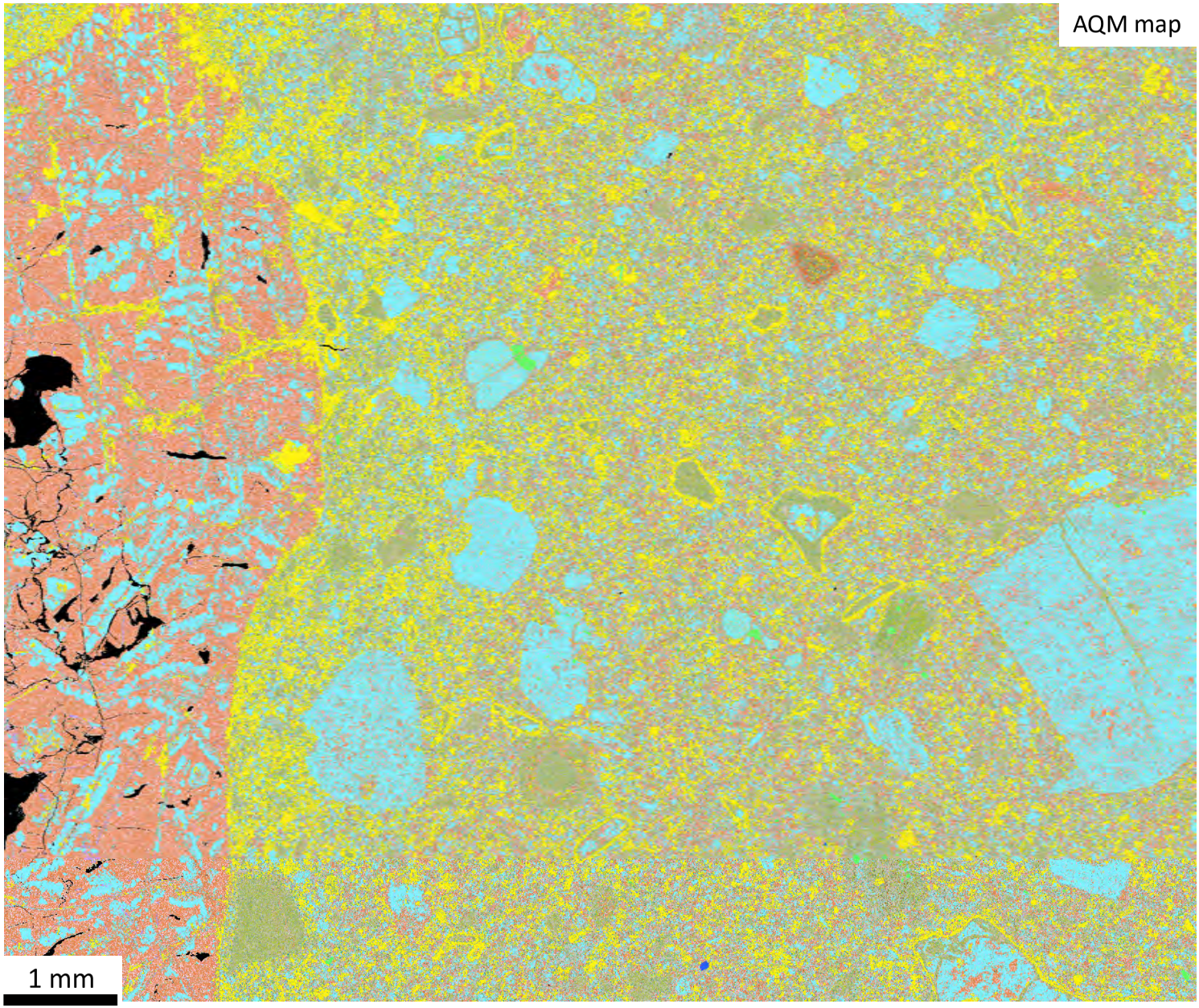

524514_02: Lamprophyre body with crustal xenoliths

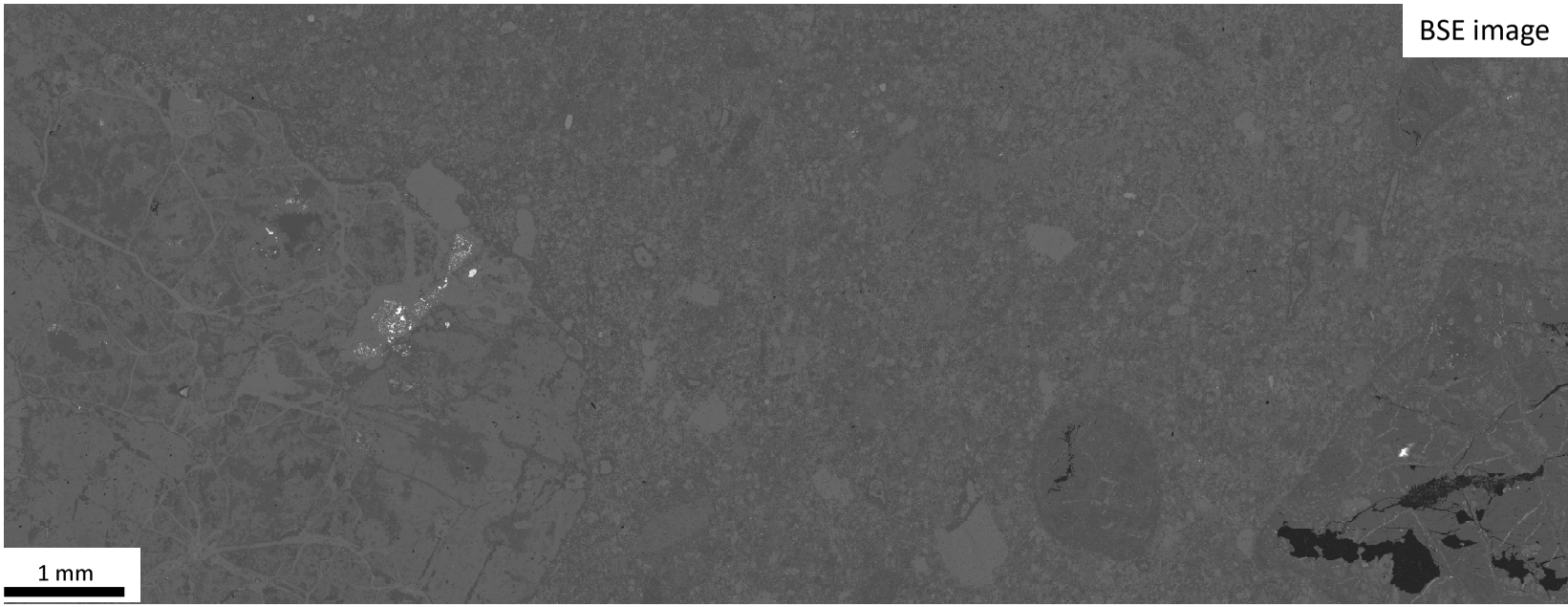

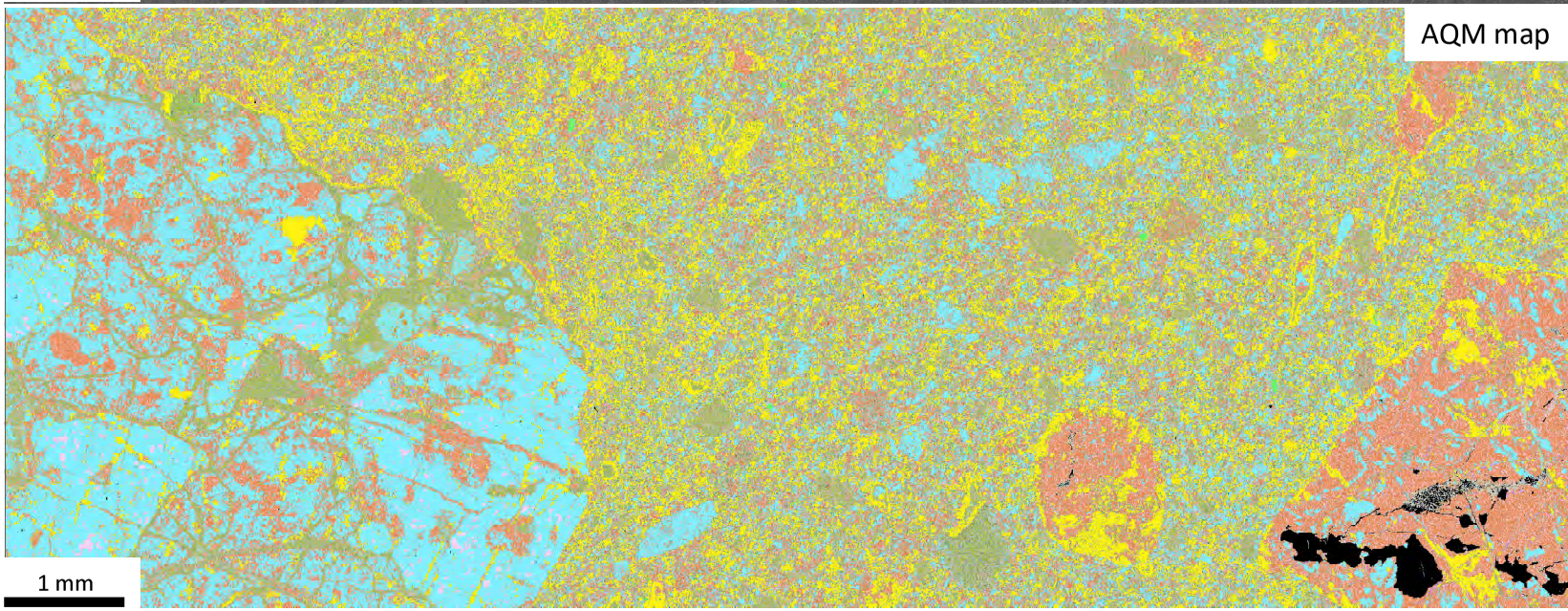

- Apatite
- Calcite
- Dozyite
- Orthoclase
- Quartz
- Rutile
- Sericite_Al-celadonite
- Weathered amphibole

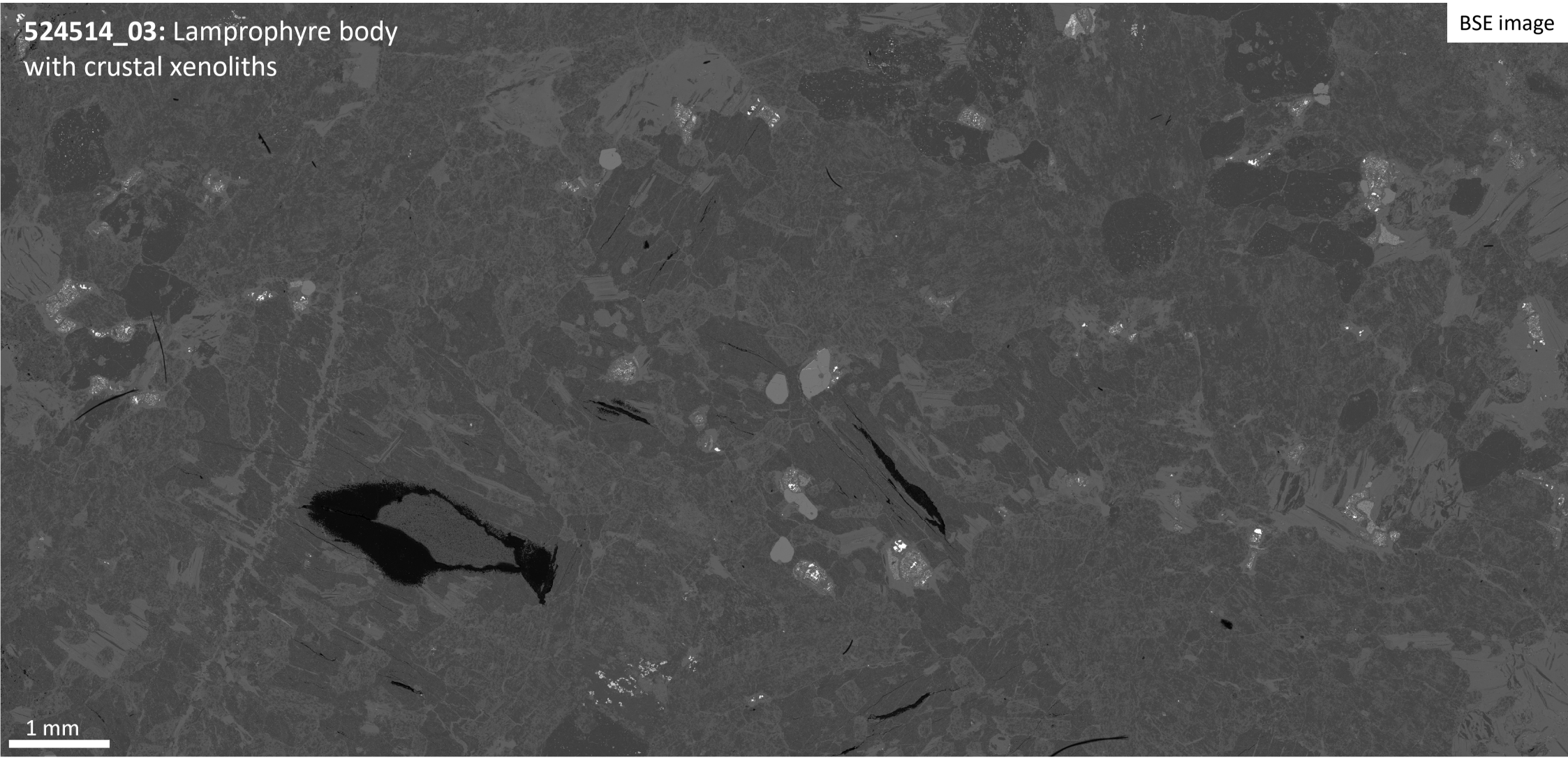
524514_03: Lamprophyre body
with crustal xenoliths
BSE image
1 mm

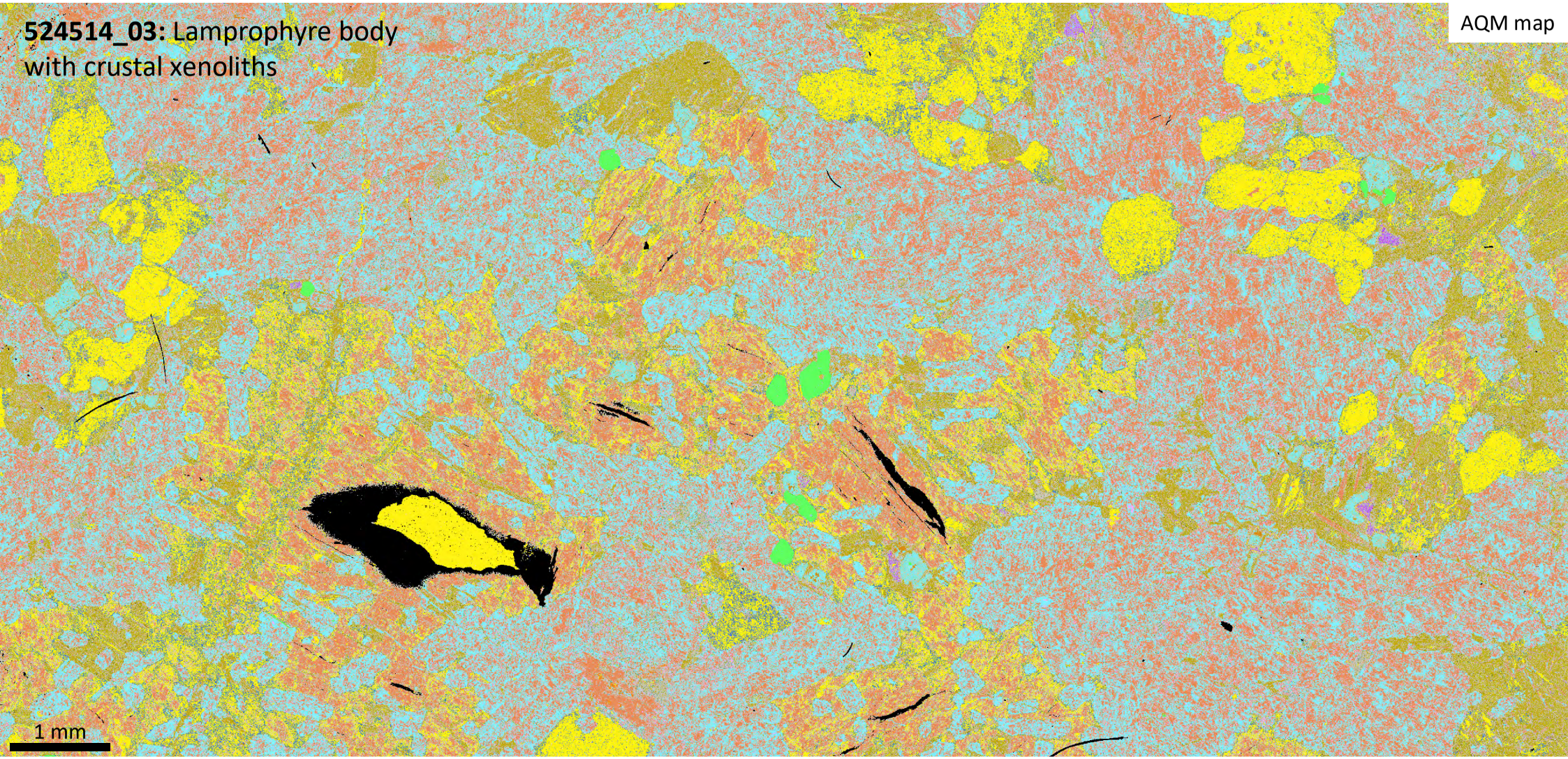
524514_03: Lamprophyre body with crustal xenoliths
AQM map
1 mm
Albite
Anorthite
Apatite
Augite-Diopside
Calcite
Chamosite/Chlorite
Fe/Mg/Ca-carbonate/hydroxide
Pseudobrookite/leucoxene
Quartz
Sericite_Al-celadonite
Weathered amphibole

524514_04: Lamprophyre body with crustal xenoliths

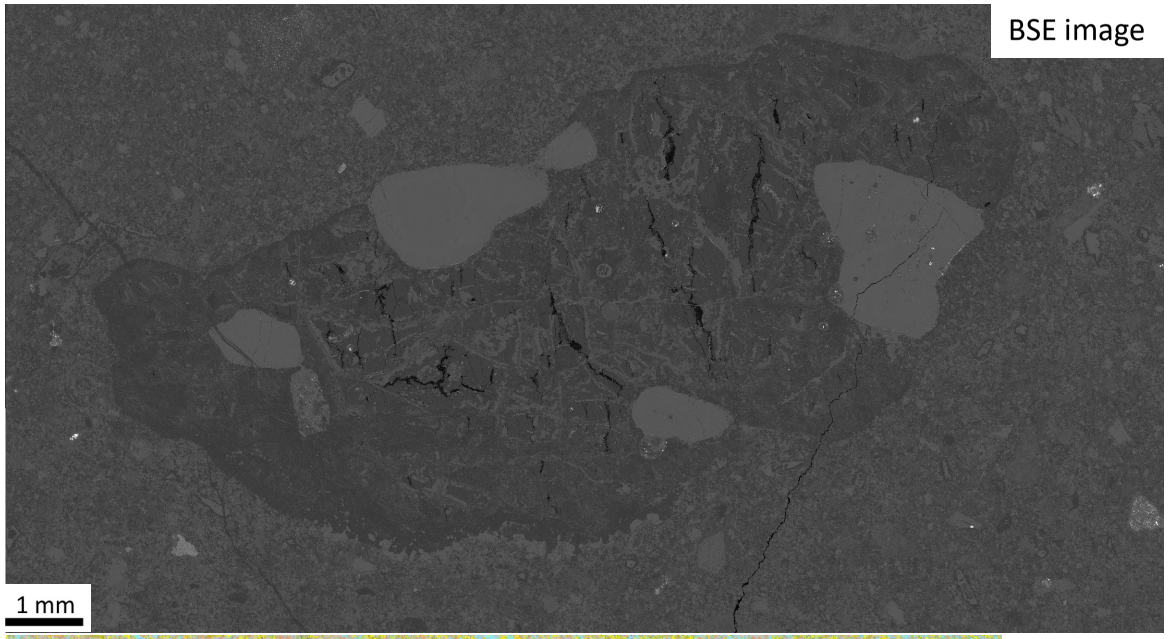

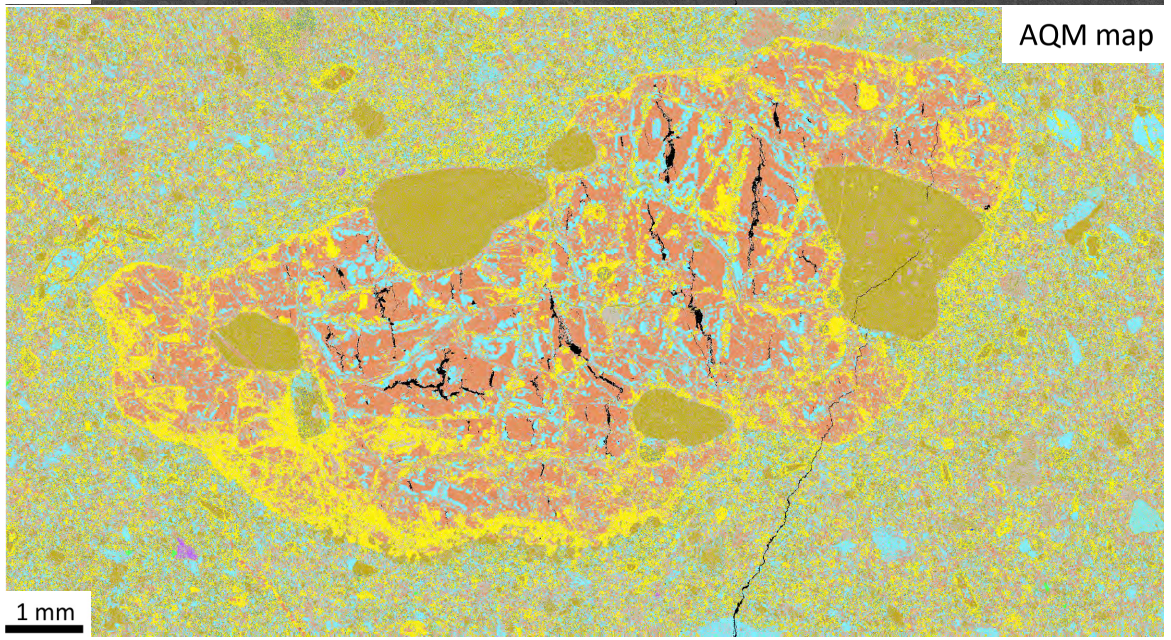

524515: Float sample of ultramafic lamprohyre with crustal xenoliths

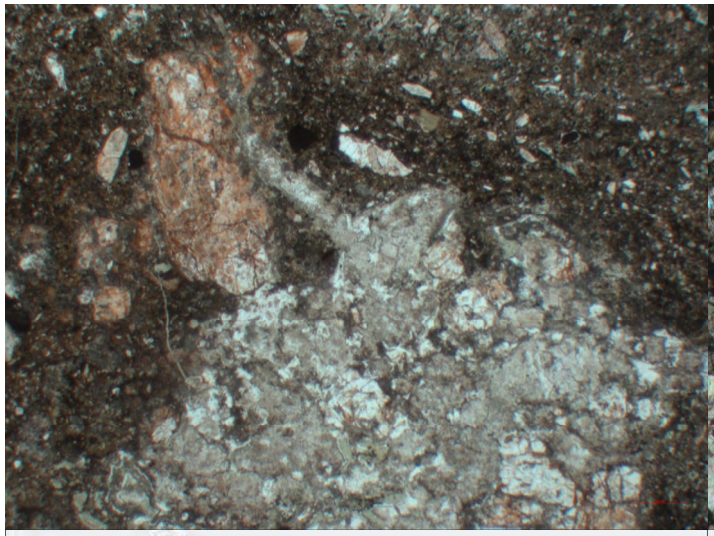

524515-01 PPL

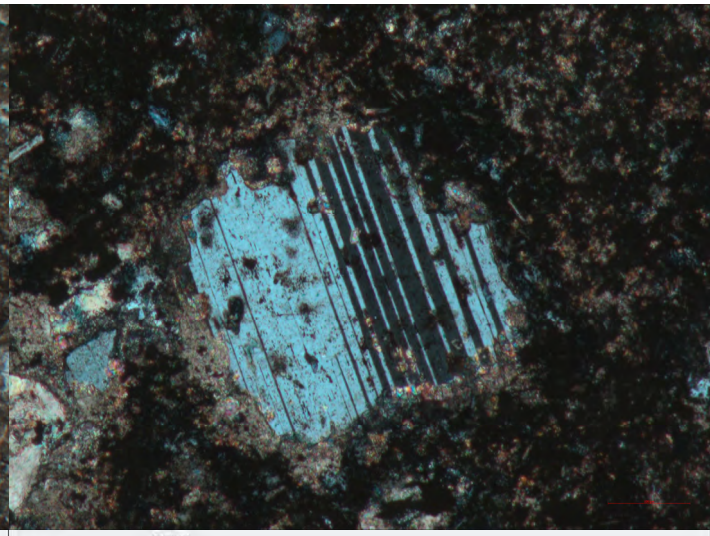

524515-02 PPL

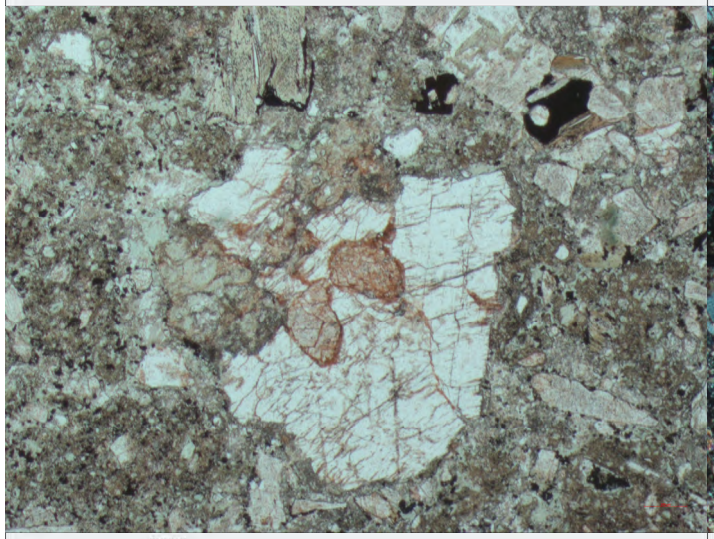

524515-03 PPL

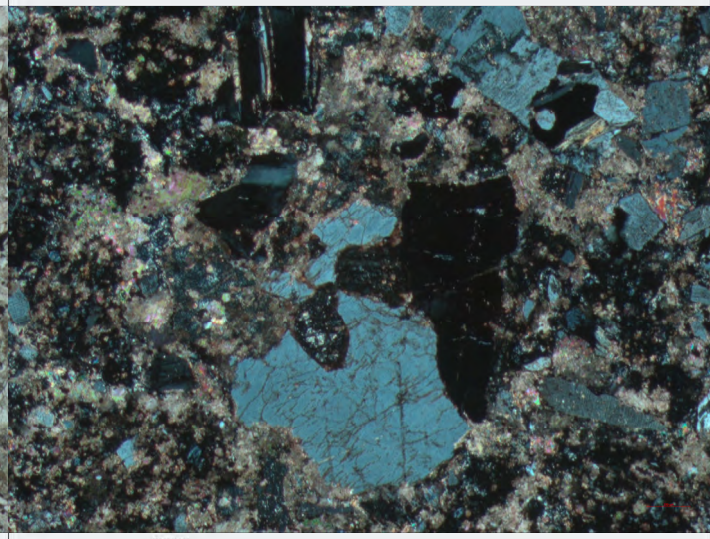

524515-03 XPL

524515: Float sample of ultramafic lamprohyre with crustal xenoliths

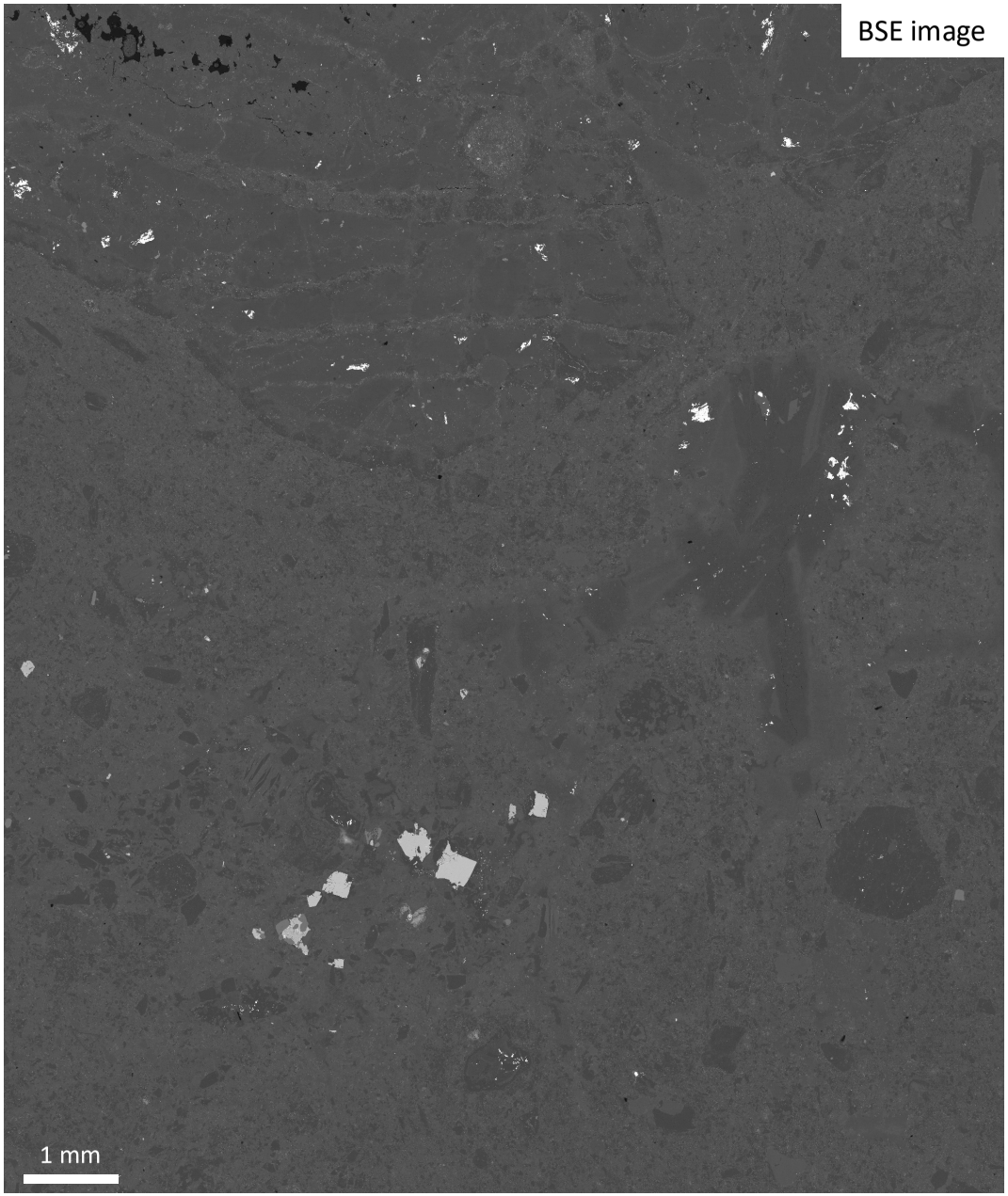

524515: Float sample of ultramafic lamprohyre with crustal xenoliths

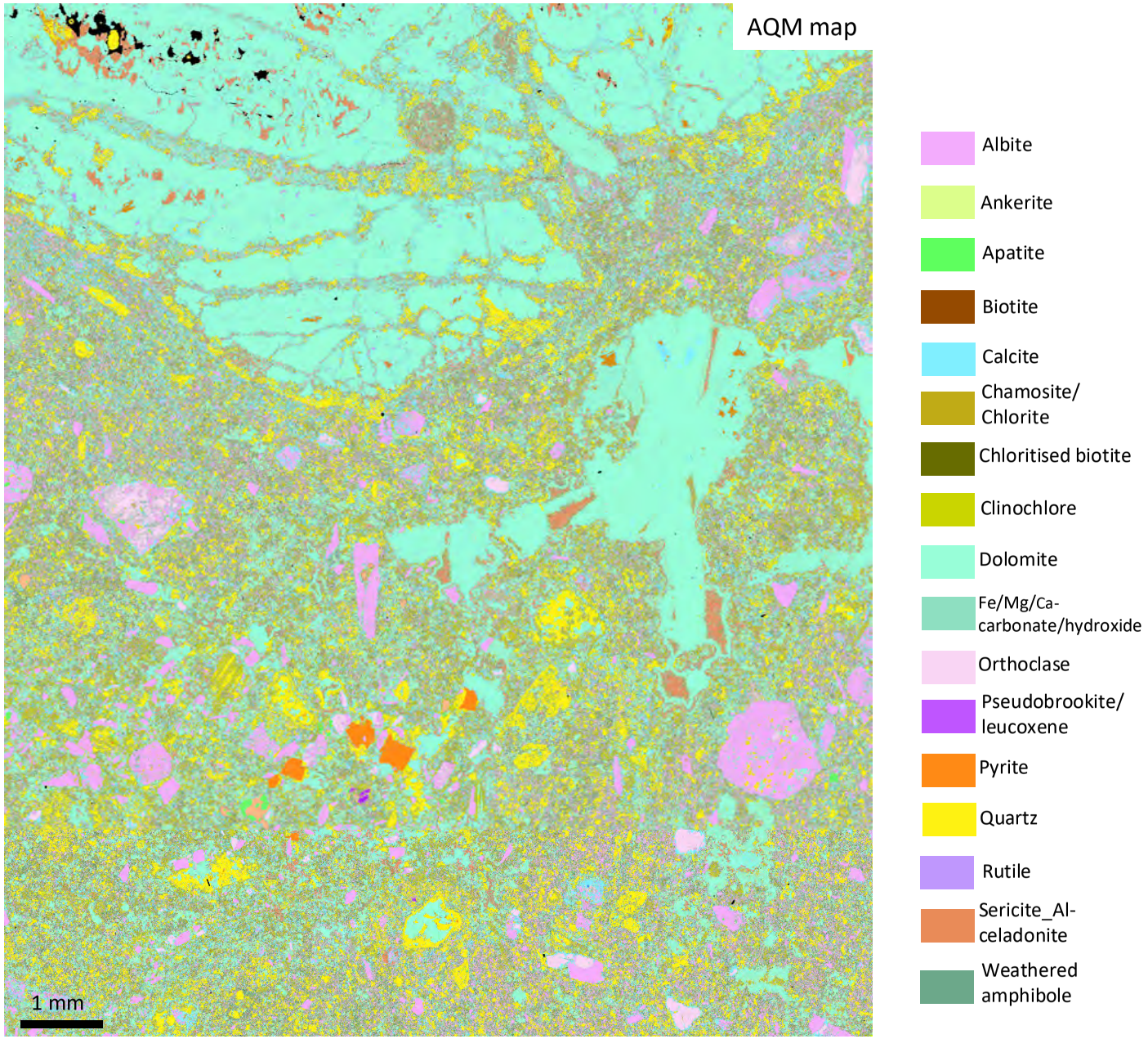

524515_02:
Float sample of ultramafic lamprophyre with crustal xenoliths

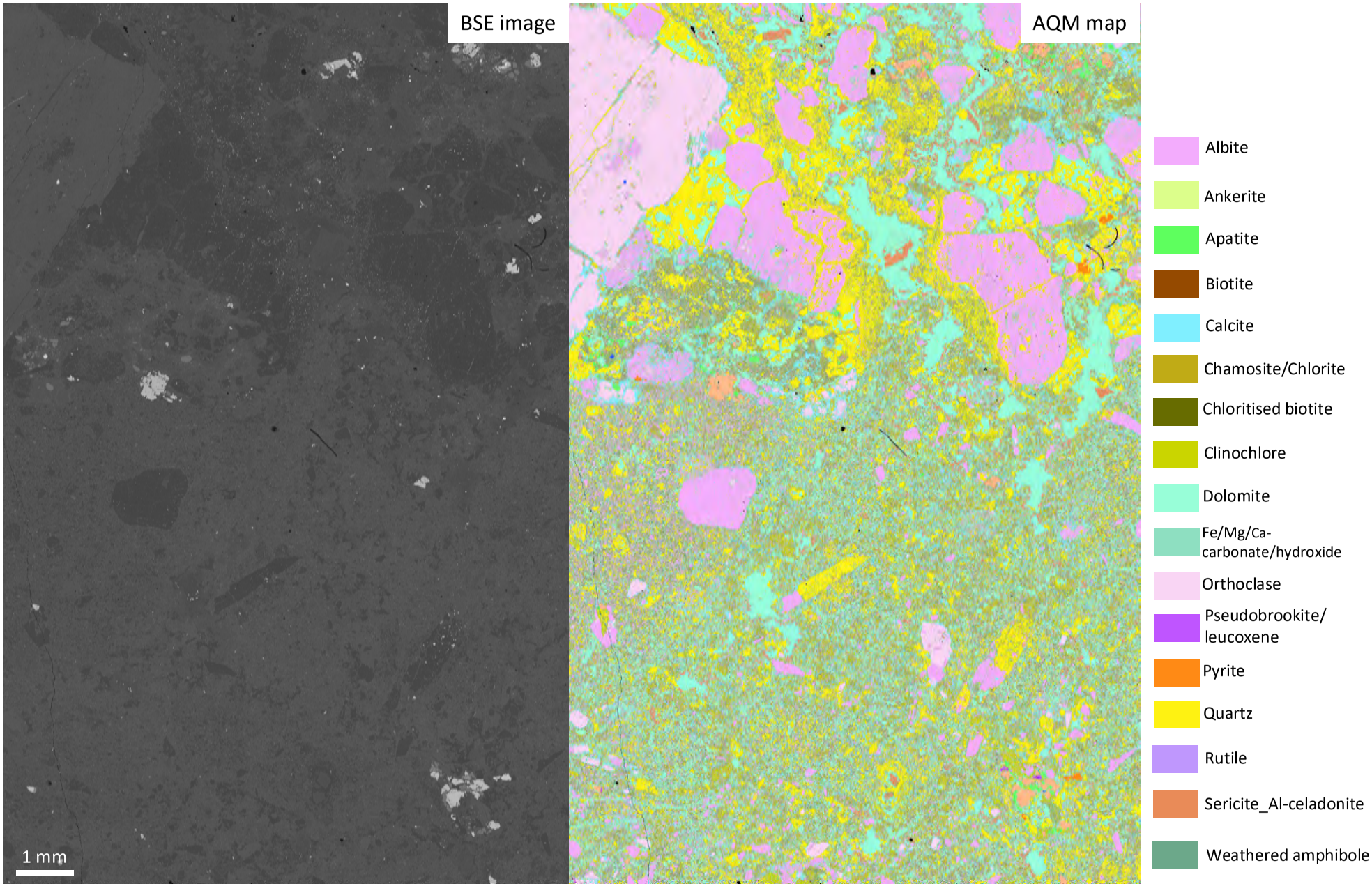

524515_03: Float sample of ultramafic lamprophyre with crustal xenoliths

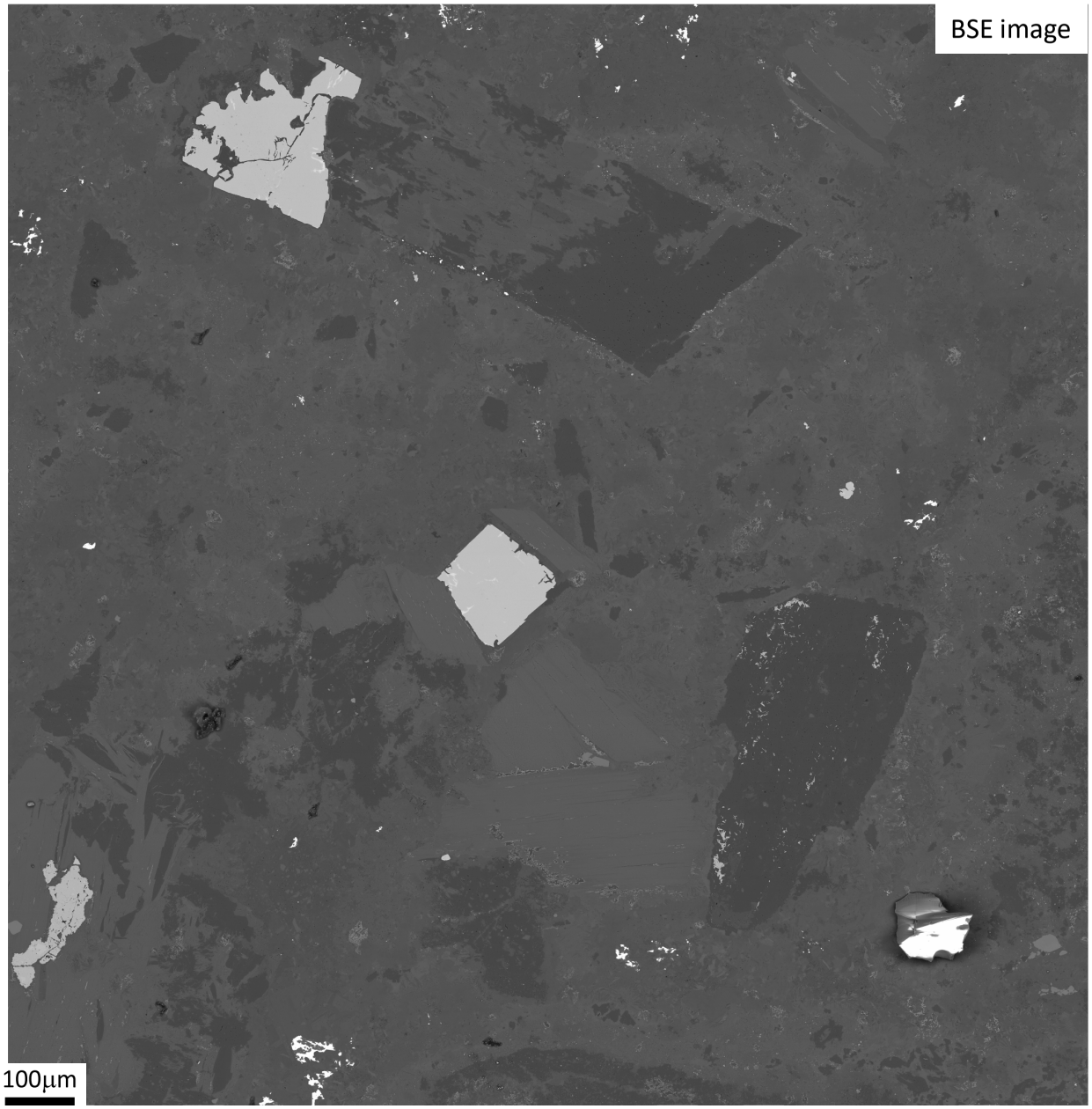

524515_03: Float sample of ultramafic lamprophyre with crustal xenoliths

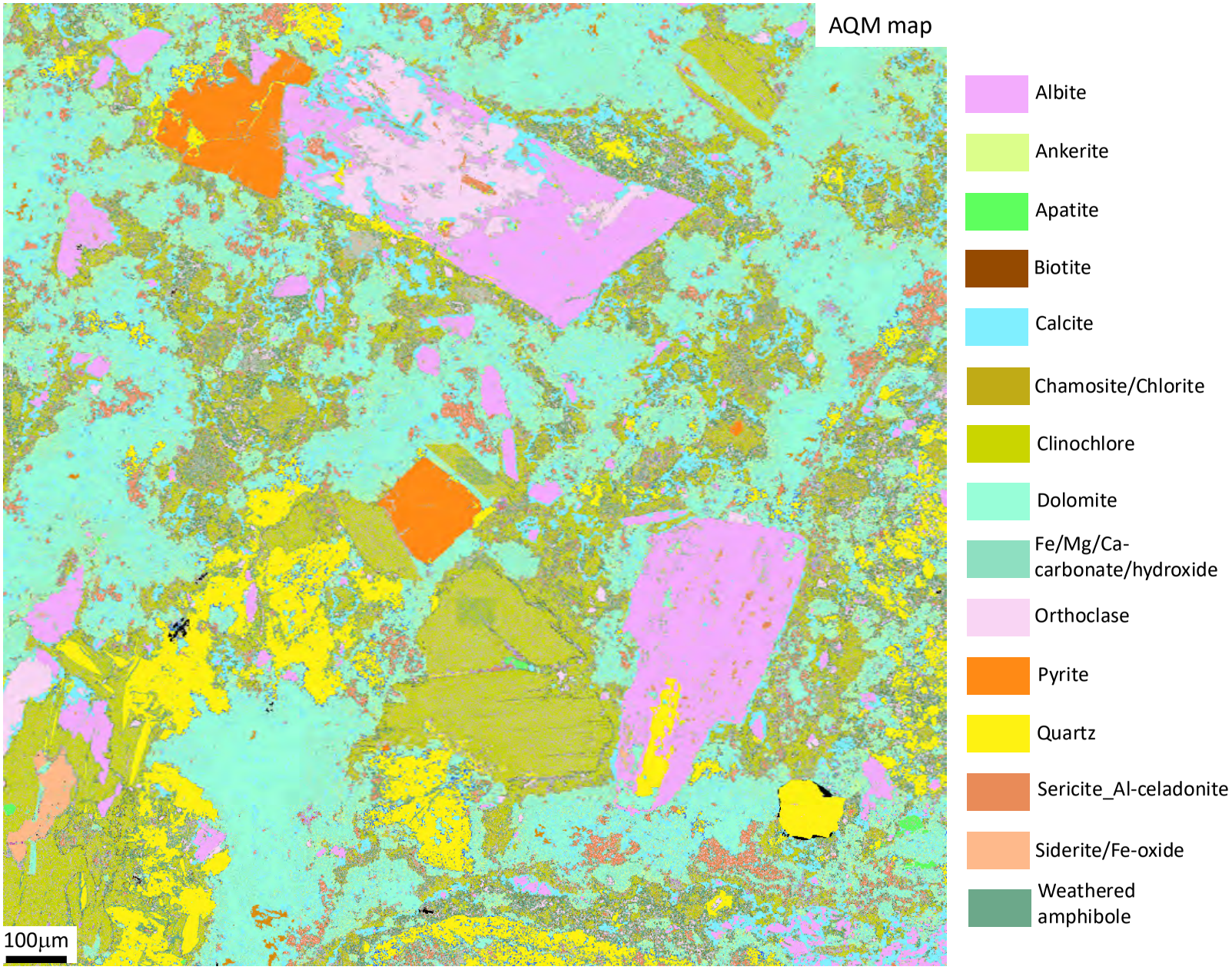

524515_04: Float sample of ultramafic lamprophyre with crustal xenoliths

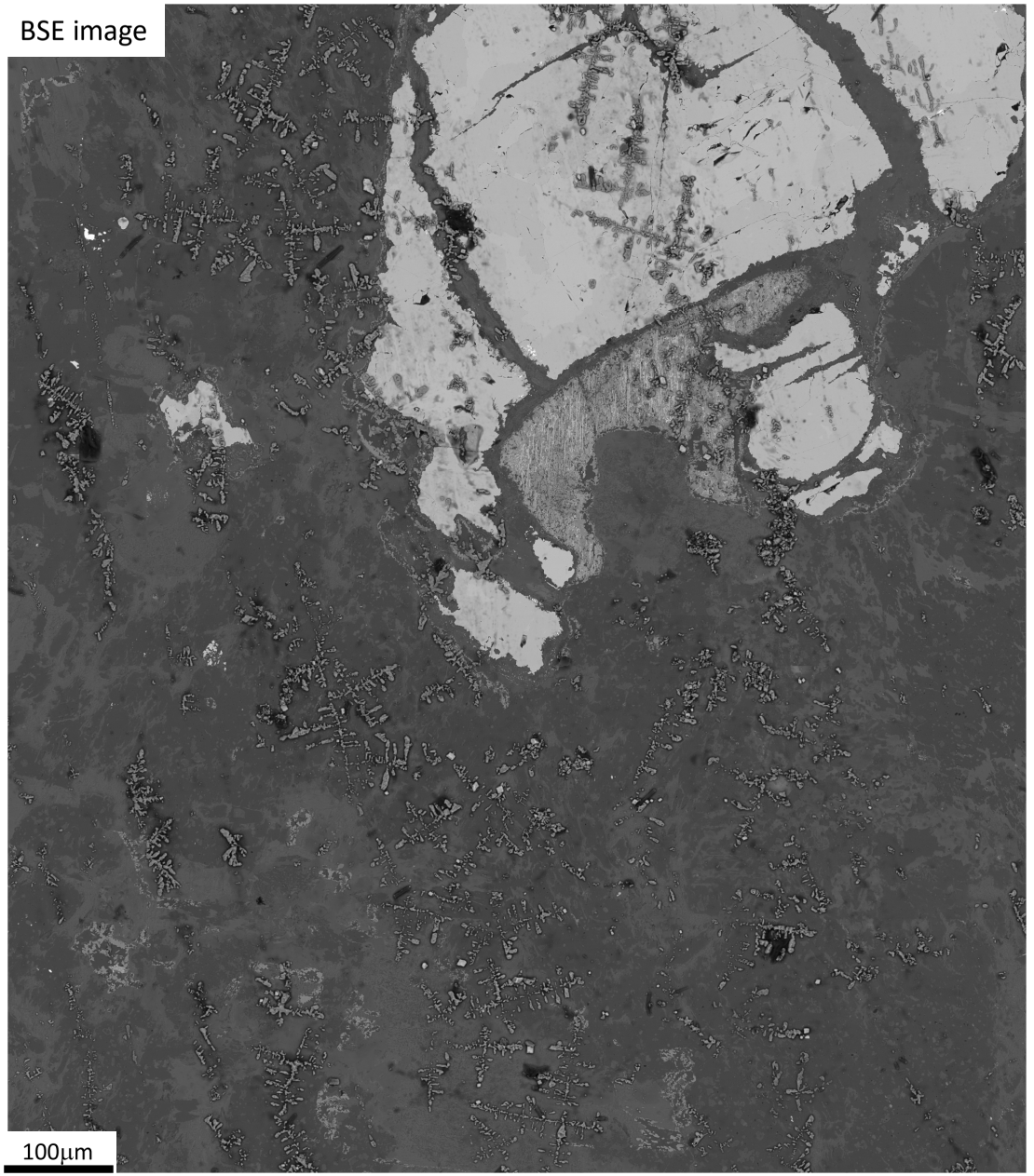

524515_04: Float of altered ultramafic lamprophyre with crustal xenoliths

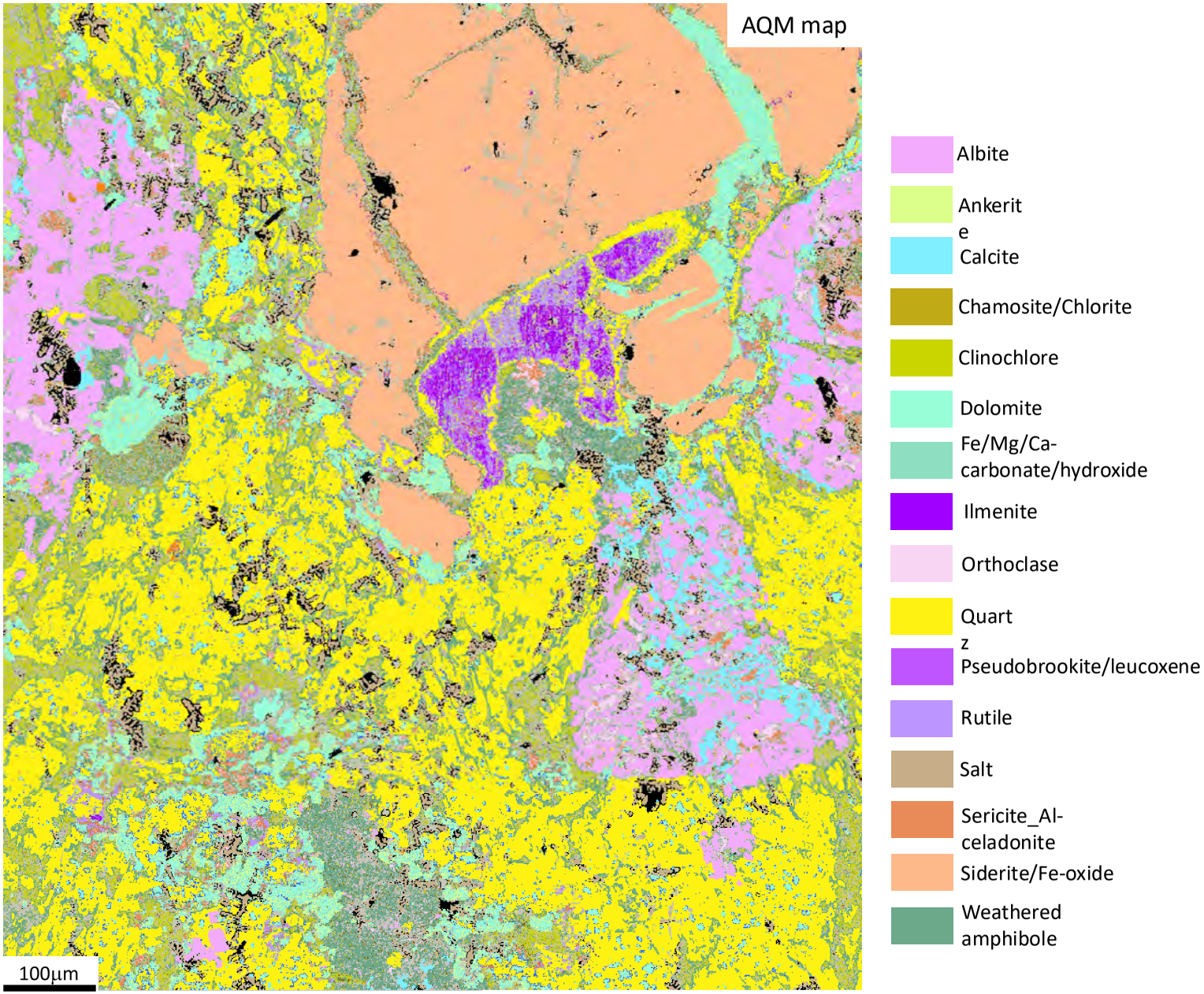

524516: Lamprophyre dyke with crustal xenoliths

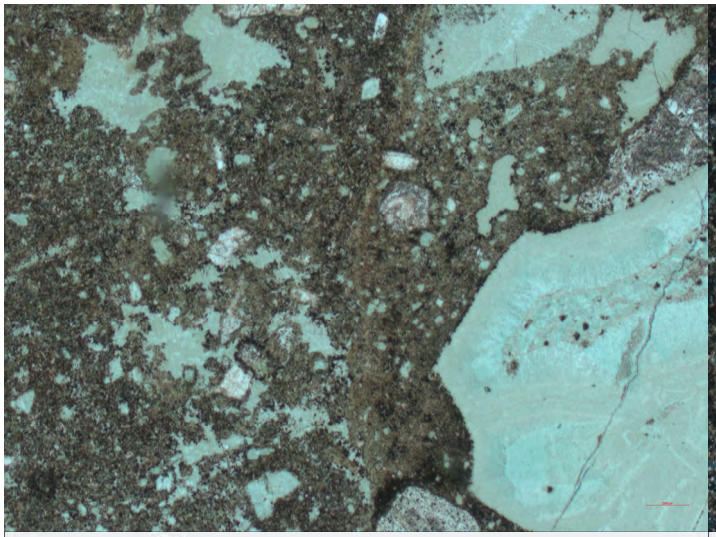

524516-01A PPL

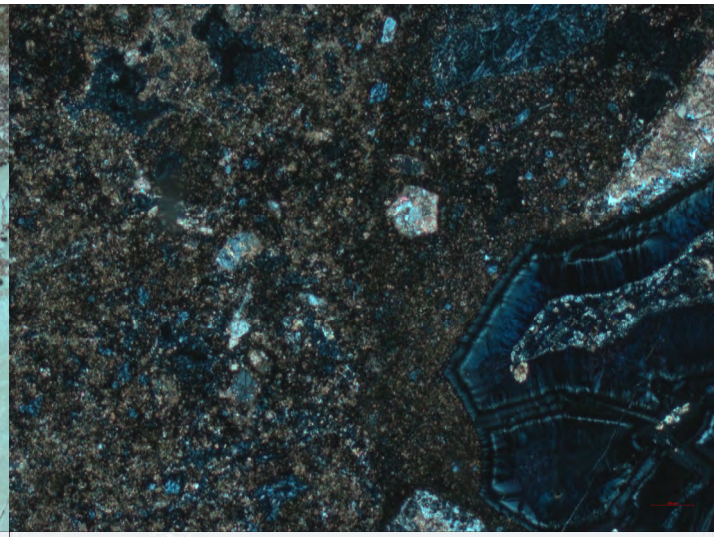

524516-01A XPL

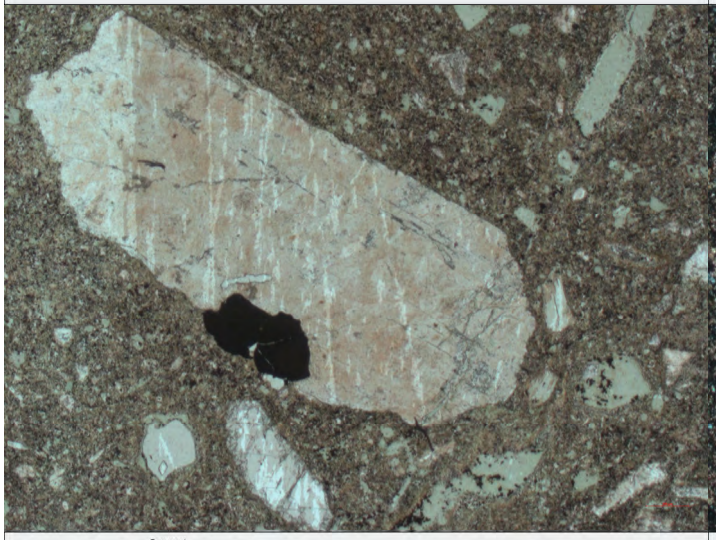

524516-03 PPL

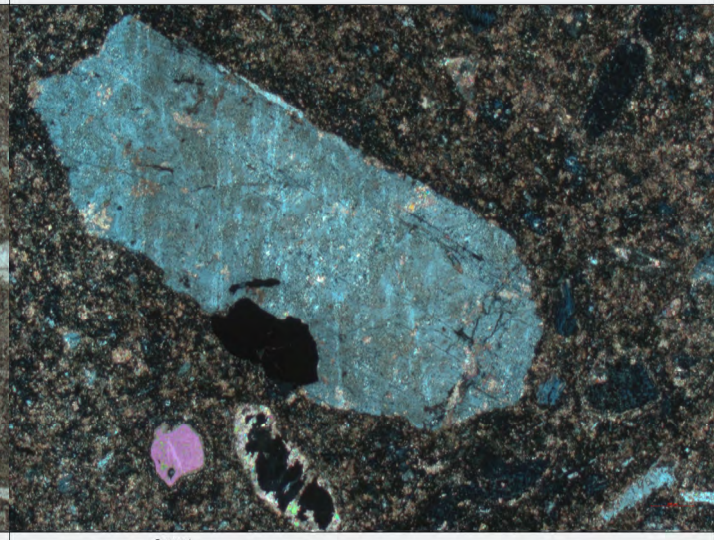

524516-03 XPL

524516_01A:
Lamprophyre dyke with crustal xenoliths

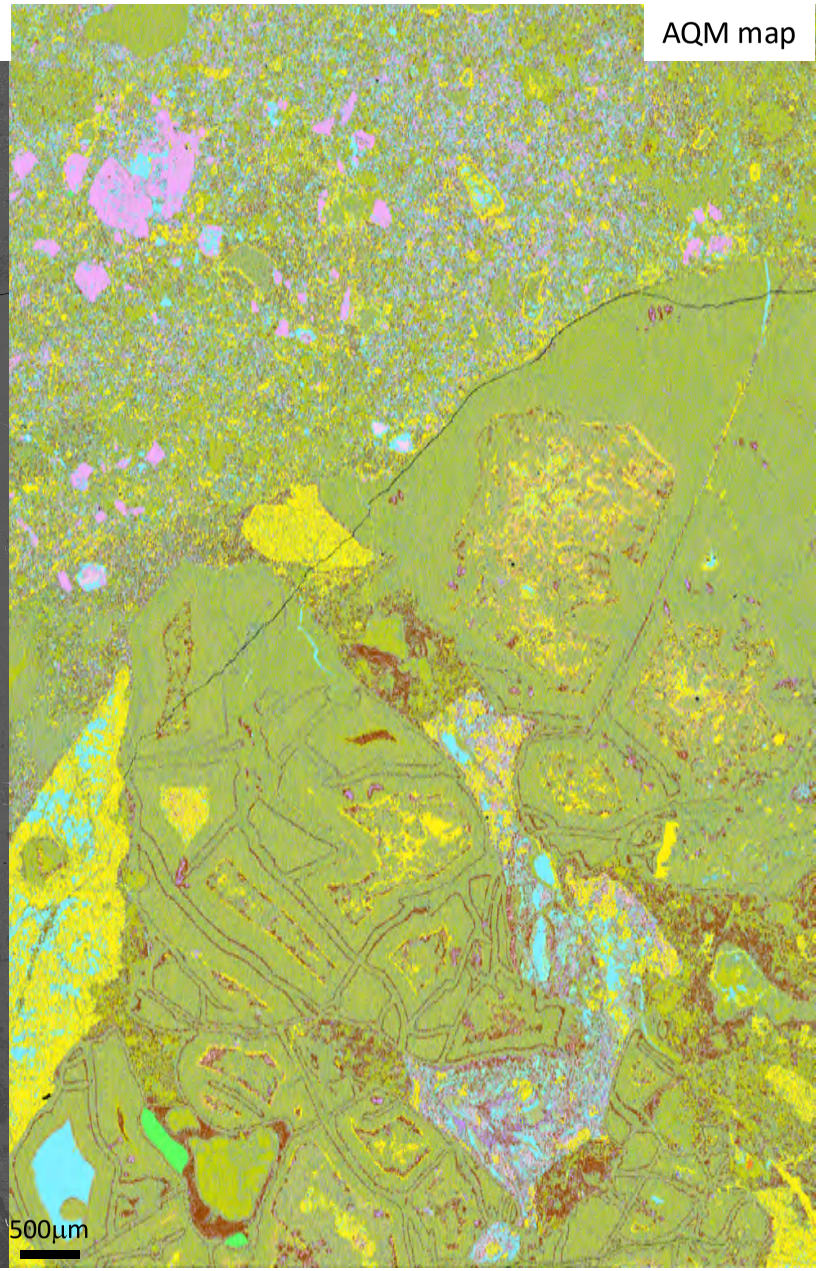

524516_01A: Lamprophyre dyke with crustal xenoliths

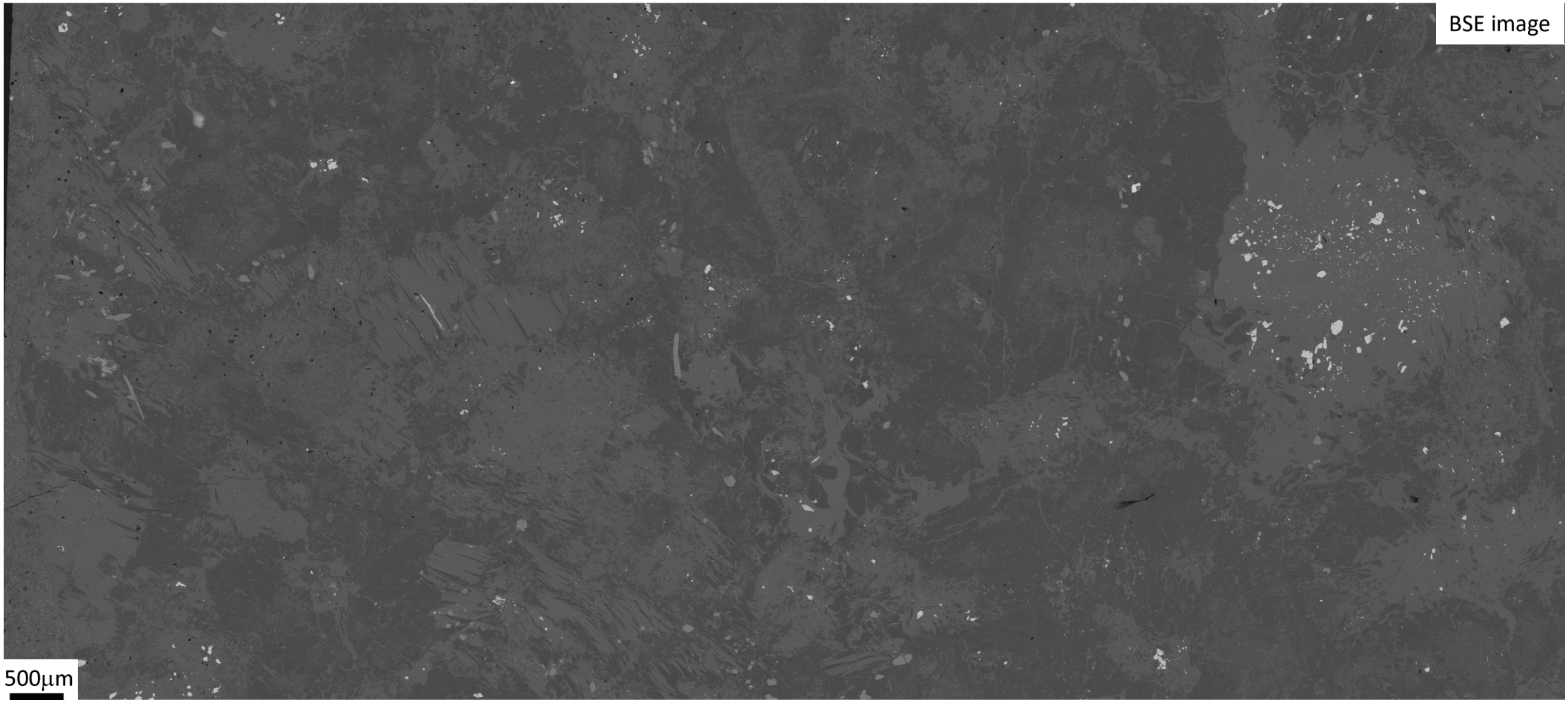

524516_01A: Lamprophyre dyke with crustal xenoliths

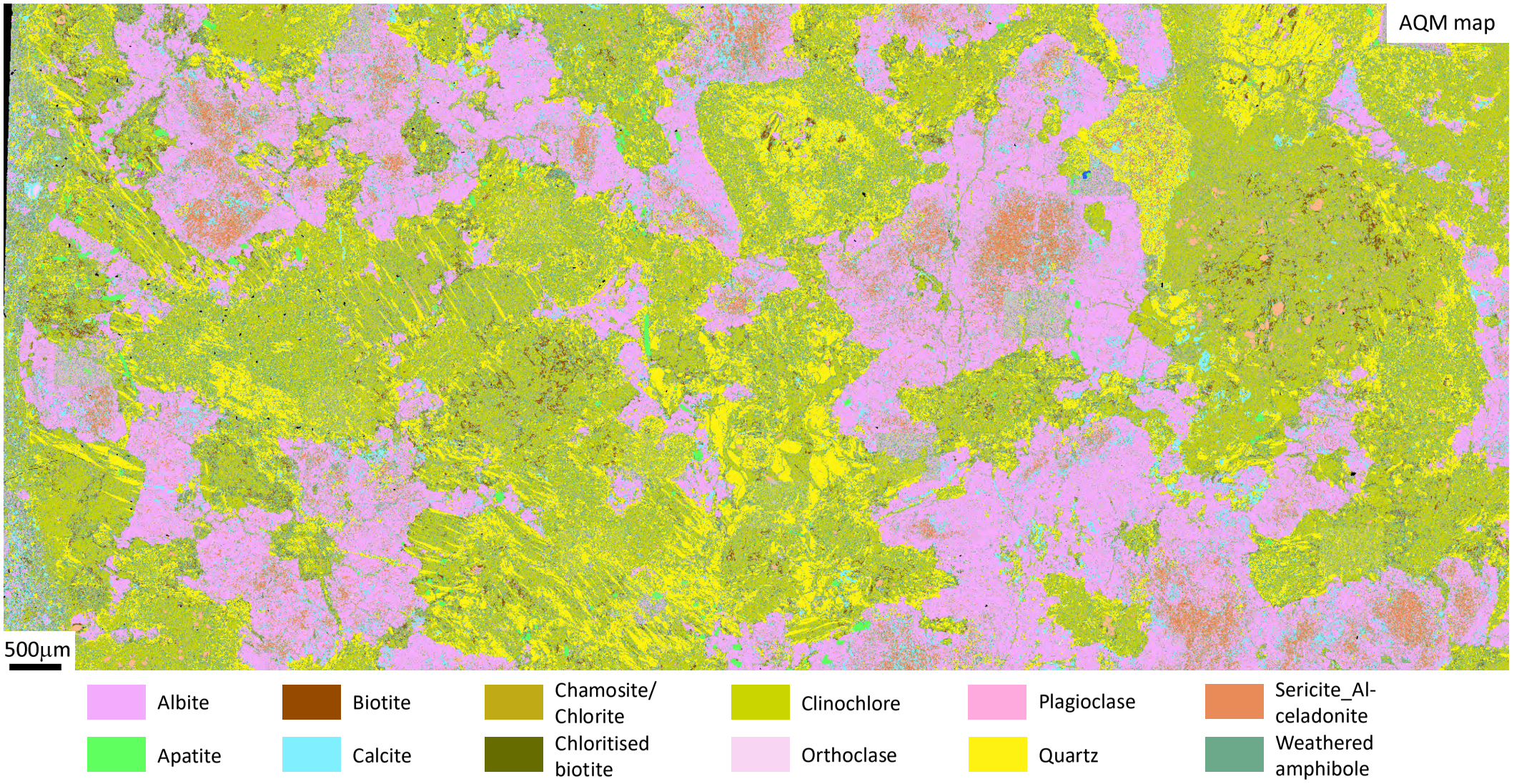

524516_02: Lamprophyre dyke with crustal xenoliths

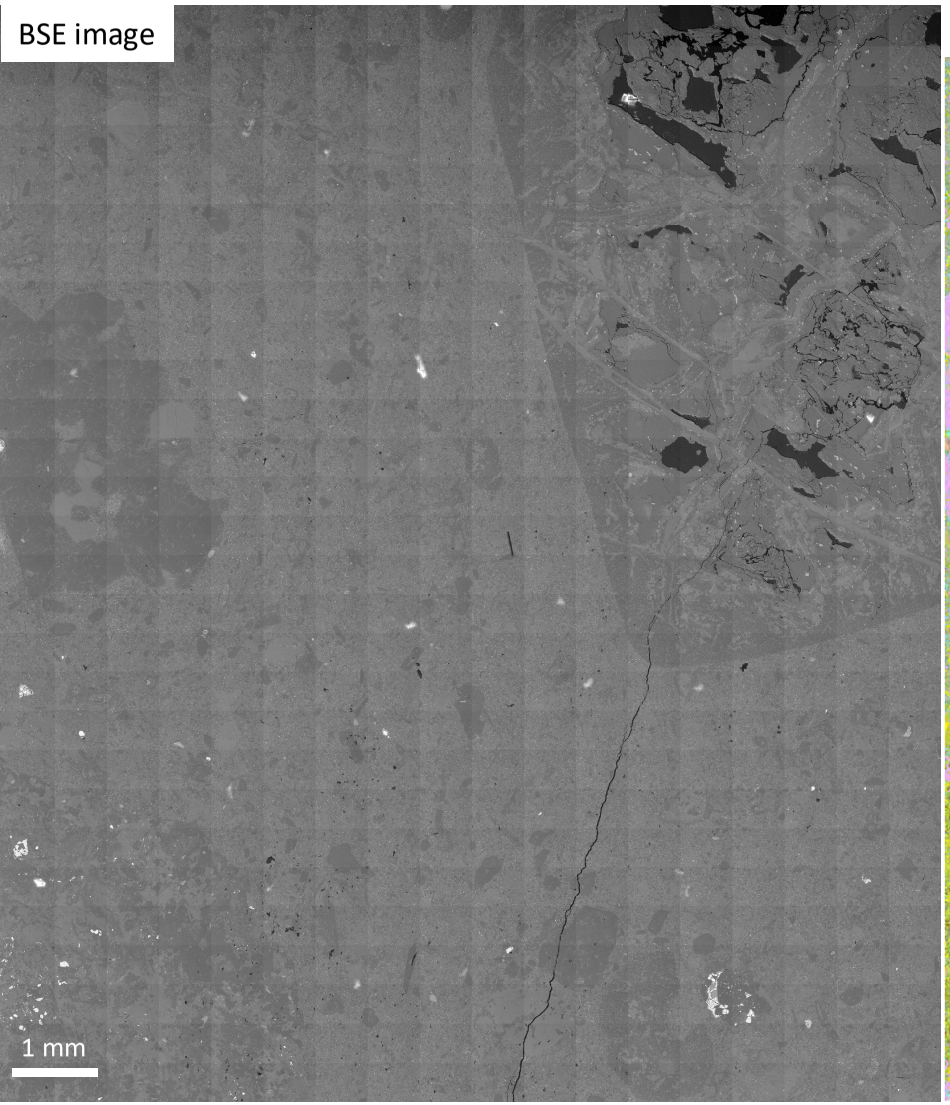

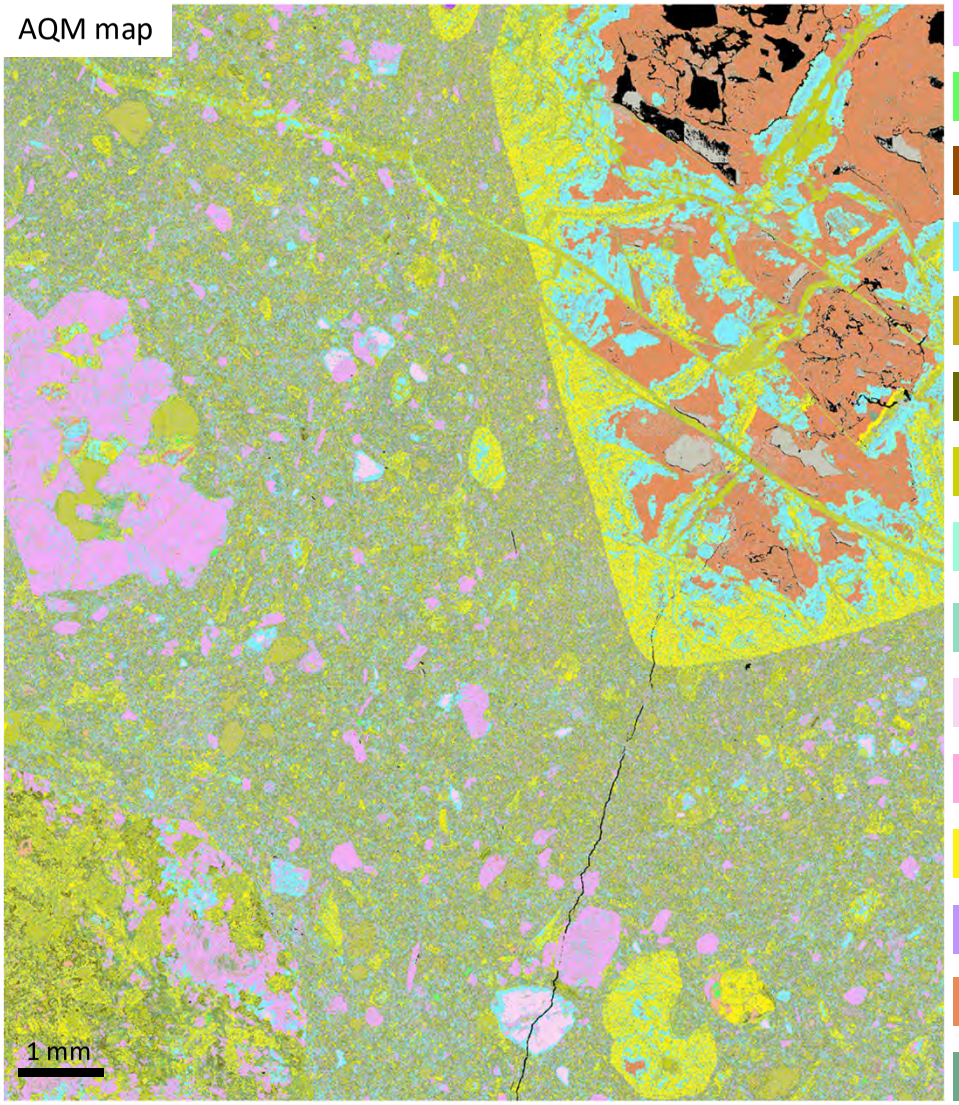

524516_03: Lamprophyre dyke with crustal xenoliths

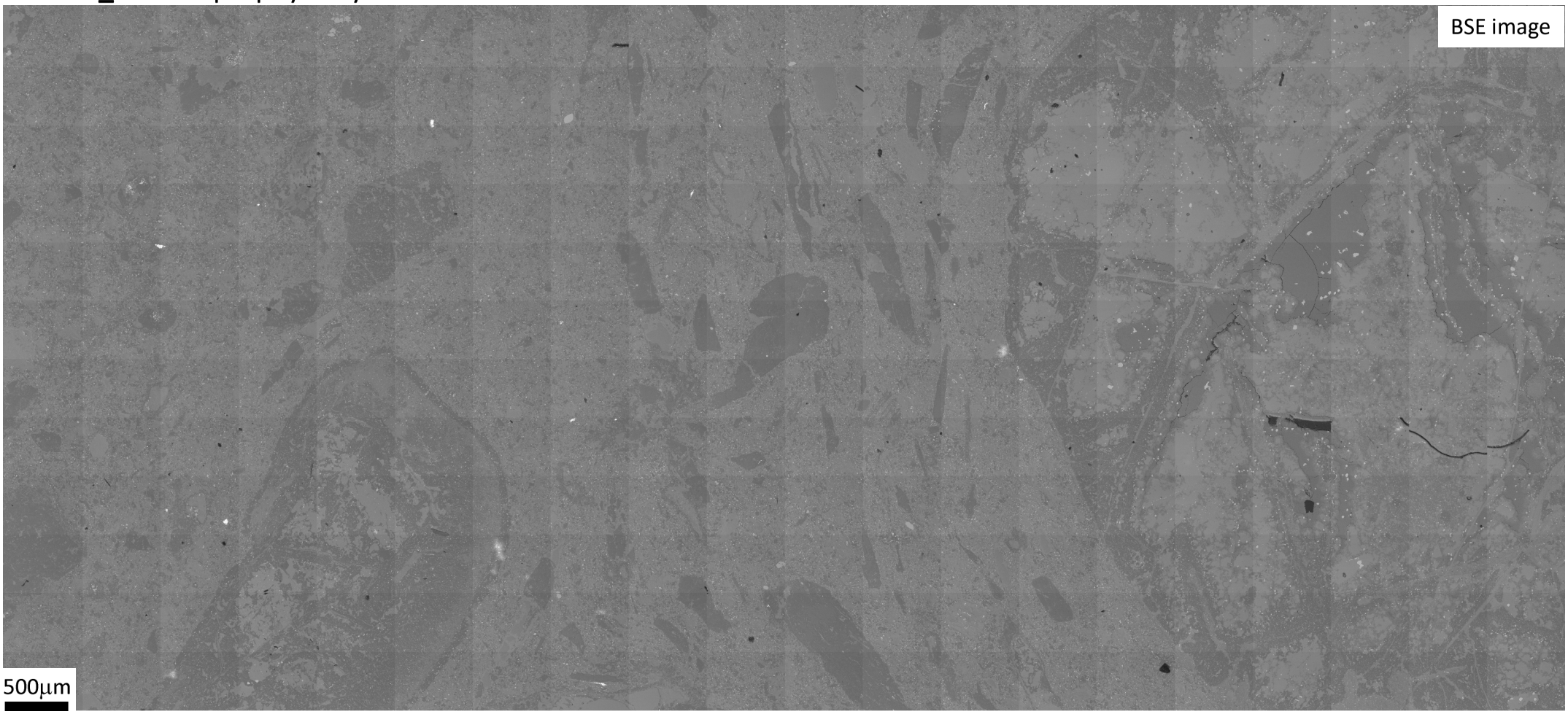

524516_03: Lamprophyre dyke with crustal xenoliths

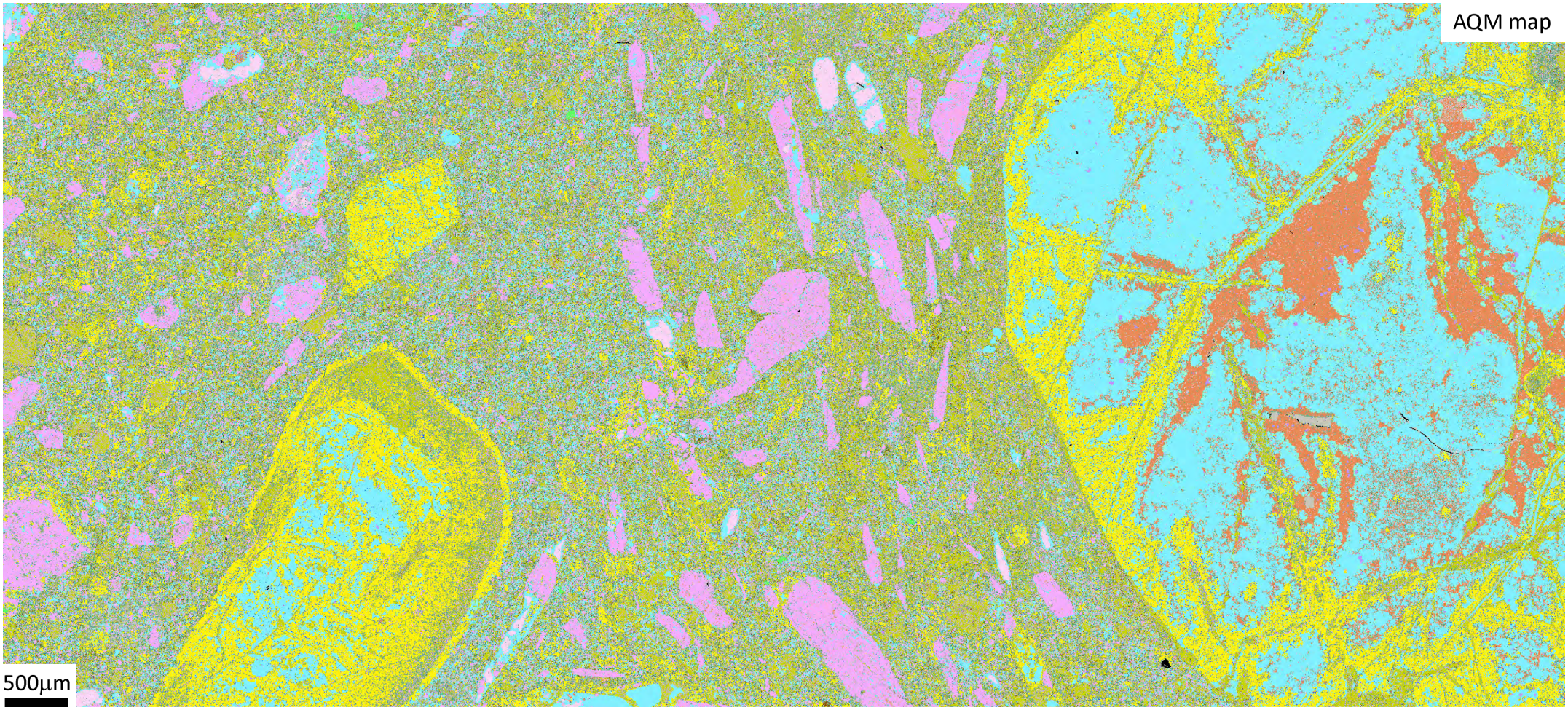

591202_01: Lamprophyre with olivine megacrysts

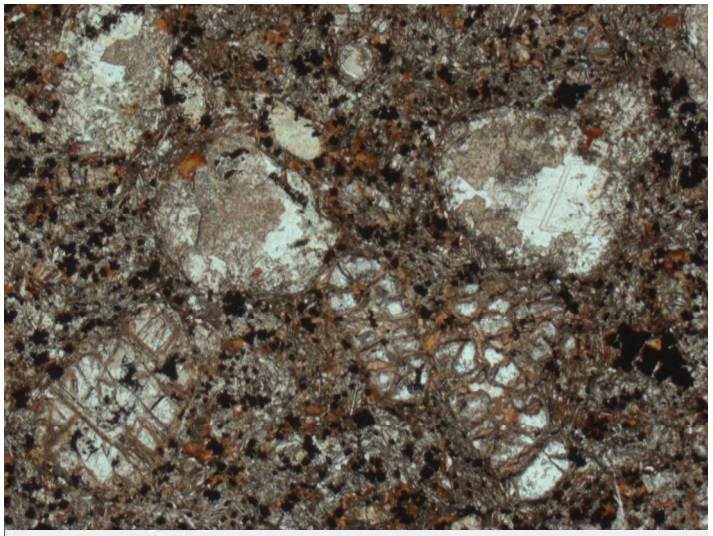

591202_01 PPL

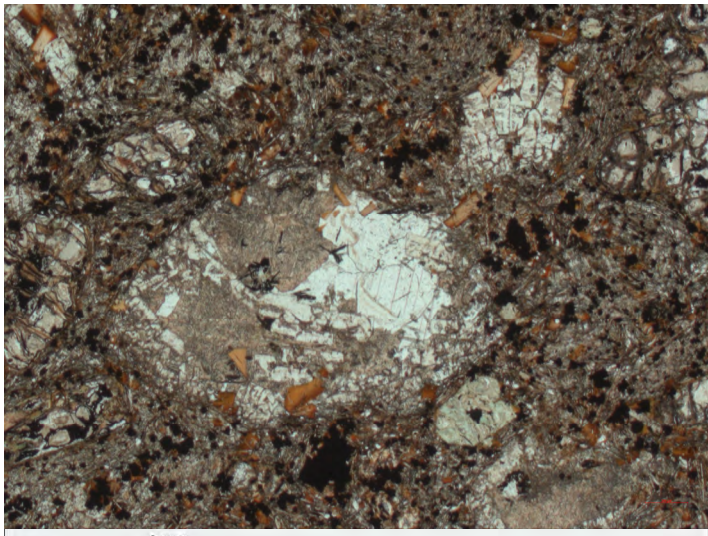

591202_01 PPL

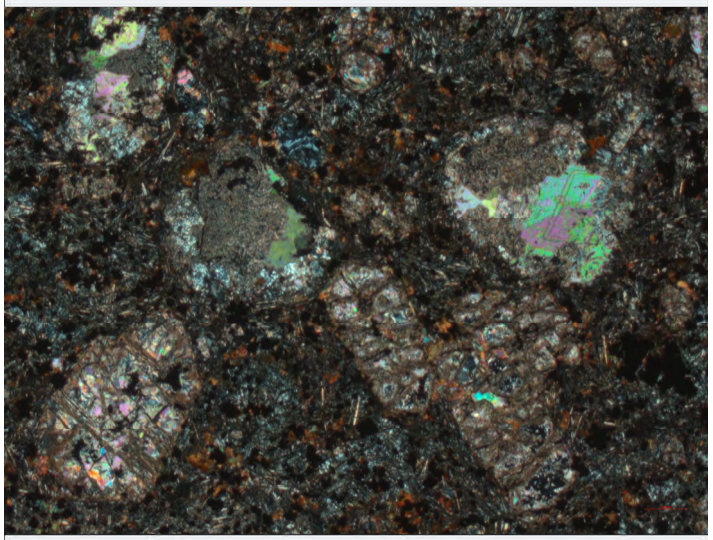

591202_01 XPL

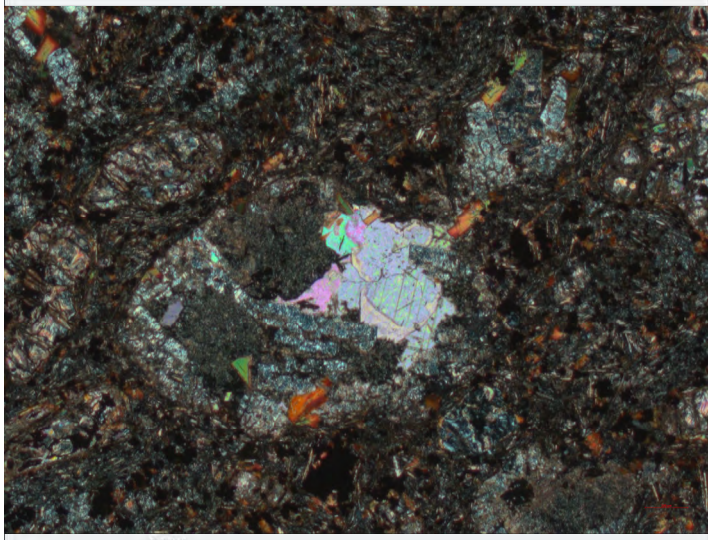

591202_01 XPL

591202_01: Lamprophyre with olivine megacrysts

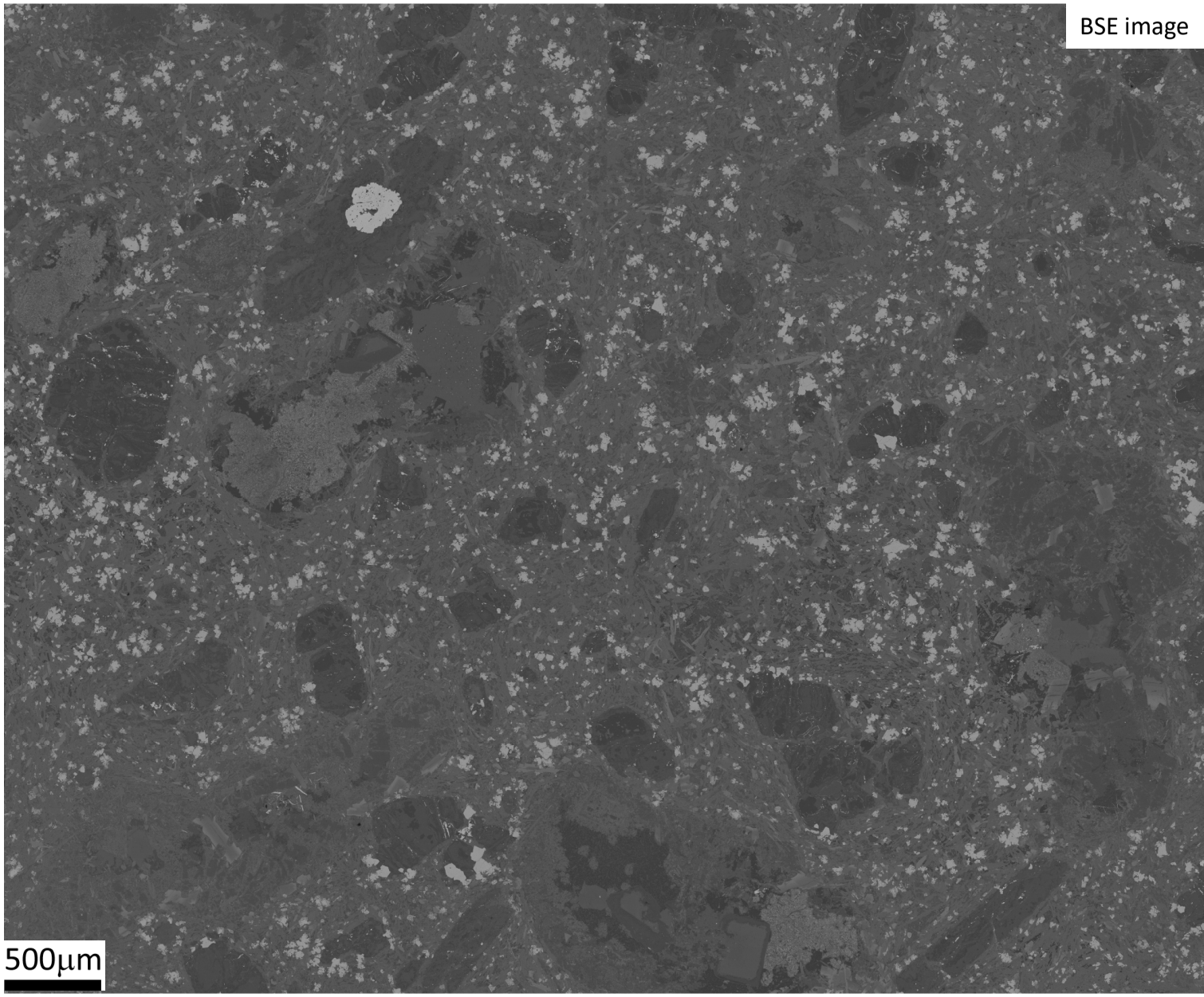

591202_01: Lamprophyre with olivine megacrysts

- Albite
- Annite
- Anthophyllite/ Cummingtonite
- Apatite
- Augite-Diopside
- Biotite
- Calcite
- Chloritised biotite
- Chlorite/Gedrite
- Dolomite
- Fe/Mg/Ca-carbonate/hydroxide
- Ilmenite
- Orthoclase
- Pyrite
- Quartz
- Sericite_Al-celadonite
- Titanomagnetite
- Weathered amphibole

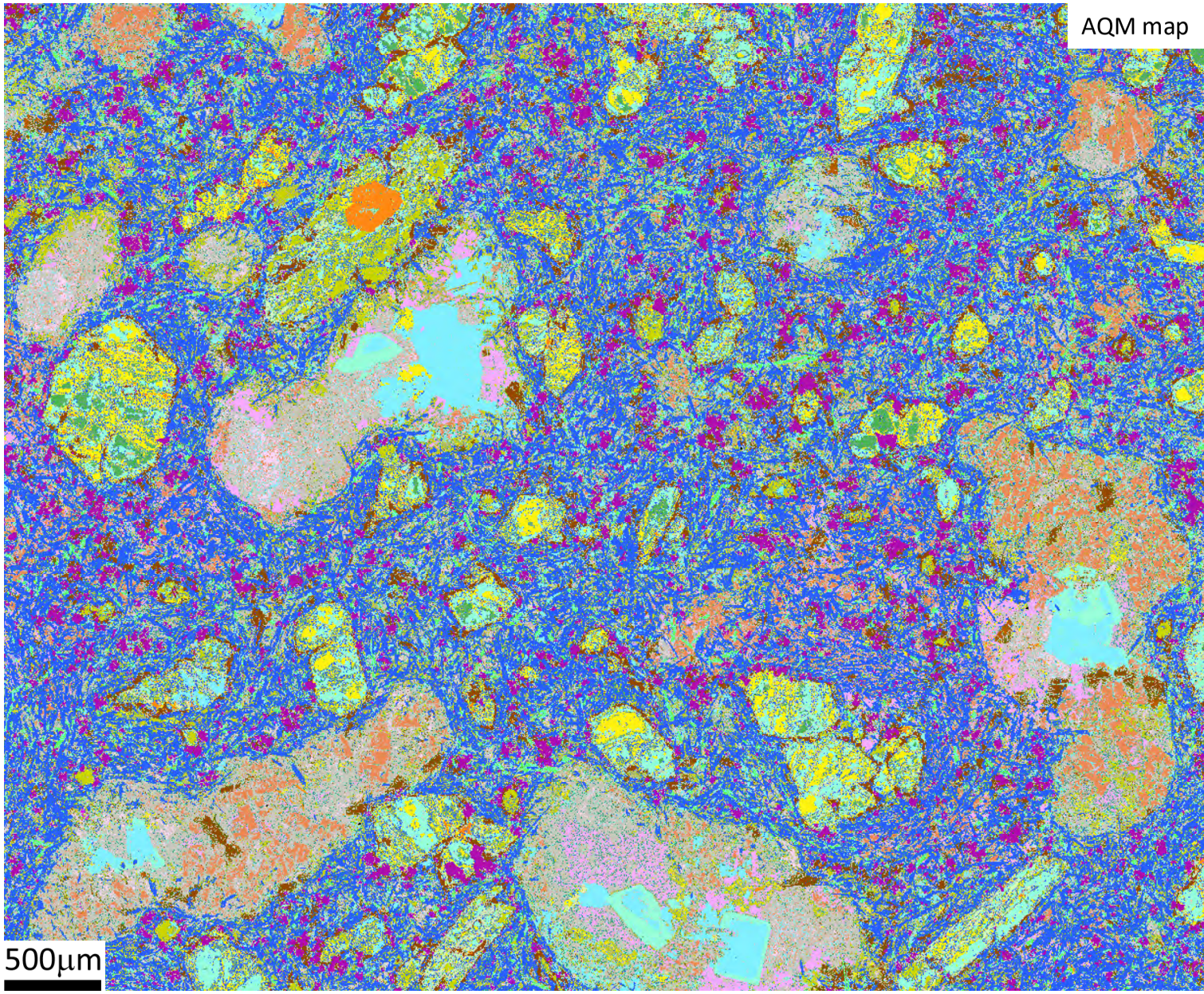

591202_01: Lamprophyre with olivine megacrysts

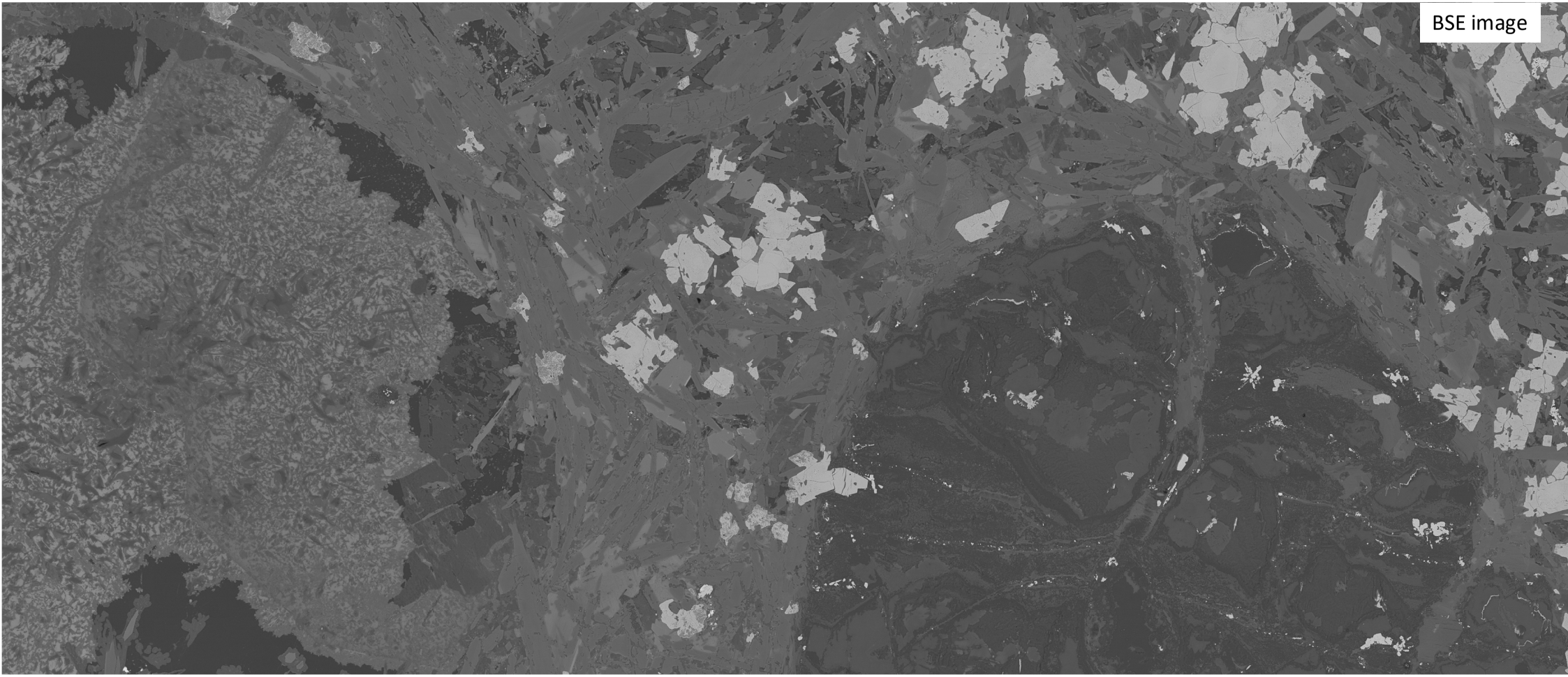

591202_01: Lamprophyre with olivine megacrysts, strongly altered

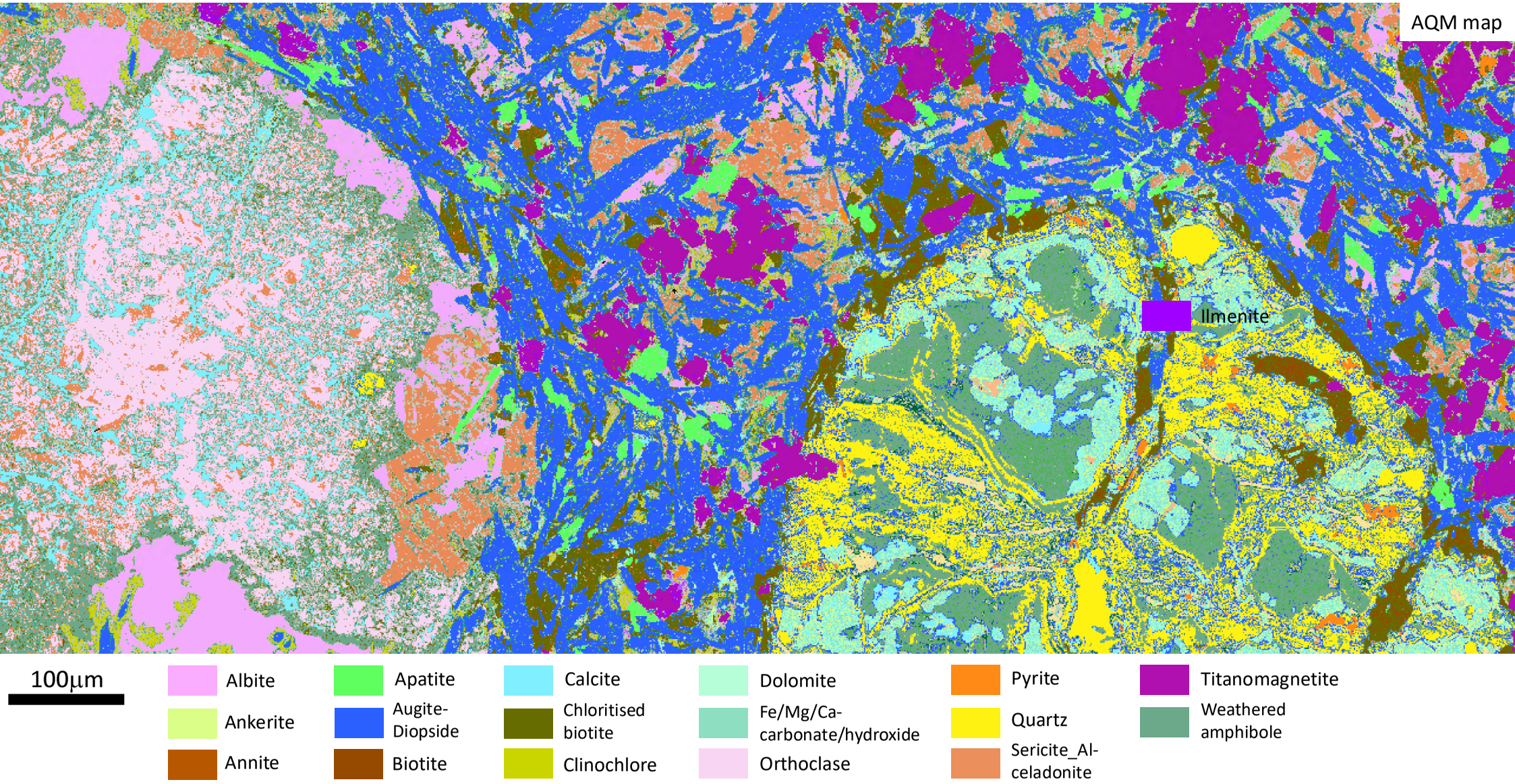

591202_01: Lamprophyre with olivine megacrysts

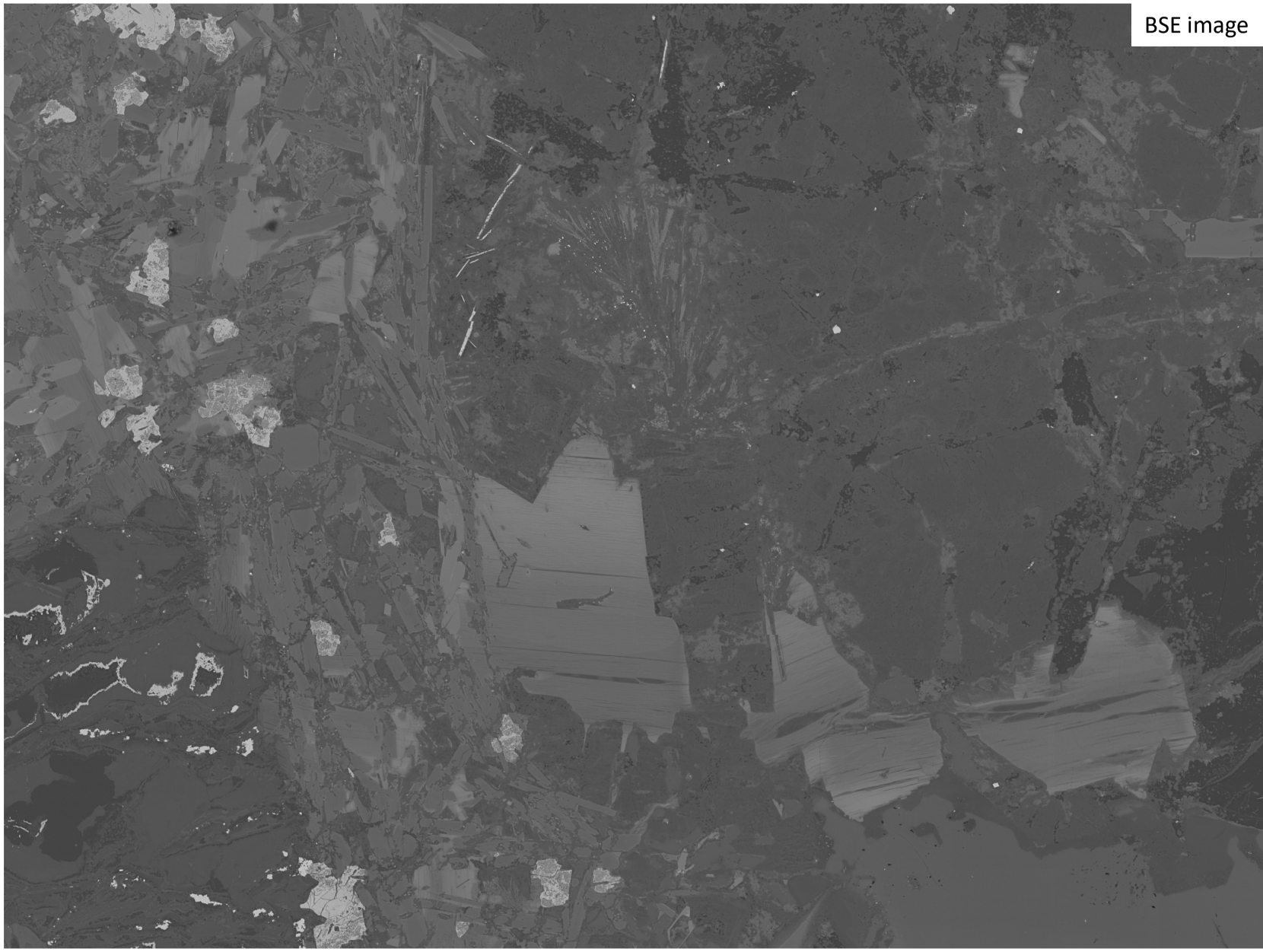

591202_01: Lamprophyre with olivine megacrysts

- Albite
- Ankerite
- Annite
- Apatite
- Augite-Diopside
- Biotite
- Calcite
- Chlorite
- Chloritised biotite
- Clinochlore
- Dolomite
- Fe/Mg/Ca-Carbonate/hydroxide
- Mg-Siderite (sideroplesite)
- Orthoclase
- Quartz
- Sericite_Al-celadonite
- Titanomagnetite
- Weathered amphibole

100µm

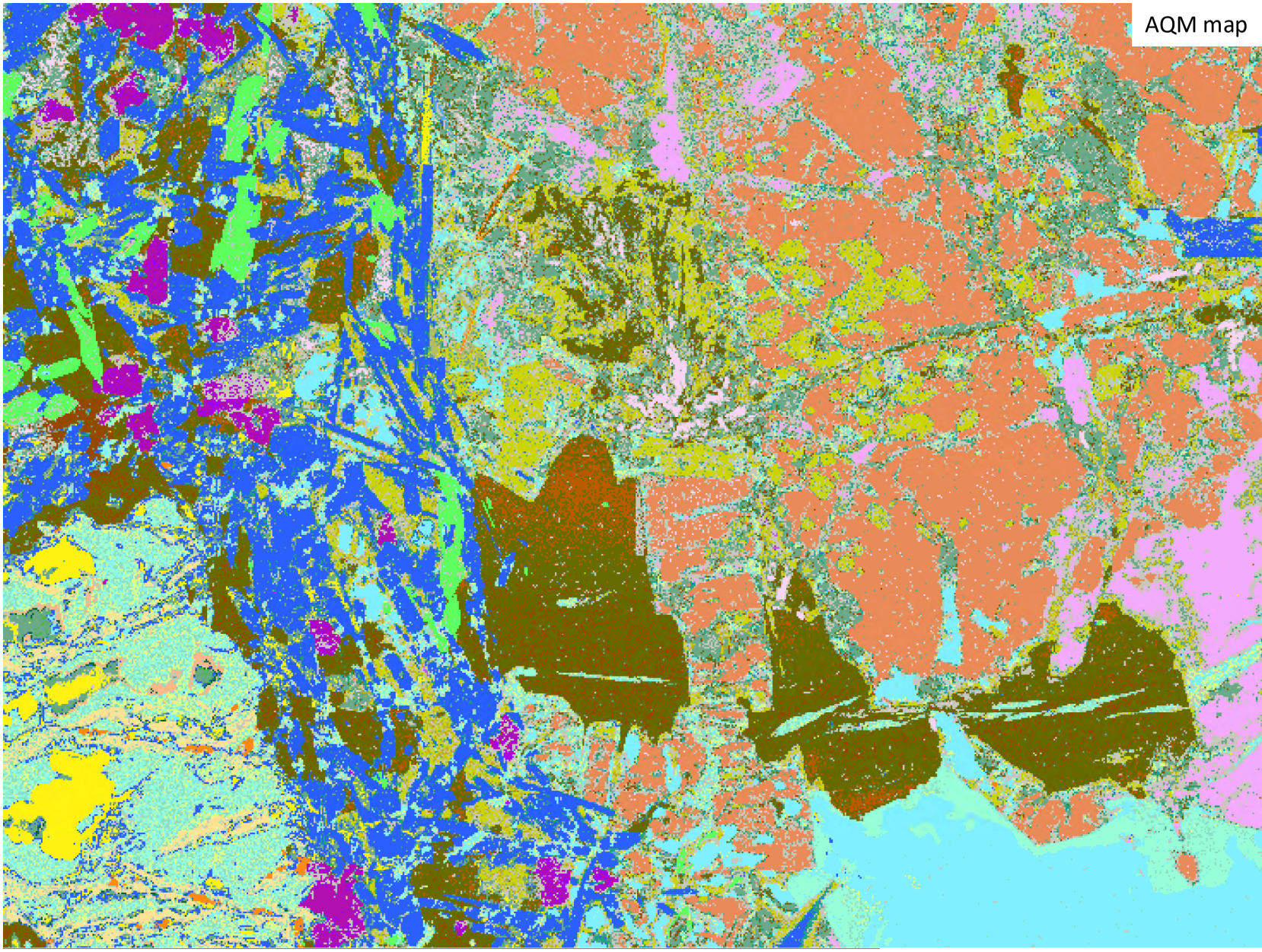

591206_01: Ultramafic lamprophyre

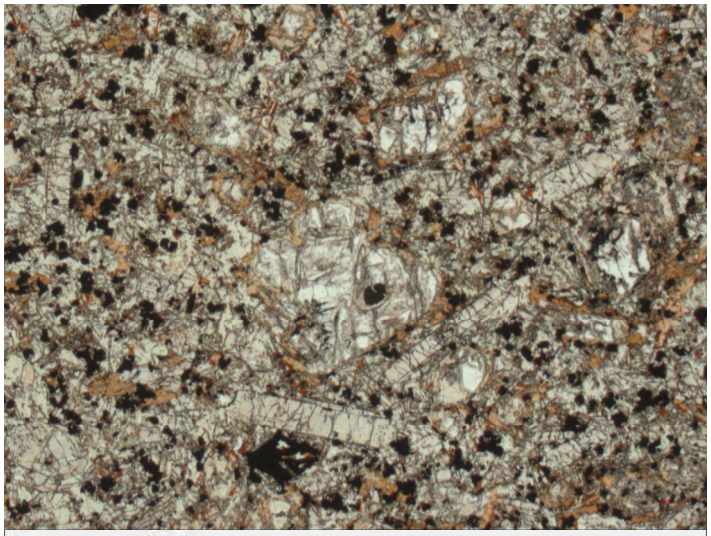

591206_01 PPL

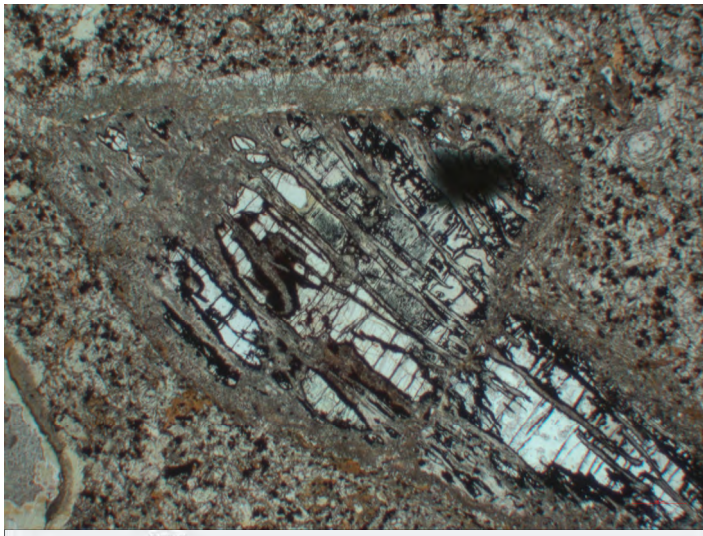

591206_02 PPL

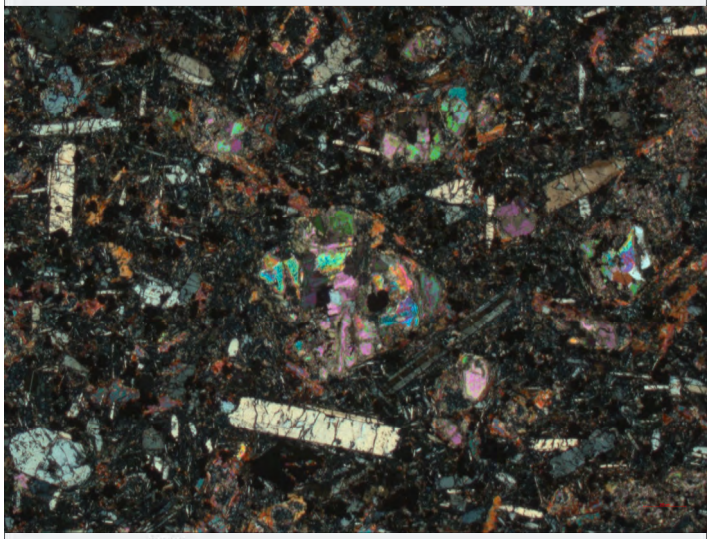

591206_01 XPL

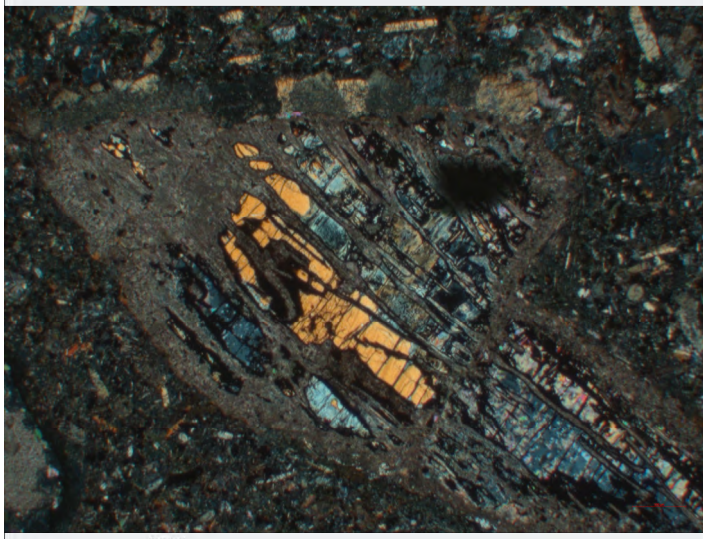

591206_02 XPL

591206_01: Ultramafic lamprophyre

591206_03 XPL

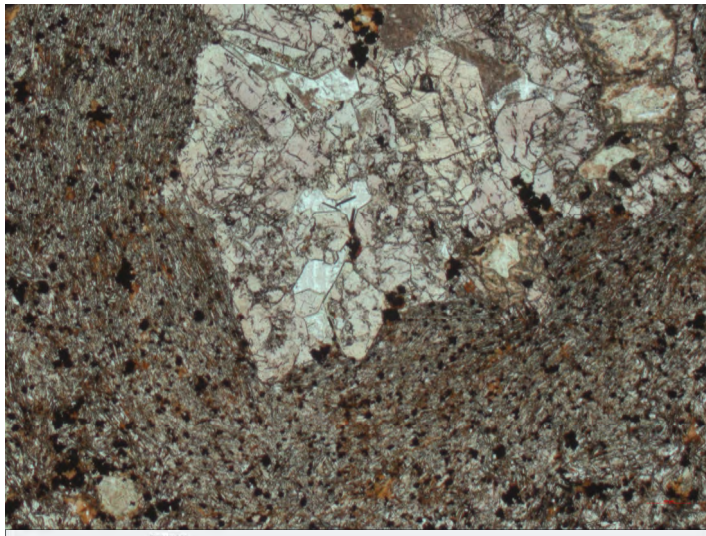

591206_04 PPL

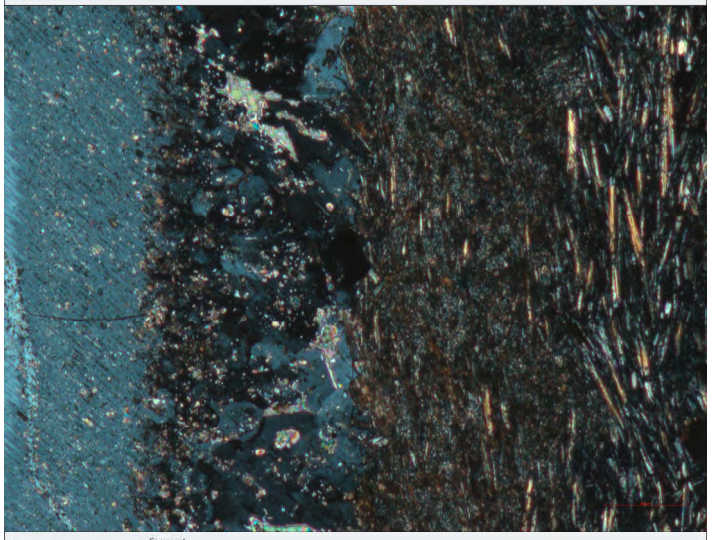

591206_03 XPL

591206_04 XPL

591206_01:
Ultramafic lamprophyre

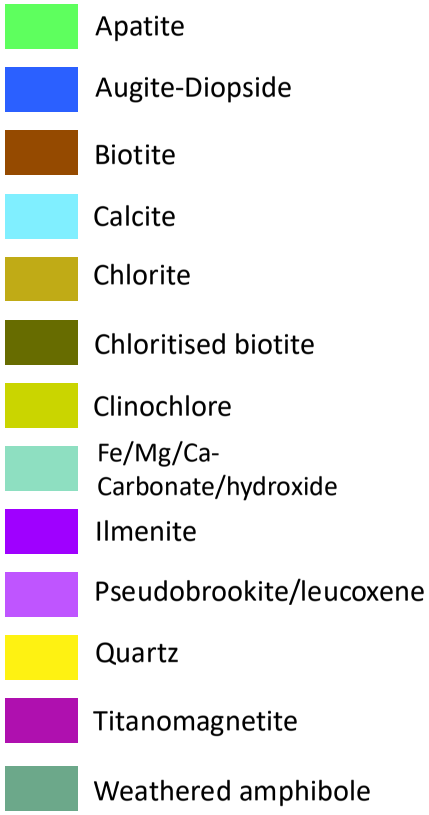

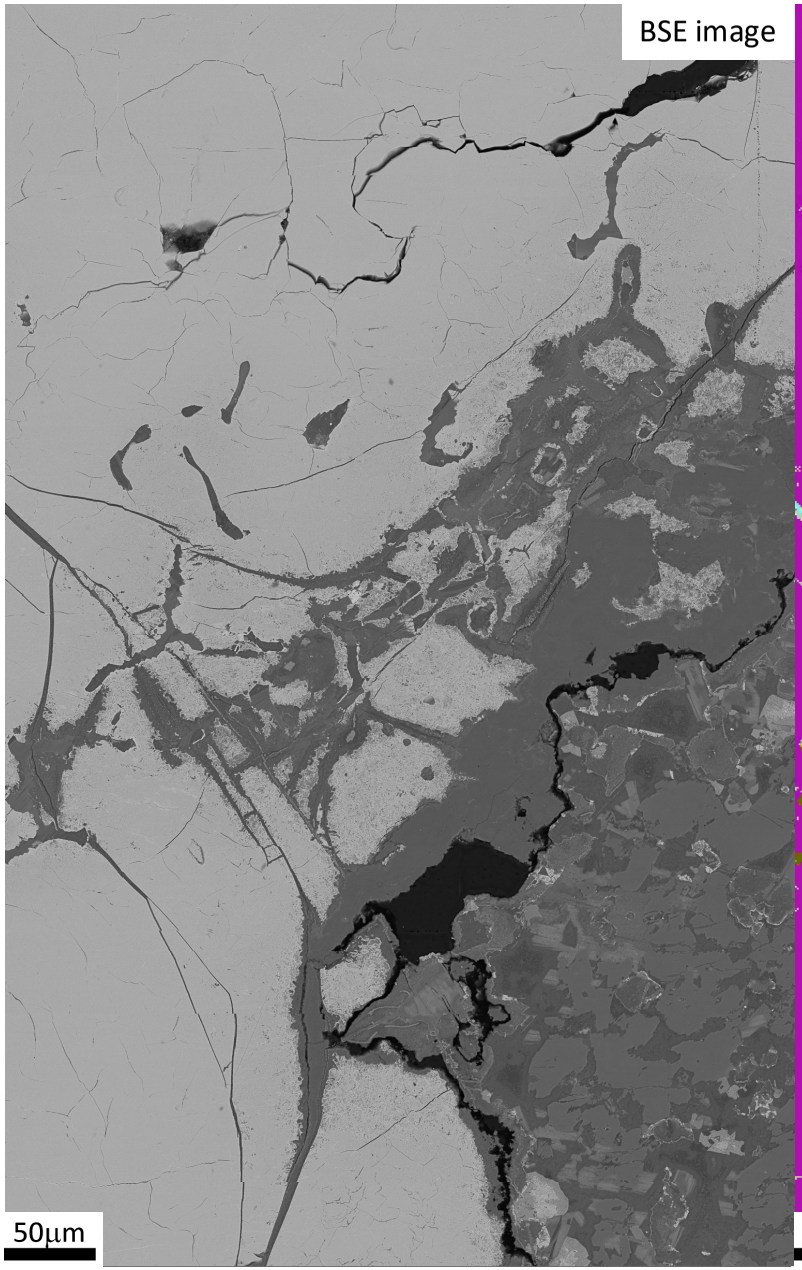

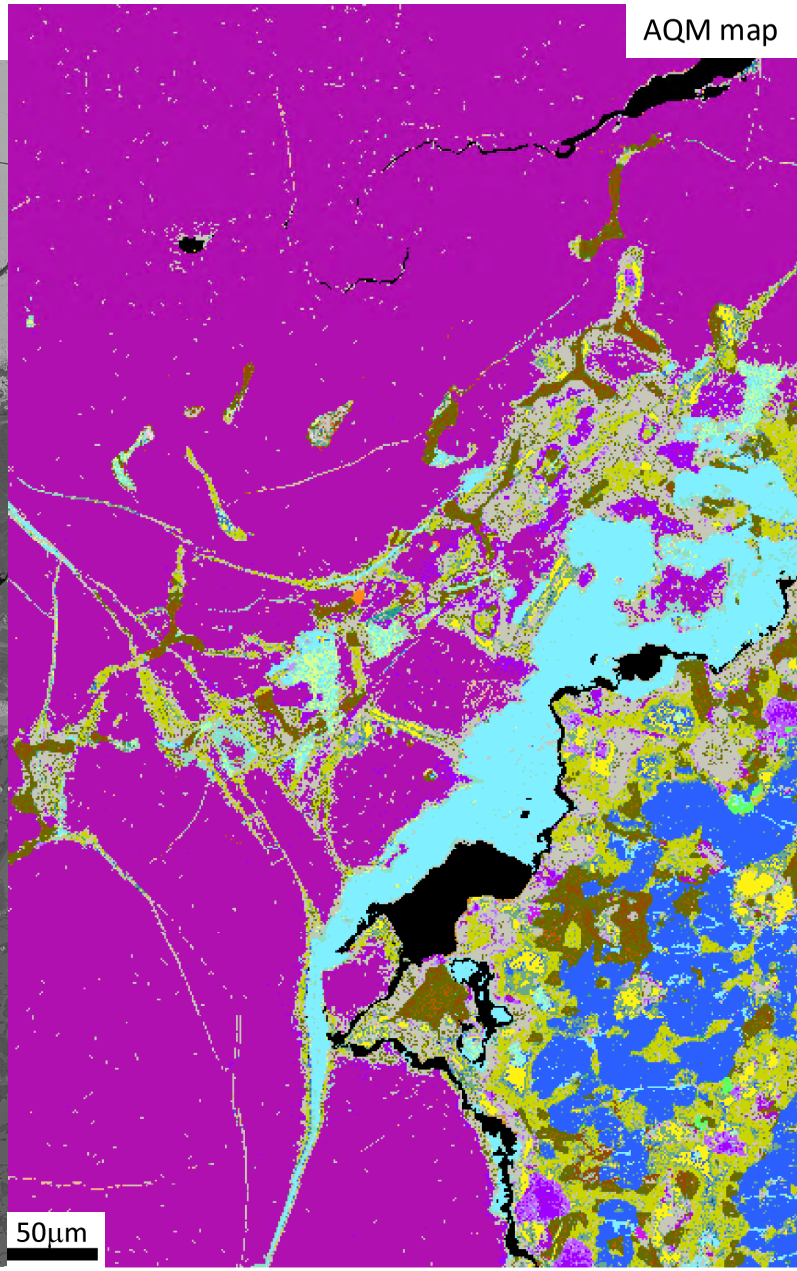

591206_02:
Ultramafic lamprophyre with altered olivine megacrysts

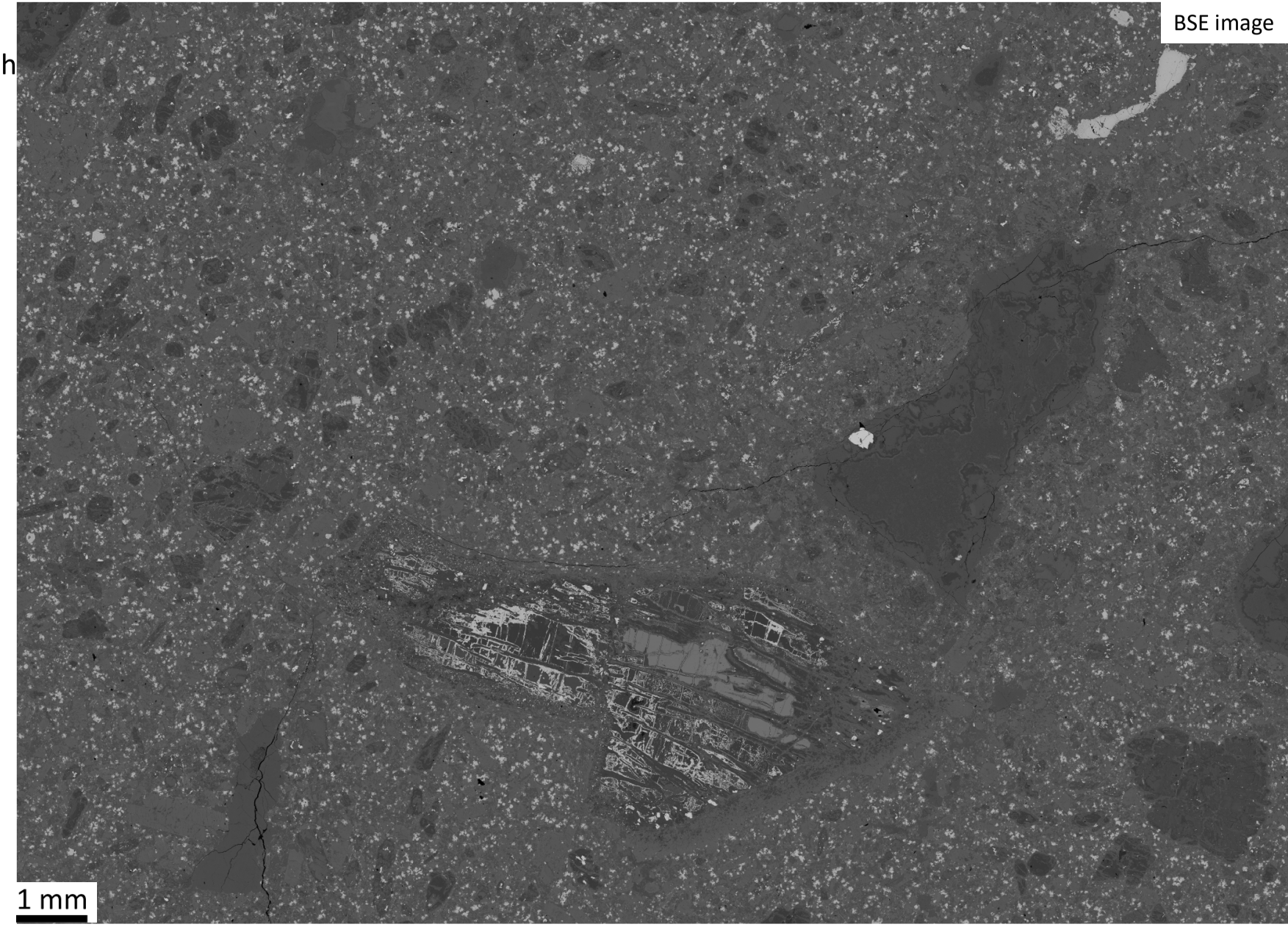

591206_02:
Ultramafic lamprophyre

- Ankerite
- Annite
- Anthophyllite/ Cummingtonite
- Apatite
- Augite-Diopside
- Biotite
- Calcite
- Chloritised biotite
- Clinochlore
- Dolomite
- Fe/Mg/Ca-Carbonate/hydroxide
- Ilmenite
- Mg-Siderite (sideroplesite)
- Olivine
- Quartz
- Sericite_Al-celadonite
- Titanomagnetite
- Weathered amphibole

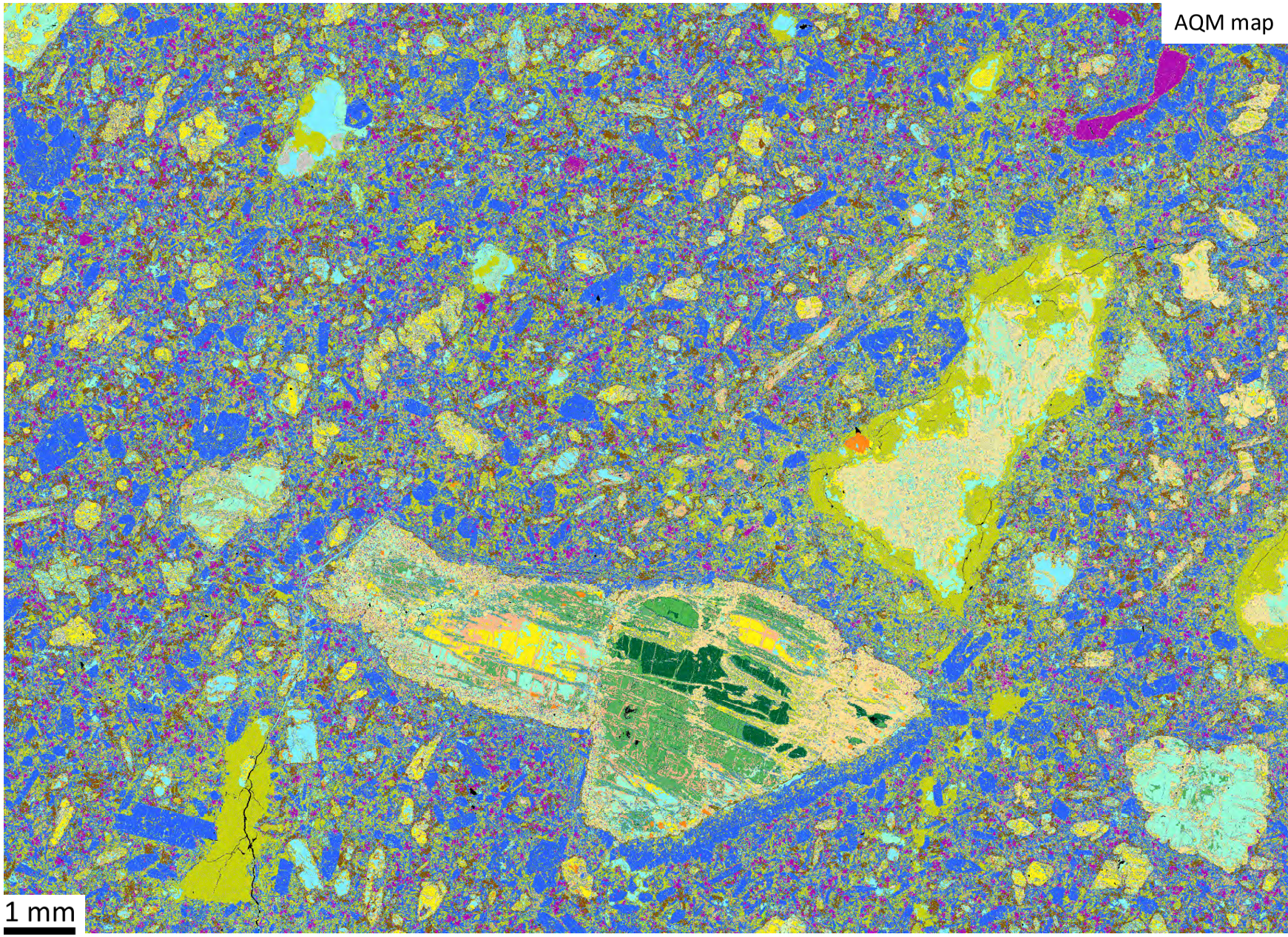

591206_02:
Ultramafic lamprophyre with altered olivine megacrysts

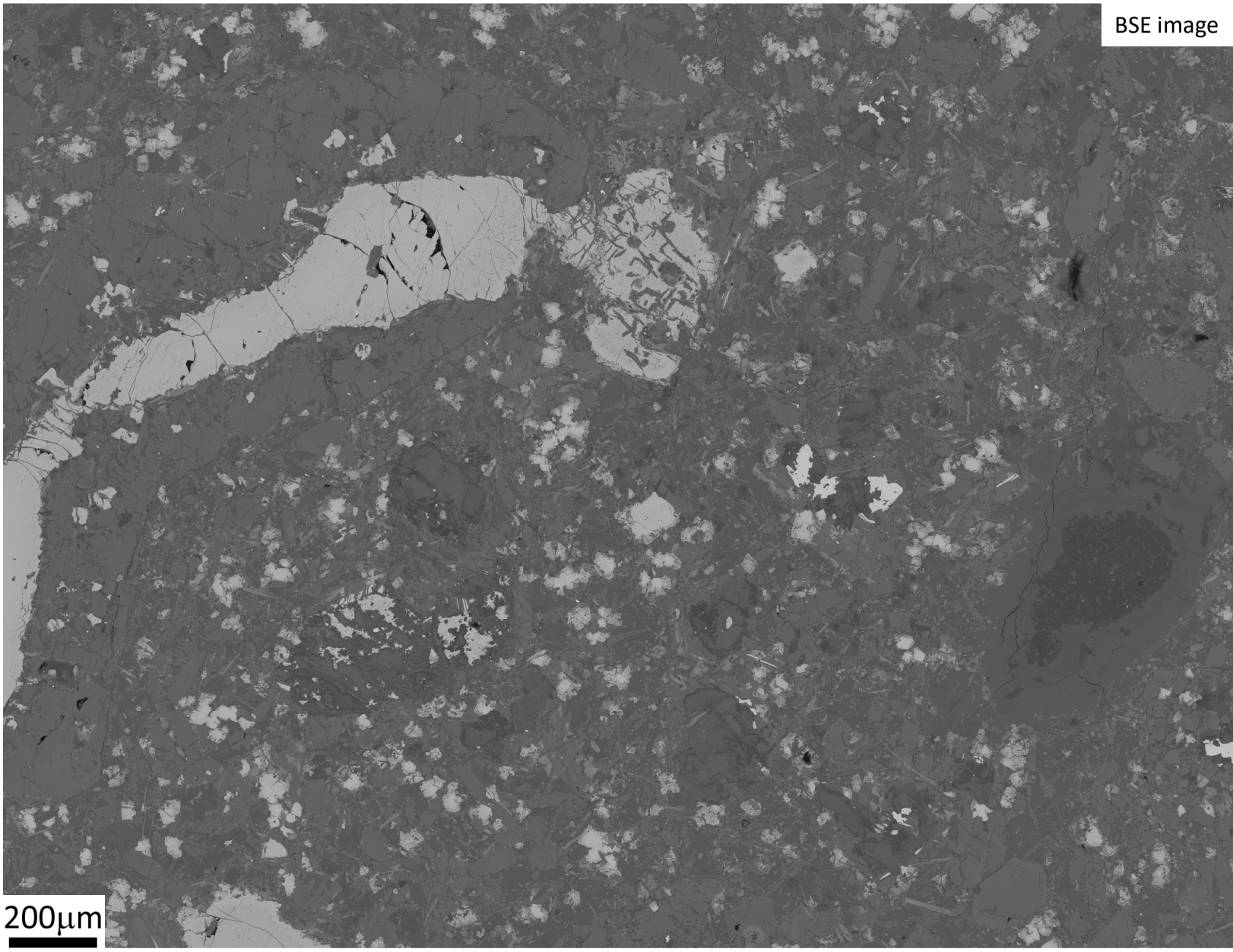

591206_02:
Ultramafic lamprophyre with altered olivine megacrysts

- Ankerite
- Annite
- Apatite
- Augite-Diopside
- Biotite
- Calcite
- Chlorite/Chamosite
- Chloritised biotite
- Clinochlore
- Dolomite
- Fe/Mg/Ca-Carbonate/hydroxide
- Ilmenite
- Mg-Siderite (sideroplesite)
- Pyrite
- Quartz
- Sericite_Al-celadonite
- Titanomagnetite
- Weathered amphibole

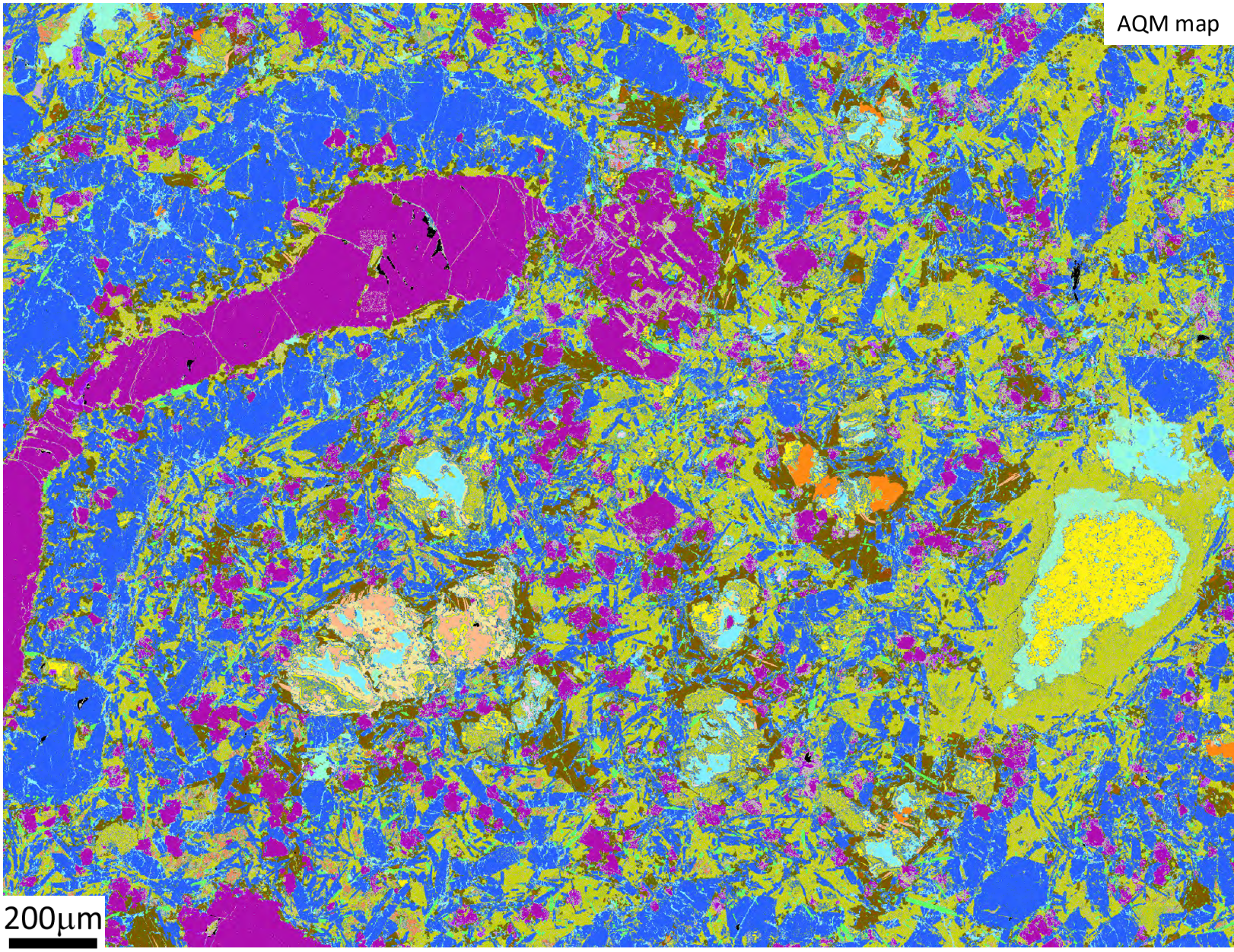

591206_03:
Ultramafic lamprophyre

- Ankerite
- Annite
- Apatite
- Augite-Diopside
- Biotite
- Calcite
- Chlorite/Chamosite
- Chloritised biotite
- Clinochlore
- Dolomite
- Fe/Mg/Ca-Carbonate/hydroxide
- Ilmenite
- Mg-Siderite (sideroplesite)
- Pyrite
- Quartz
- Siderite/Fe-oxide
- Titanomagnetite
- Weathered amphibole

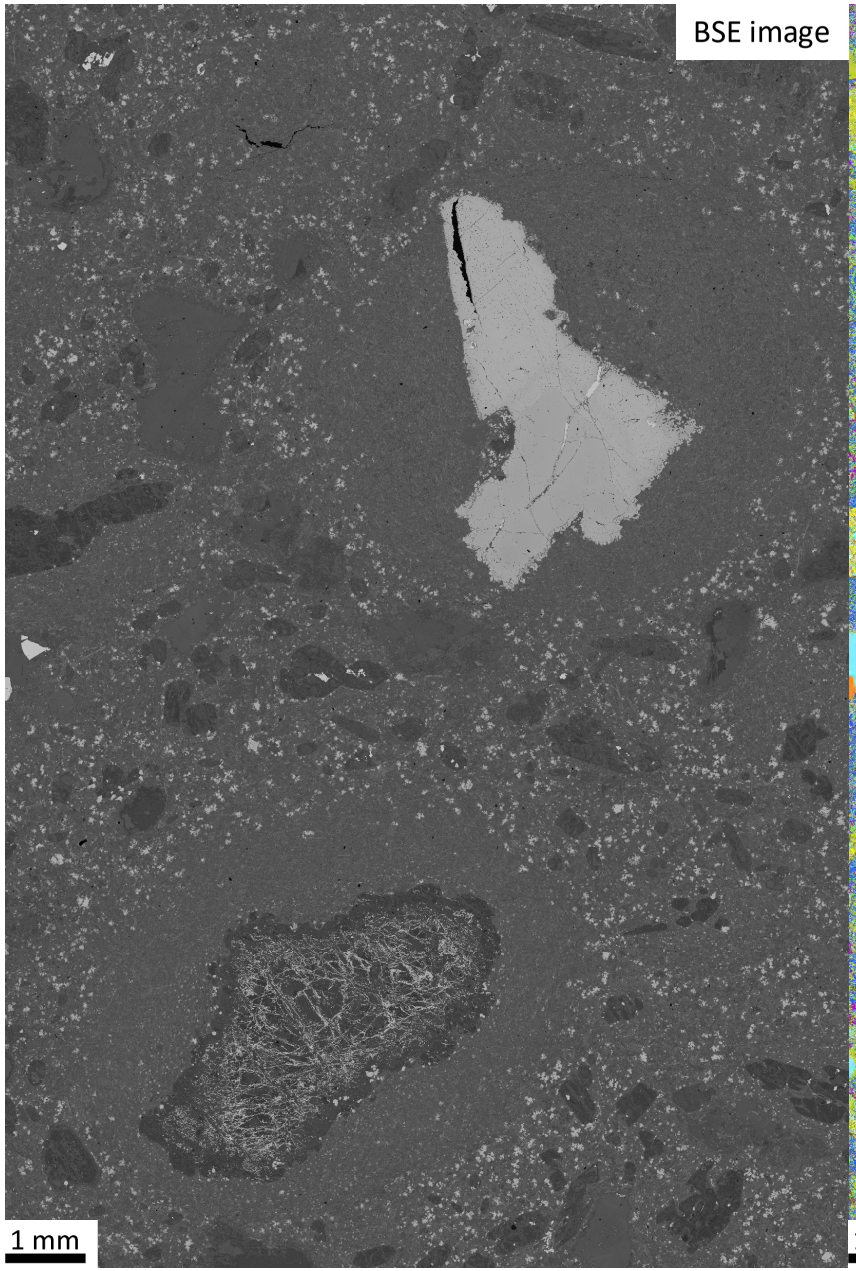

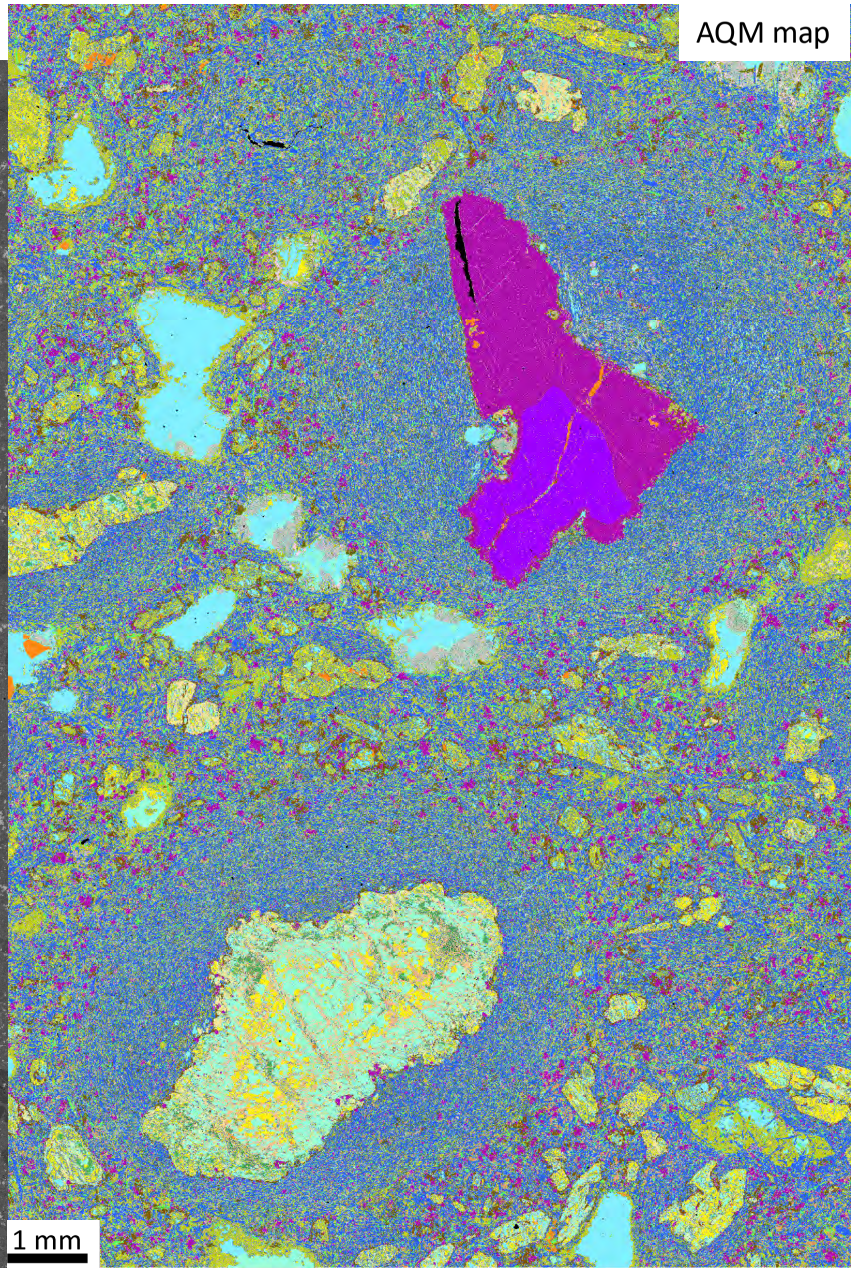

591206_04:
Ultramafic lamprophyre

- Ankerite
- Annite
- Anthophyllite/ Cummingtonite
- Apatite
- Augite-Diopside
- Biotite
- Calcite
- Chlorite/Chamosite
- Chloritised biotite
- Clinochlore
- Dolomite
- Fe/Mg/Ca-Carbonate/hydroxide
- Ilmenite
- Mg-Siderite (sideroplesite)
- Pyrite
- Quartz
- Sericite_Al-celadonite
- Titanomagnetite
- Weathered amphibole

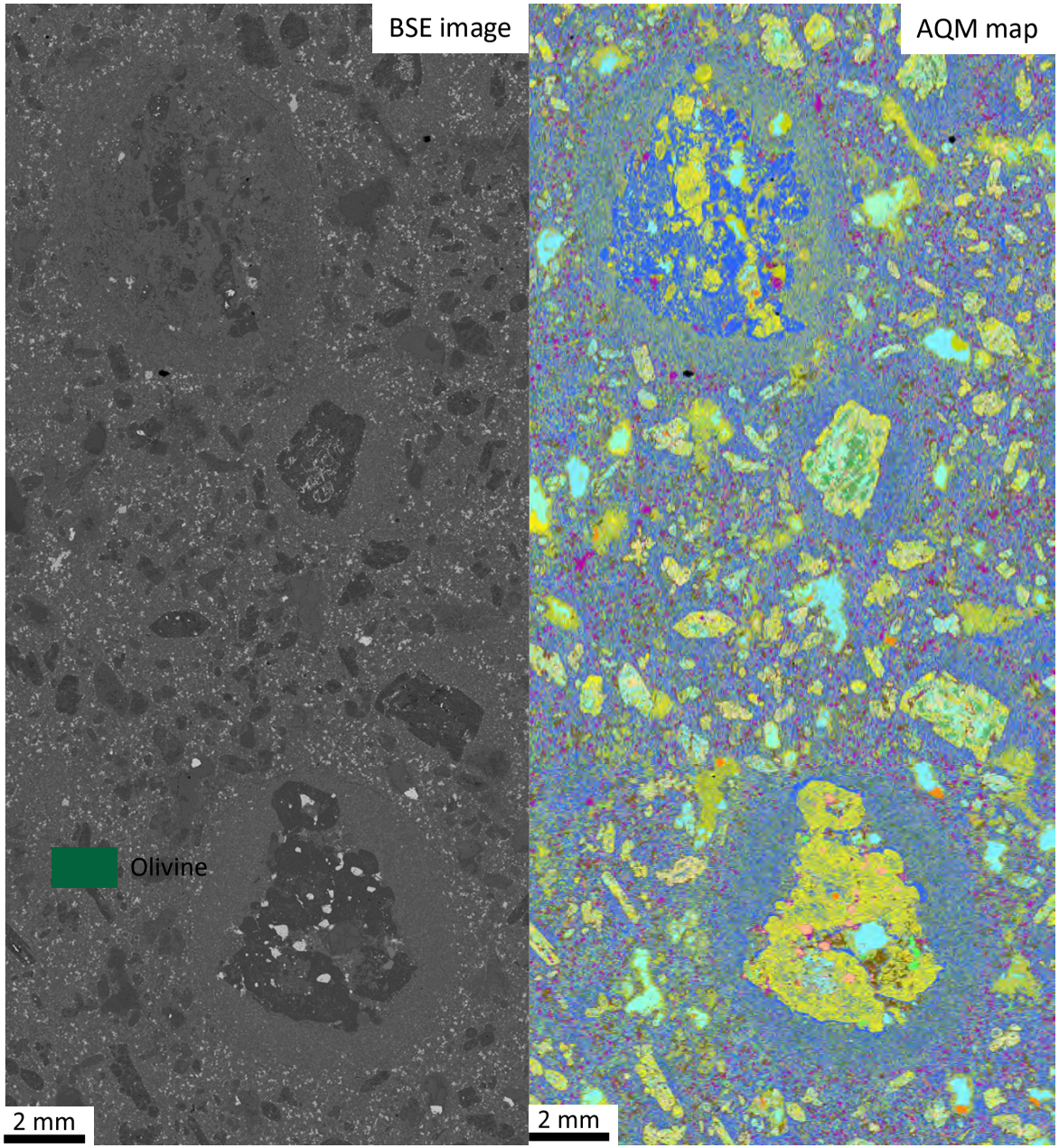

591206_04: Ultramafic lamprophyre

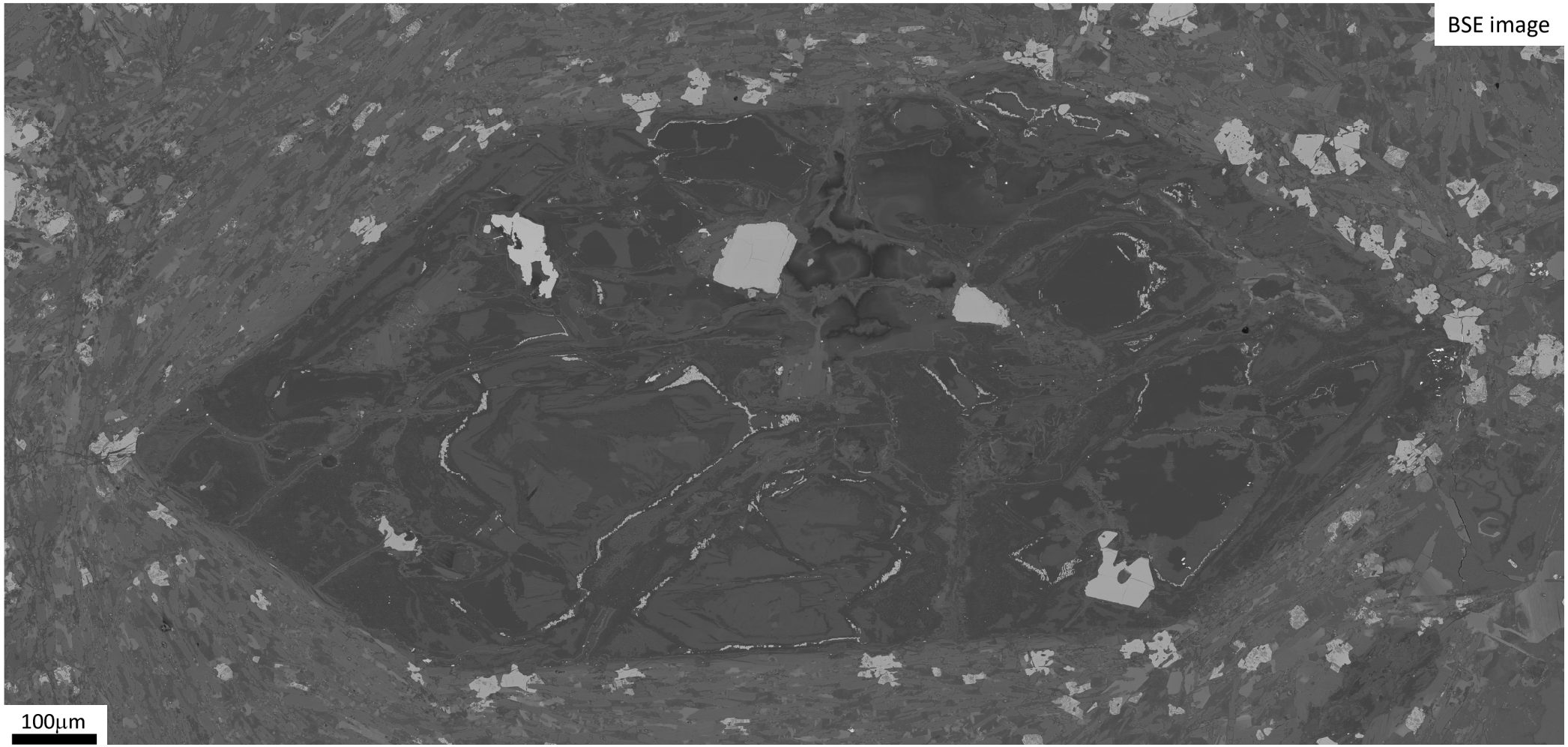

591206_04: Ultramafic lamprophyre

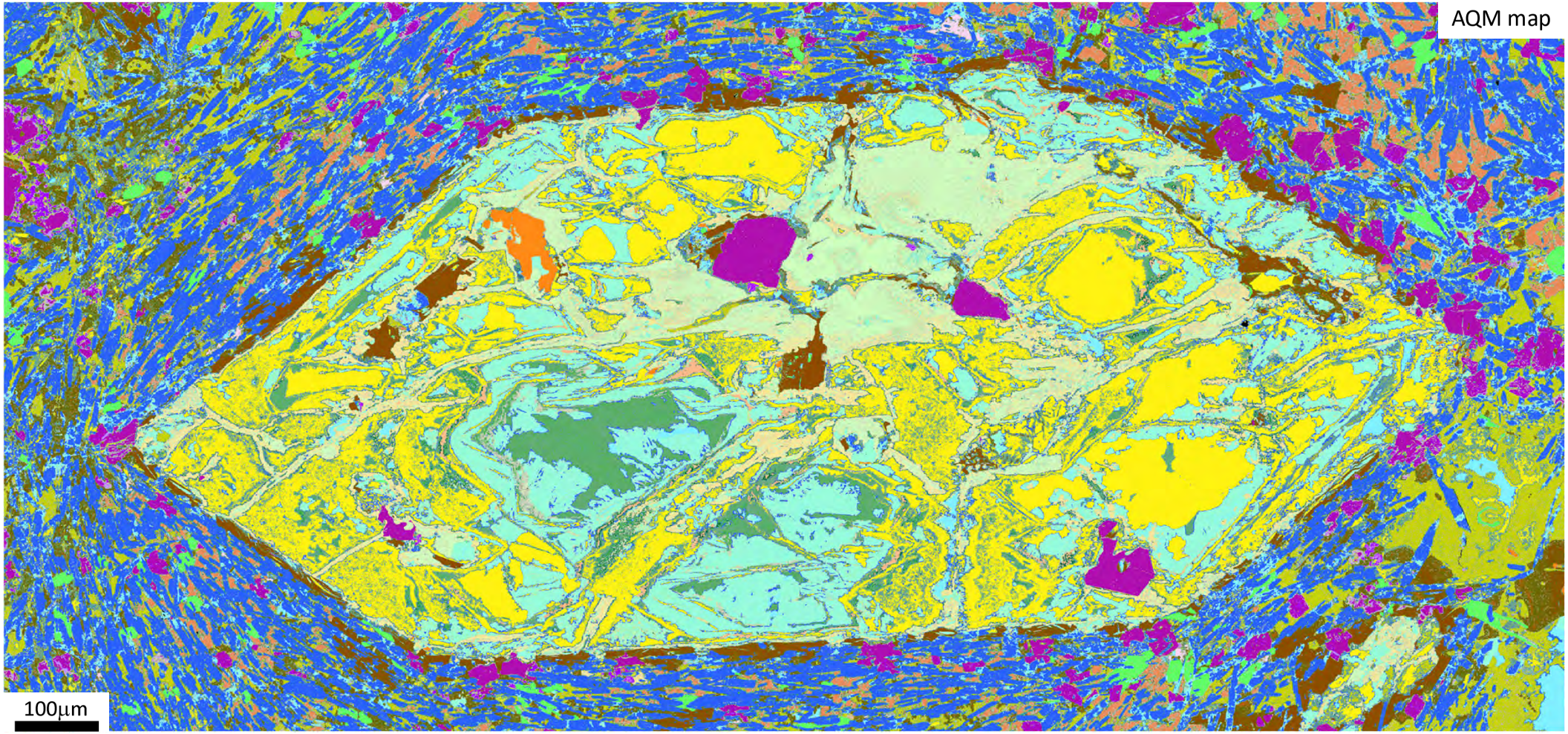

591206_05:
Ultramafic lamprophyre

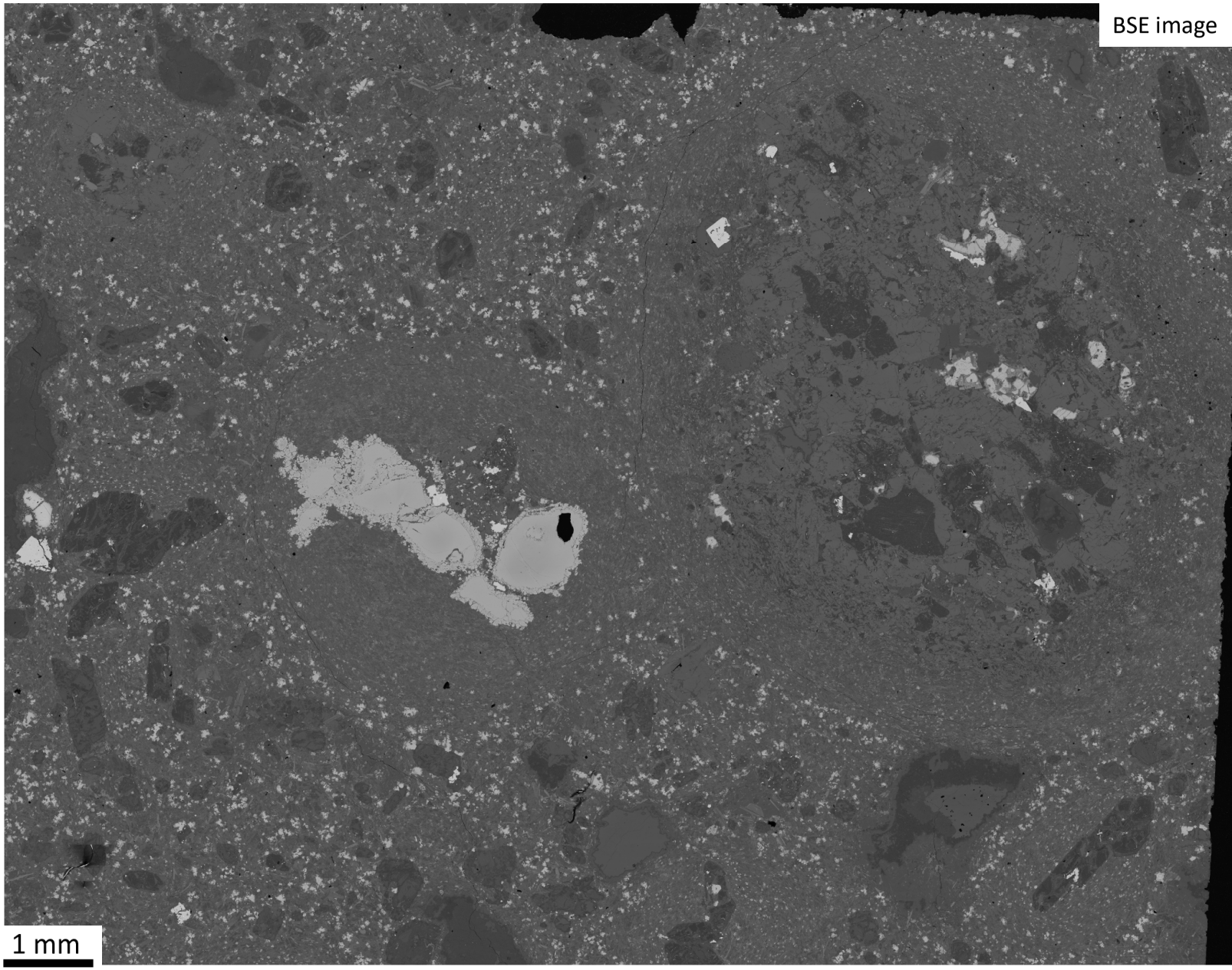

591206_05:
Ultramafic lamprophyre

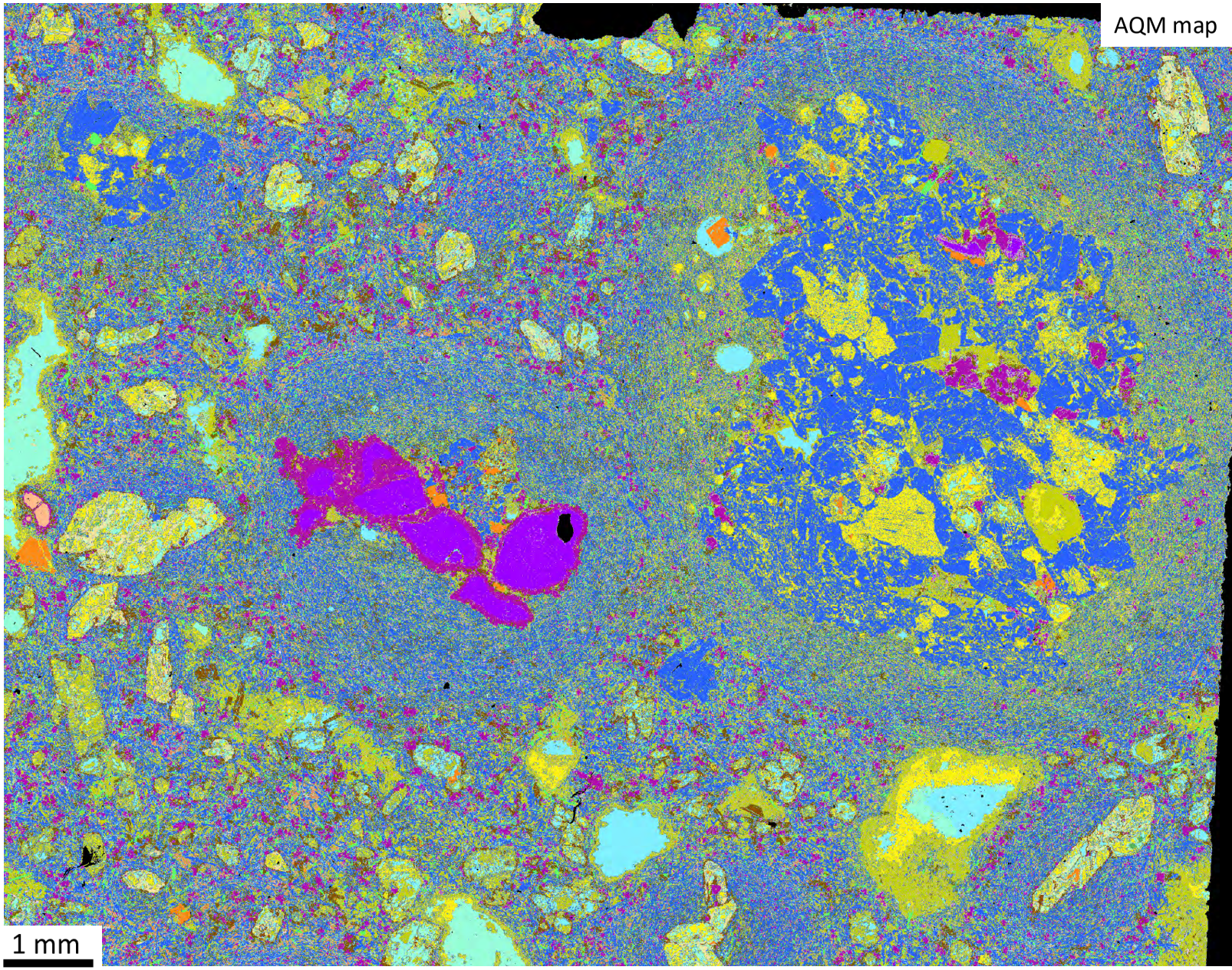

- Annite
- Apatite
- Augite-Diopside
- Biotite
- Calcite
- Chlorite/Chamosite
- Chloritised biotite
- Clinochlore
- Dolomite
- Fe/Mg/Ca-Carbonate/hydroxide
- Ilmenite
- Mg-Siderite (sideroplesite)
- Pyrite
- Quartz
- Sericite_Al-celadonite
- Titanomagnetite
- Weathered amphibole

591208:
Ultramafic lamprophyre

591208: Ultramafic lamprophyre

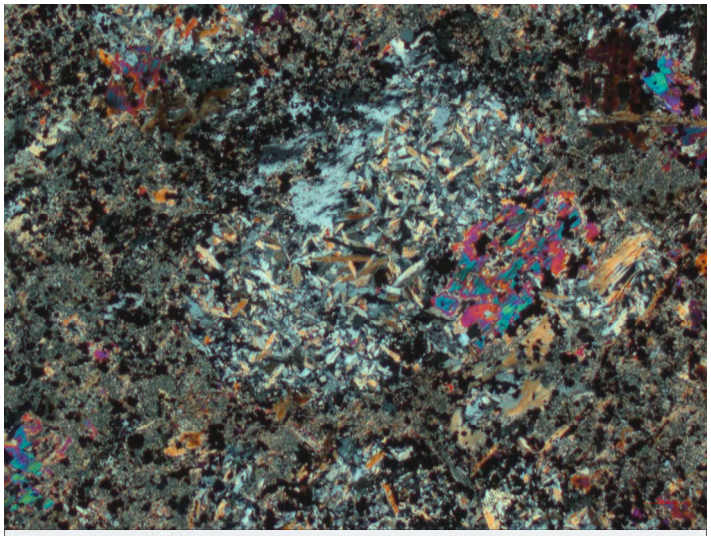

591208_01 XPL

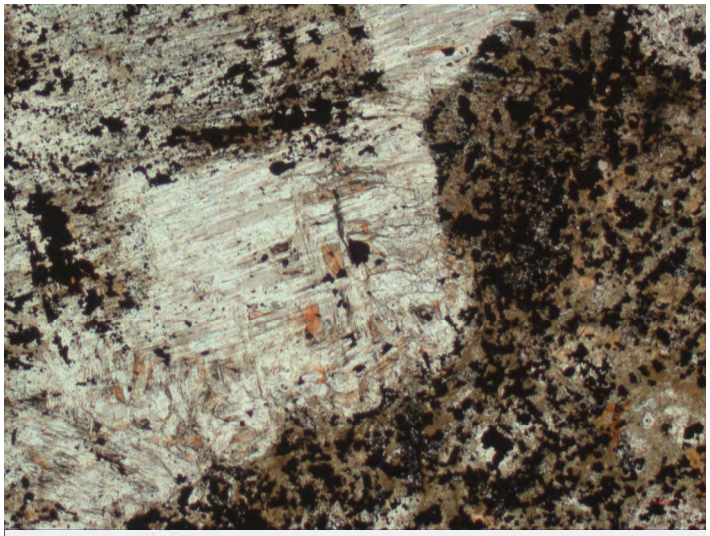

591208_02 PPL

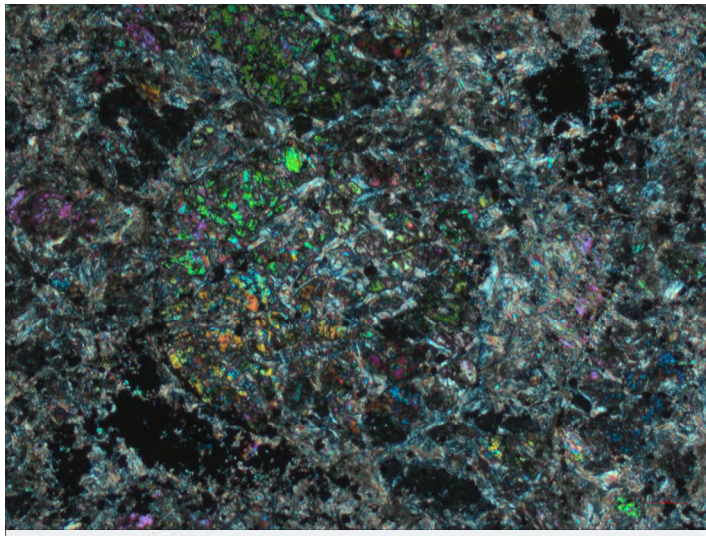

591208_04 XPL

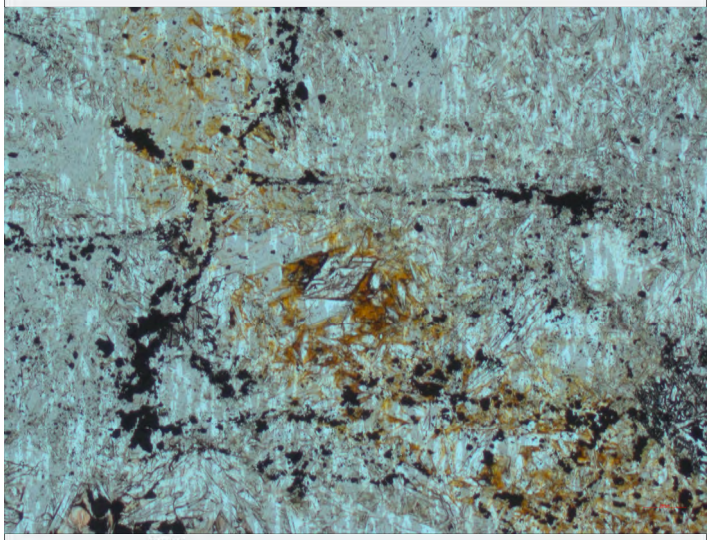

591208_03 PPL

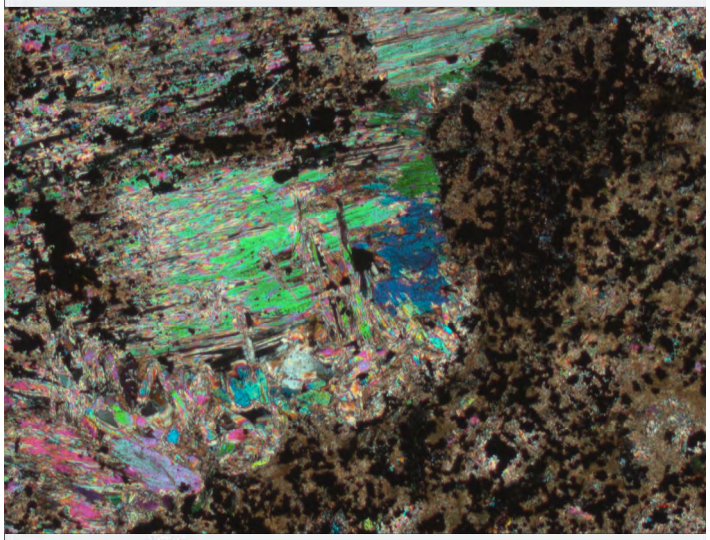

591208_02 XPL

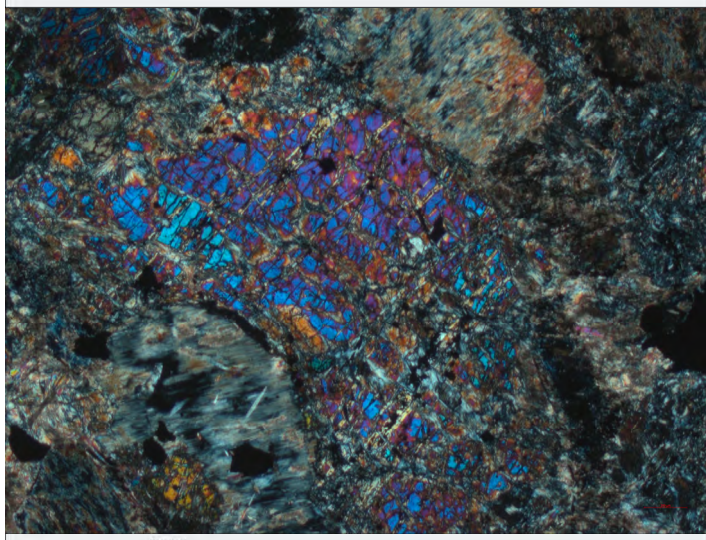

591208_08 XPL

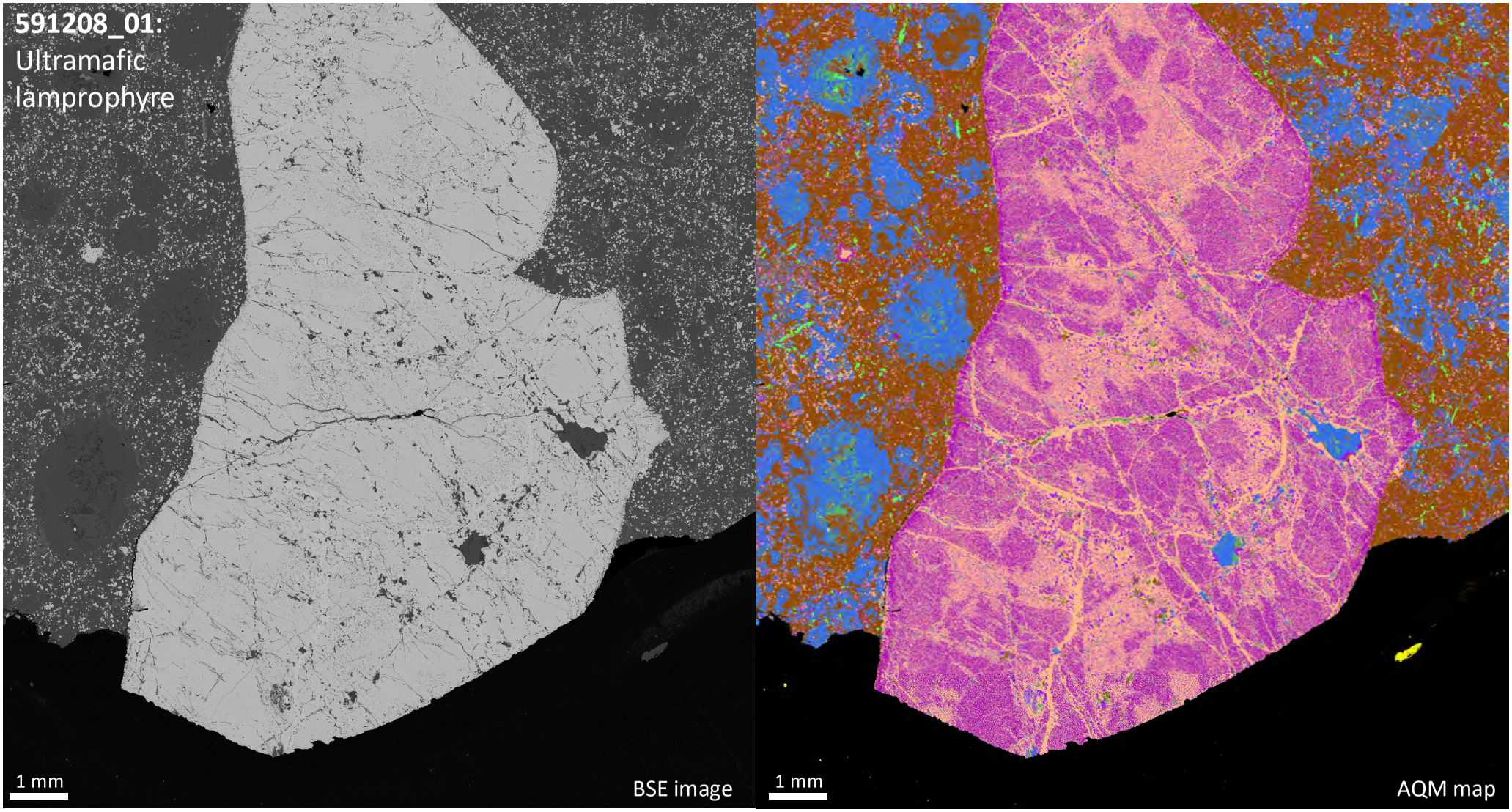
591208_01:
Ultramafic
lamprophyre
1 mm
BSE image
1 mm
AQM map
Anthophyllite/
Cummingtonite
Augite-
Diopside
Chloritised
biotite
Siderite/
Fe-oxide
Titanomagnetite
Apatite
Biotite
Ilmenite
Sphene
Weathered
amphibole

591208_02:
Ultramafic lamprophyre

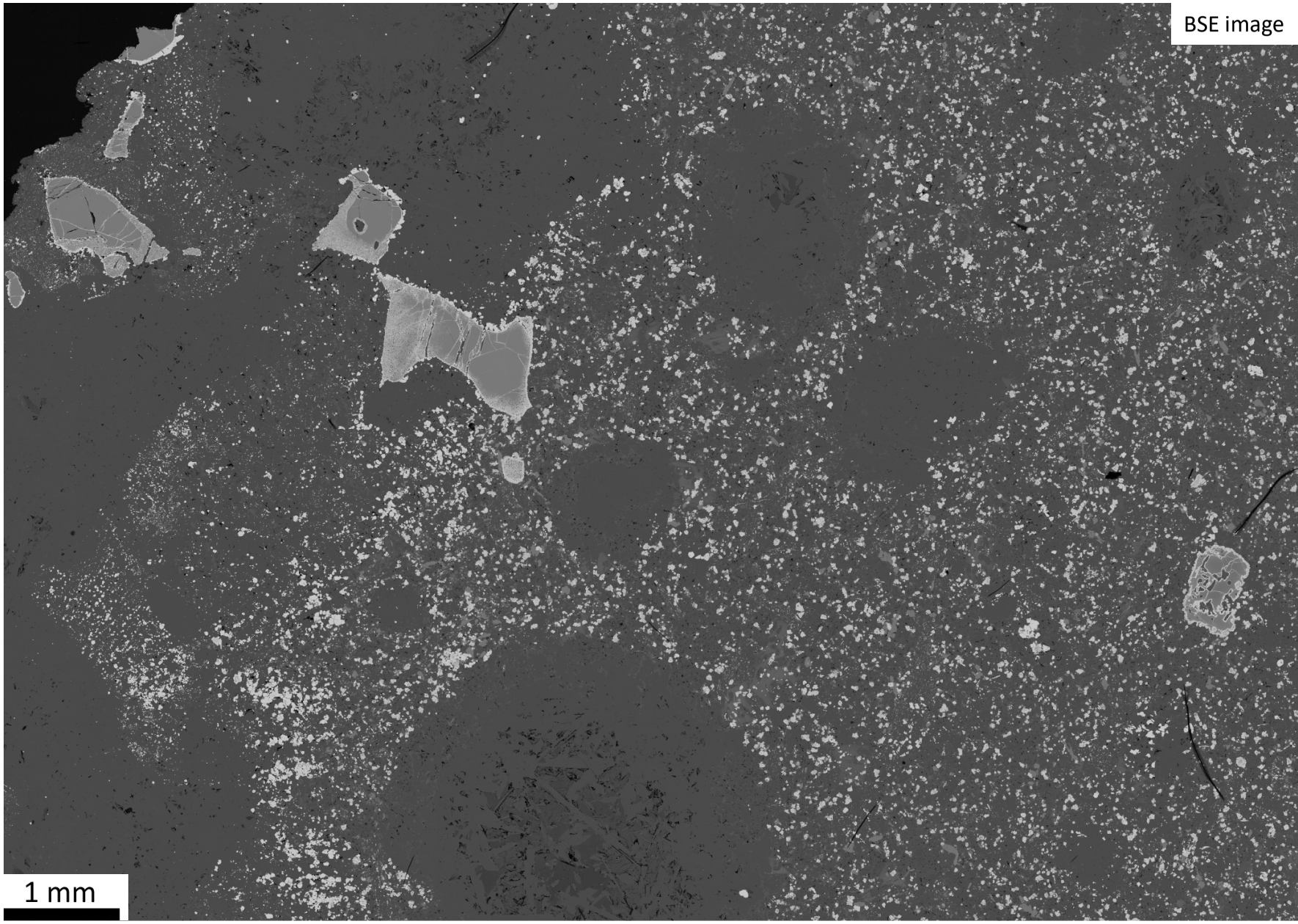

591208_02:
Ultramafic lamprophyre

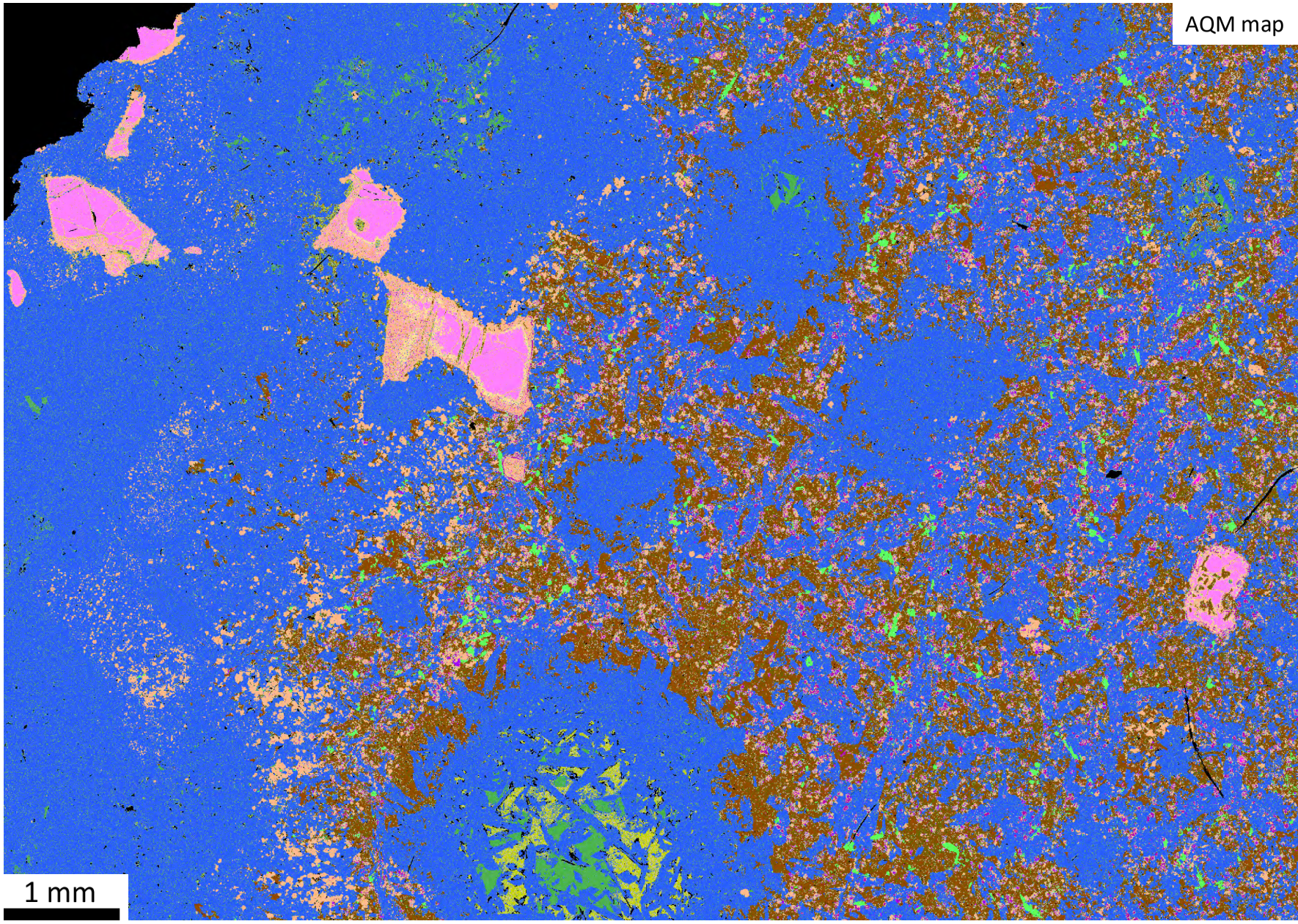

- Anthophyllite/ Cummingtonite
- Apatite
- Augite-Diopside
- Biotite
- Chloritised biotite
- Clinochlore
- Fe/Mg/Ca-Carbonate/hydroxide
- Ilmenite
- Siderite/Fe-oxide
- Sphene
- Spinel
- Titanomagnetite
- Weathered amphibole

591208_02:
Ultramafic lamprophyre

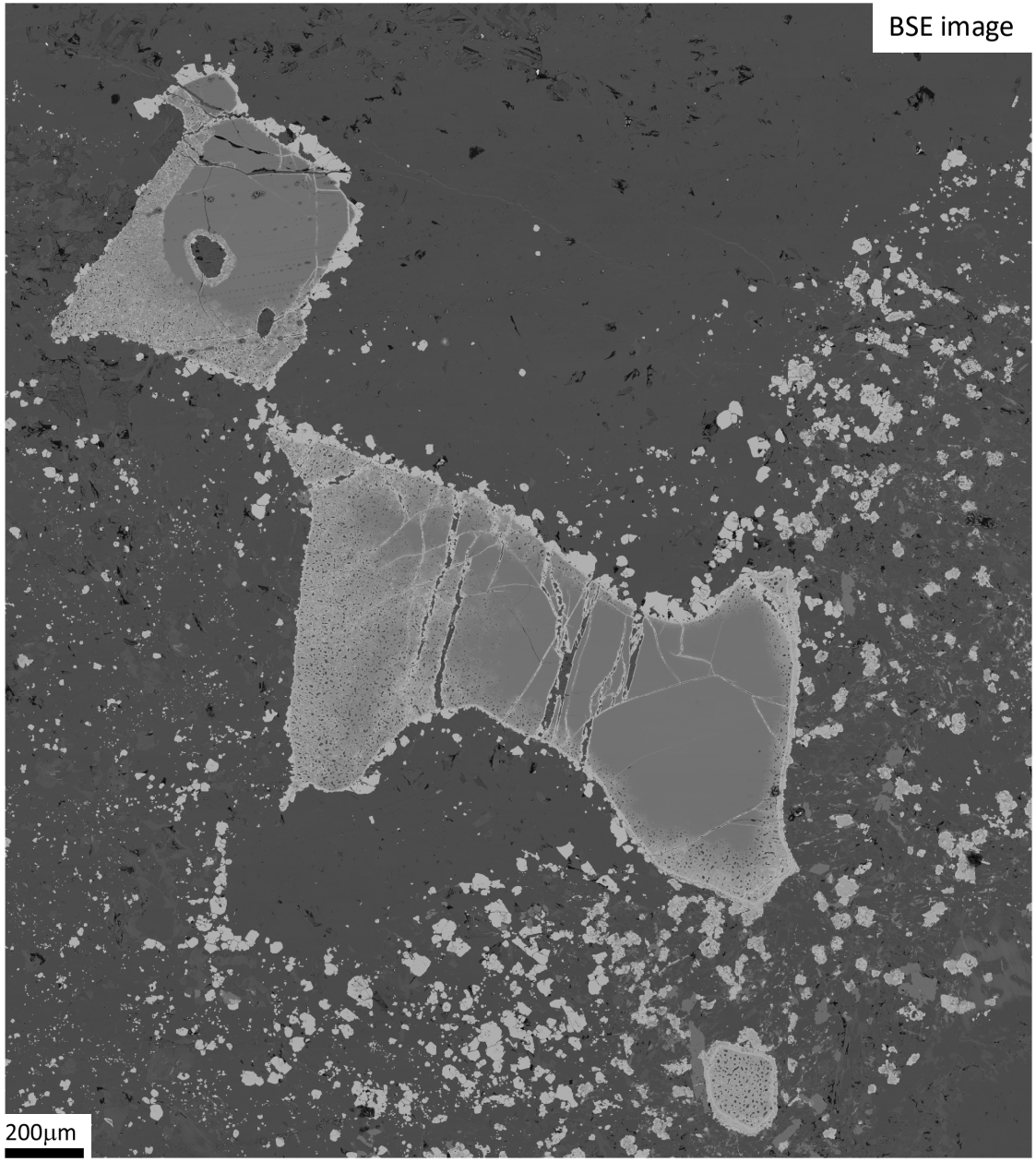

591208_02:
Ultramafic lamprophyre

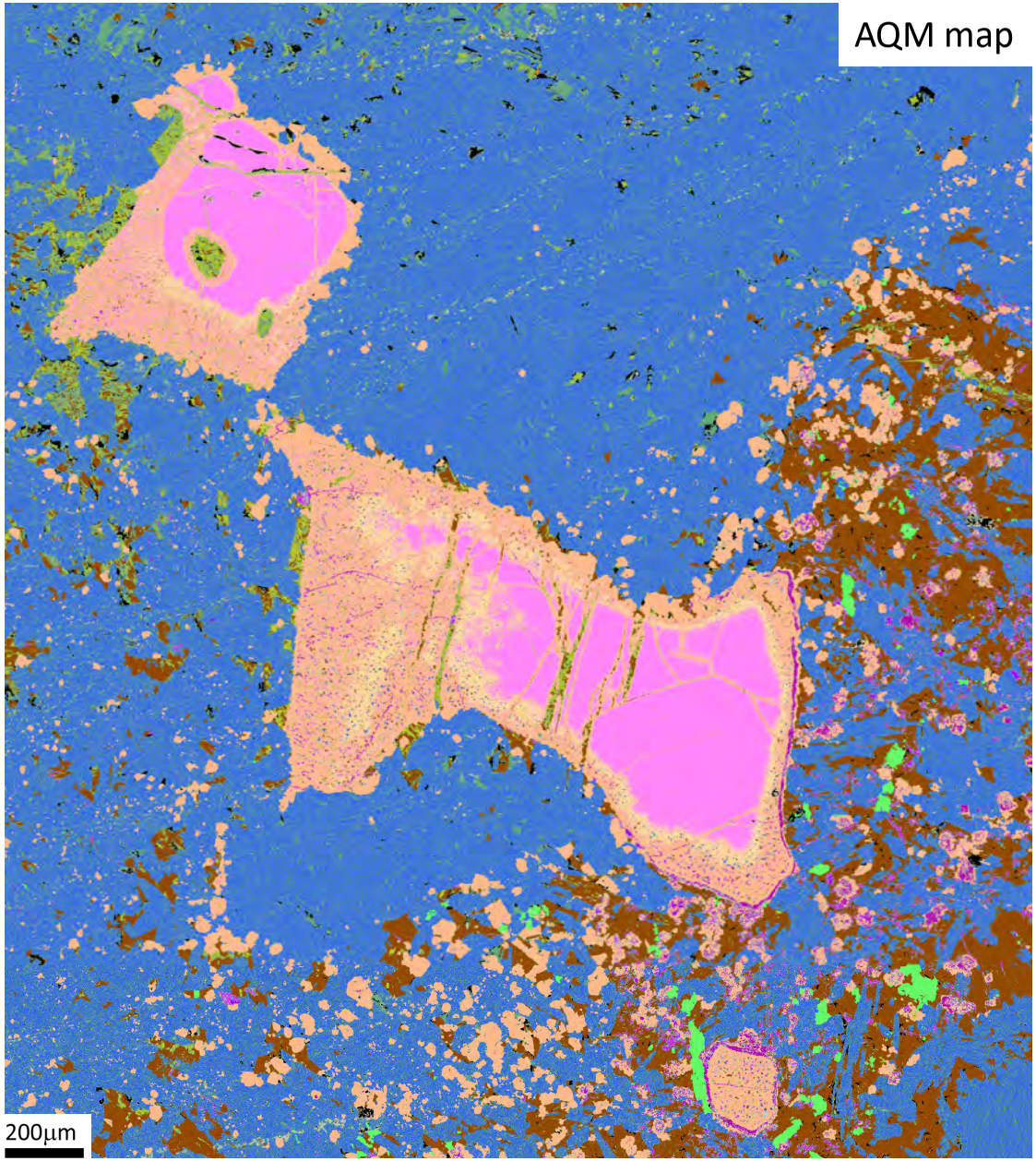

- Anthophyllite/ Cummingtonite
- Apatite
- Augite-Diopside
- Biotite
- Chloritised biotite
- Clinochlore
- Mg-Siderite (sideroplesite)
- Siderite/Fe-oxide
- Sphene
- Spinel
- Titanomagnetite

591208_06:
Ultramafic lamprophyre

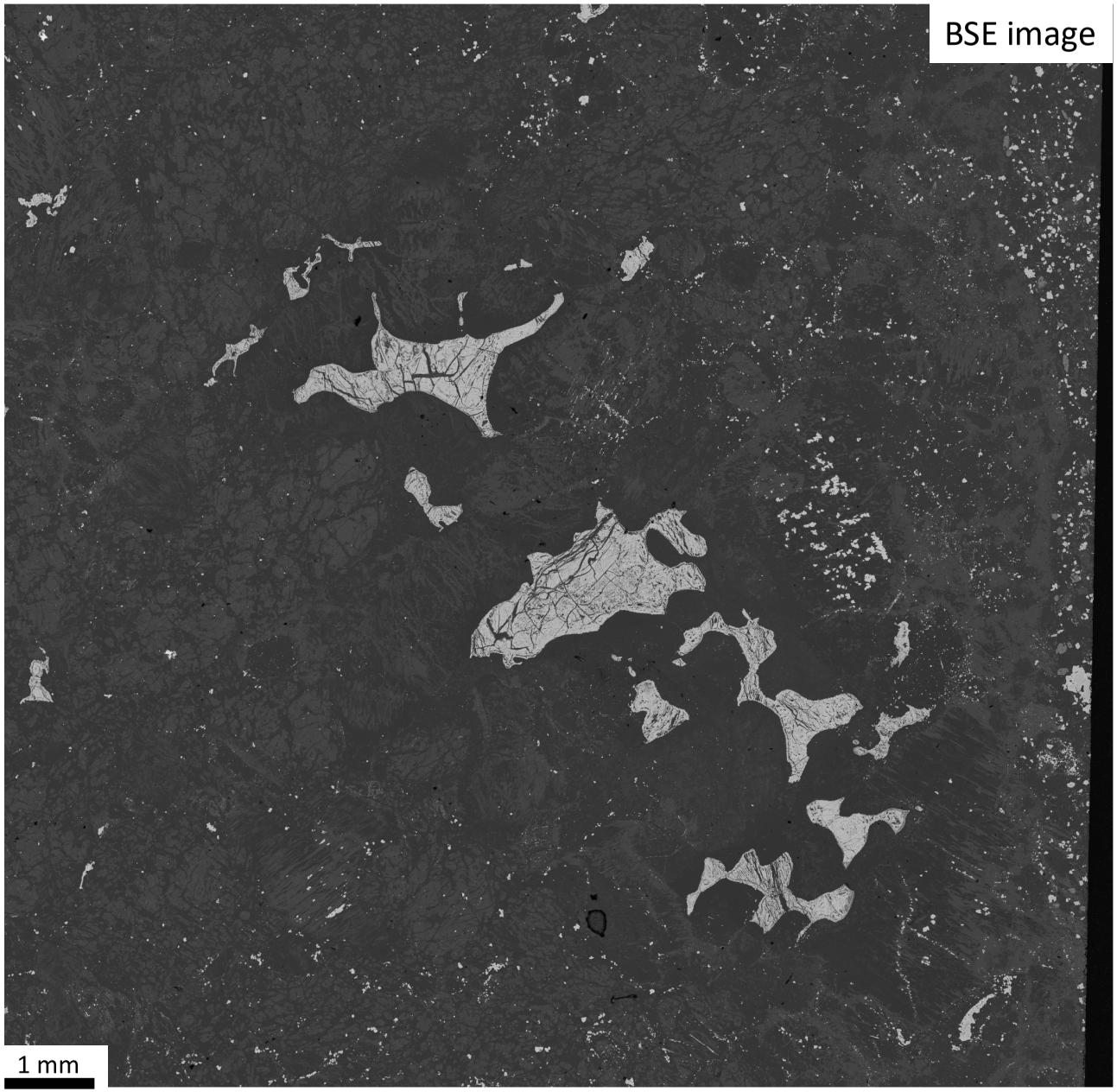

591208_06:
Ultramafic lamprophyre

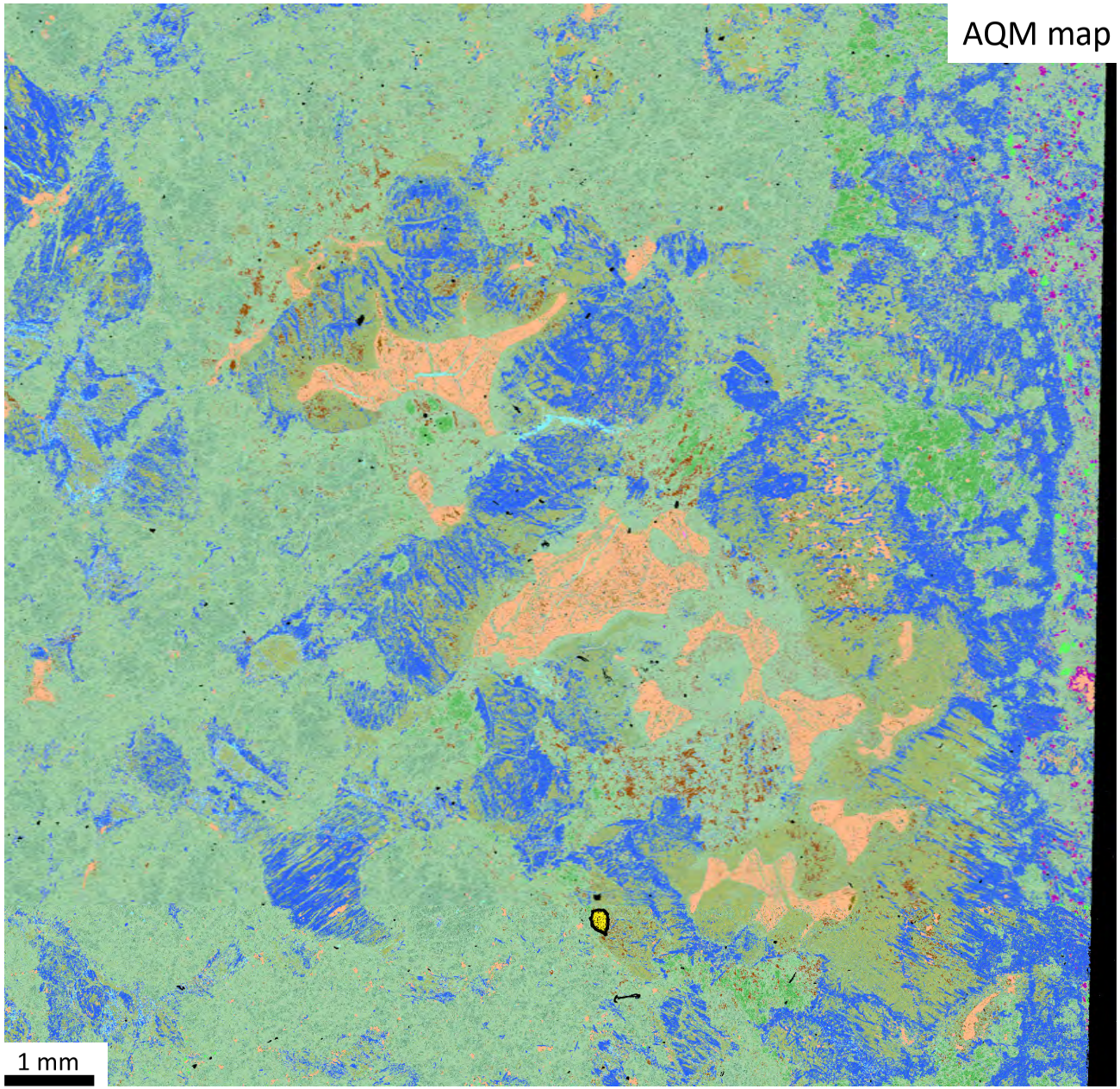

- Anthophyllite/ Cummingtonite
- Apatite
- Augite-Diopside
- Biotite
- Chrysotile
- Dozyite
- Olivine
- Siderite/Fe-oxide
- Titanomagnetite
- Weathered amphibole

591212:
Ultramafic Lamprophyre dyke